

REVISING THE ROLE OF THE
VENTROLATERAL PERIAQUEDUCTAL GRAY
IN THE FEAR CIRCUIT

KRISTINA M. WRIGHT

A dissertation

submitted to the faculty of the Department of
Psychology & Neuroscience in partial fulfillment
of the requirements for the degree of
Doctor of Philosophy

Boston College
Morrissey College of Arts and Sciences
Graduate School

April 2021

© Copyright 2021 Kristina M. Wright

Title: Revising the role of the ventrolateral periaqueductal gray in the fear circuit

By: Kristina M. Wright

Advisor: Michael A. McDannald, Ph.D.

Secondary Advisor and Chair: John Christianson, Ph.D.

Tertiary Committee Member: Gorica Petrovich, Ph.D.

Outside Committee Member: Benjamin Greenwood, Ph.D.

ABSTRACT

Kristina M. Wright: Revising the role of the
ventrolateral periaqueductal gray in the fear circuit
(Under the direction of Michael A. McDannald, PhD)

The ability to accurately evaluate and respond to threats is vital to survival. Disruptions in neural circuits of fear give rise to maladaptive threat responding, and have clinical implications in fear and anxiety disorders. To better inform therapeutic interventions, it is imperative that roles for regions classically associated with fear continue to be refined, and that novel nodes are incorporated into what is most certainly a larger fear circuit. In the canonical view, threat estimates are generated at the level of the amygdala and sent to the ventrolateral periaqueductal gray (vIPAG), which organizes an appropriate behavioral response, most notably freezing. Despite a multitude of studies successfully linking the vIPAG and Pavlovian fear behavior, evidence of a direct neural correlate for fear expression in the vIPAG is lacking. By contrast, a role for the caudal substantia nigra (cSN) in fear, stands apart from its canonical associations with movement and reward processes. Although there is new interest in examining a role for the nigra in fear modulation, this is essentially an uncharted area of discovery. The goals of this dissertation are three-fold. First, to propose a role for vIPAG activity in threat estimation, a function previously restricted to the upstream amygdala. Second, to scrutinize vIPAG neural activity using a novel multi-cue Pavlovian procedure and identify the long-anticipated, direct neural correlate for fear expression. Third, to present causal evidence supporting the cSN as a potential node in a circuit that most certainly extends beyond regions canonically associated with fear.

Dedicated to my grandmother, who has been by my side every step of the way,
and to the memory of my mother and uncle.

I hope I have made you all proud.

ACKNOWLEDGEMENTS

To those in my personal life that have contributed to this journey, your efforts have not gone unnoticed. To my grandmother, Elena - I would not be where I am today if you had not raised me. Thank you for turning your life upside down and welcoming me into your home as if I were your own. It is impossible to articulate everything you have done for me over so many years of development, and I am eternally grateful. In my lifetime, I'm sure my attempts to return the favor will fall short of your contributions to my life, but I will never stop trying. To the Gossels family - Andrea for the encouragement when I needed it most, Leanne for pushing me to transfer to Boston College, and Warren and Lisa for the kind of support only the best fake parents can provide. To Cathy Hazeltine-Fallon - for your mentorship and friendship, and believing that I could become something someday. And lastly, to my dearest friends - thank you for your words of encouragement, bouts of belly laughter, magnificent music, breathtaking adventures, and unforgettable dancing.

To those in the Boston College Community - especially my advisor, Dr. Michael McDannald. Thank you for your dedication to my personal and professional growth. I'm incredibly proud of the research questions we answered and raised, and the quality of work we produced. Can you believe it? Seven years ago, you hired someone with one semester of lab experience to help build your new lab. At this point, I think it's safe to say - we did alright. Your ambitious and tireless optimism stands in stark contrast to my constant questioning; I cannot count the times I thought to myself, "*Will this* [insert: technique, modification, assay etc.] *actually work?!*" On a more serious note, thank you for believing in me when I haven't had the gusto to do it myself, telling me that I either

had to get a PhD or get out, and providing me with a mantra that has become a regular part of my life: “The only way to ensure you will not get something, is to not try”. Finally, thank you for providing me with the best two years of my life and Alyssa, the best coworker and friend I could have imagined. Graduate school was pretty good, too.

It is hard to believe I was twenty-one years old when I first entered the Boston College Campus. I can say with certainty, that I didn’t intend to celebrate my thirtieth birthday before leaving. Fortunately, it is under favorable circumstances! It should come as no surprise that I have encountered many, incredible people during my time on campus who have significantly contributed to my path toward this dissertation. I would like to take this opportunity to acknowledge them now, in the order I met them. *Dr. Marilee Ogren* - I often reflect on the term paper I wrote for your Abnormal Psychology course, as my very first opportunity to investigate a research question. I cannot overemphasize the impact that paper had on my personal growth, nor the impact your continued support and mentorship has had on my professional path. I have developed a plethora of new skills by way of the opportunities you have extended to me, and benefited immensely from your advice when life was most challenging. *Dr. Gorica Petrovich* - I always knew I wanted to work in a lab. Despite being a second-semester senior, you gave me a chance to work in yours. I’m not sure where I would have ended up without this opportunity, but I am eternally grateful that I didn’t have to find that out. Friday nights were for mounting tissue; the pursuit of a perfect slide was meditative, and these evenings were the glue that held each of my busy weeks together. However, your contribution to my path did not stop there. You recommended me to someone named Mike, which gave rise to a connection that would dramatically shape the third decade of my life. For this, and your continued support through my time

as a graduate student, thank you. *Dr. John Christianson* - Ironically, all this time I wanted to be in *your* lab, the timing just never worked out! Jokes aside, I have always admired you as a scientist, and was thrilled when I finally had the chance to take one of your courses during graduate school. I have always felt the support of your lab from above (literally), and your advice and mentorship from McGuinn Hall. Finally, thank you for thinking of and believing in me as a scientist; I will never forget the recognition I received for my research contributions at the Department level and beyond BC, nor how incredible, valued and supported they made me feel.

To the previously mentioned members of my dissertation committee along with Dr. Benjamin Greenwood, thank you for your interest in my project and your willingness to support this part of my academic journey. Finally, thank you and best of luck to both current, past and future members of the McDannald lab; especially to my excellent undergraduate students, for contributing considerable amounts of time and effort to critical aspects of experiments detailed in this dissertation: Danny, Shannon, & Claire.

TABLE OF CONTENTS

ABSTRACT	iii
ACKNOWLEDGEMENTS	v
LIST OF TABLES	xi
LIST OF FIGURES	xiii
ESSENTIAL ABBREVIATIONS	xv
GLOSSARY OF KEY TERMS	xvii
CHAPTER 1: Introduction to the Ventrolateral Periaqueductal Gray and Defensive Behavior	1
1.1 Adaptive Fear	2
1.2 Periaqueductal Gray	3
1.3 Fear Conditioning	4
1.4 Ventrolateral periaqueductal gray	5
1.5 Conditioned suppression as a measure of fear	6
1.6 Direct electrophysiological support is lacking	9
1.7 Additional weakness in current literature	10
1.8 A Canonical fear circuit	12
1.9 Substantia nigra	13
1.10 Summary	14
CHAPTER 2: Do cue-excited vIPAG single-units signal threat probability or fear output?	15
2.1 Introduction	16
2.2 Methods	17
2.2.1 Subjects	17
2.2.2 Electrode Assembly	18
2.2.3 Surgery	18
2.2.4 Behavior Apparatus	19
2.2.5 Behavioral Procedures	20
2.2.5.1 Pellet Exposure	20
2.2.5.2 Nose Poke Acquisition	20
2.2.5.3 Cue Pre-exposure	20
2.2.5.4 Pavlovian Fear Discrimination	21
2.2.6 Histology	21

2.2.7 Single-unit Data Acquisition.....	22
2.2.8 Statistical Analyses.....	23
2.2.8.1 Calculating Suppression Ratios.....	23
2.2.8.2 Behavior Analysis.....	23
2.2.8.3 K-means Clustering.....	23
2.2.8.4 Identifying Cue-excited vIPAG Neurons.....	24
2.2.8.5 Z-score normalization.....	25
2.2.8.6 Determining Observed and Expected Cue Firing Patterns.....	26
2.2.8.7 Population and Single-unit Firing Analyses.....	26
2.2.8.8 Single-unit Linear Regression.....	26
2.2.8.9 Threat Probability Tuning Curve.....	29
2.3 Results.....	29
2.3.1 vIPAG neurons are responsive at cue onset or ramp over cue.....	32
2.3.2 vIPAG neurons show differential firing that is maximal to danger.....	36
2.3.3 Population biases are evident in vIPAG single-units.....	39
2.3.4 Onset neurons signal threat probability.....	42
2.3.5 Ramping neurons prioritize threat probability over fear output.....	44
2.4 Discussion.....	45

CHAPTER 3: Do cue-inhibited vIPAG single-units signal

threat probability or fear output?	49
3.1 Introduction.....	50
3.2 Methods.....	50
3.2.1 Statistical Analyses.....	51
3.2.2.1 Behavior Analysis.....	51
3.2.2.2 95% bootstrap confidence intervals.....	51
3.2.2.3 Identifying cue-inhibited vIPAG neurons.....	51
3.2.2.4 Z-Score Normalization.....	52
3.2.2.5 Identifying Flip and Sustain Neurons.....	52
3.2.2.6 Waveform Analyses.....	52
3.2.2.7 Population Firing Analyses.....	53
3.2.2.8 Single-unit Linear Regression.....	53
3.2.2.9 Threat probability tuning curve.....	54
3.3 Results.....	55
3.3.1 vIPAG neurons flip to excitation or sustain inhibition over cue.....	56
3.3.2 Flip and sustain populations show differential cue firing.....	60
3.3.3 Population biases are evident in single-units.....	63
3.3.4 Flip neurons switch to threat probability signaling from early to late.....	65

3.3.5 Sustain neurons signal fear output and threat probability throughout.....	66
3.3.6 Differential threat tuning in flip and sustain neurons.....	68
3.4 Discussion.....	70
CHAPTER 4: Is endogenous cSN necessary for fear suppression?	73
4.1 Introduction.....	74
4.2 Methods.....	75
4.2.1 Subjects.....	75
4.2.2 Optogenetic Ferrule and Fiber Optic Cable Assembly.....	76
4.2.3 Surgery.....	77
4.2.4 Behavior Apparatus.....	78
4.2.5 Behavioral procedures.....	79
4.2.5.1 Pellet Exposure.....	79
4.2.5.2 Nose Poke Acquisition.....	79
4.2.5.3 Cue Pre-exposure.....	79
4.2.5.4 Pavlovian Fear Discrimination.....	80
4.2.6 Light Illumination.....	80
4.2.7 Histology.....	82
4.2.8 Statistical Analysis.....	82
4.2.8.1 Behavior Analyses.....	82
4.3 Results.....	84
4.3.1 Baseline nose poking.....	88
4.3.2 Pre-illumination fear discrimination.....	89
4.3.3 Endogenous cSN activity is necessary for fear suppression.....	94
4.3.4 Global inflation of fear is specific to cue presentation.....	97
4.4 Discussion.....	98
Chapter 5: Summary of Results and Discussion.....	100
5.1 Summary of Results.....	103
5.2 Discussion.....	107
5.2.1 The vIPAG as a site of integration.....	107
5.2.2 Rethinking the functional CeA-vIPAG relationship.....	107
5.2.3 Predatory imminence continuum.....	108
5.2.4 Flip and Ramping neurons likely signal threat timing.....	110
5.2.4.1 Investigating threat timing.....	111
5.2.4.2 Threat Timing neurons are likely more than one cell type.....	112
5.2.5 A different type of disinhibition.....	115
5.2.6 A glutamatergic vIPAG Input.....	116
5.2.7 Updating Threat Timing.....	116

5.2.8 Sustain neurons are putatively GABAergic and glutamatergic.....	117
5.2.9 Substantia Nigra and the vIPAG microcircuit.....	118
5.2.10 Onset hub of signal integration.....	118
5.2.11 Conclusions.....	119
References	121

LIST OF TABLES

CHAPTER 2:

Table 2.1 Onset neuron sample regression input.....	28
---	----

CHAPTER 4:

Table 4.1 Complete ANOVA with all factors.....	93
--	----

LIST OF FIGURES

CHAPTER 1:

Figure 1.1 Diagram of caudal periaqueductal gray.....	5
Figure 1.2 Fear discrimination measured by nose poke rate.....	6
Figure 1.3 Midbrain circuit for defensive behavior.....	11

CHAPTER 2:

Figure 2.1 Fear Discrimination, Histology, and vIPAG single-unit activity.....	29
Figure 2.2 vIPAG neurons are responsive to cue onset or ramp over cue presentation.....	33
Figure 2.3 Trial by trial firing for Onset and Ramping neurons.....	35
Figure 2.4 Single-unit biases in Onset and Ramping populations.....	38
Figure 2.5 vIPAG neurons prioritize threat probability over fear output.....	41

CHAPTER 3:

Figure 3.1 Fear discrimination, histology, heat plot and waveform characteristics.. ..	55
Figure 3.2 vIPAG neurons flip to excitation or sustain inhibition over cue presentation.....	58
Figure 3.3 Trial by trial firing for Flip and Sustain neurons.....	59
Figure 3.4 Population biases are evident in single-units.....	62
Figure 3.5 Sustain and Flip populations signal threat probability and fear output.....	64
Figure 3.6 Probability tuning.....	68

CHAPTER 4:

Figure 4.1 Histology and transduction mapping.....	84
Figure 4.2 Pavlovian discrimination and experiment timeline.....	86
Figure 4.3 Baseline nose poking and pre-illumination discrimination.....	88
Figure 4.4 cSN inhibition globally inflates fear.....	91

Figure 4.5 Light illumination and suppression.....96

CHAPTER 5:

Figure 5.1 Functional populations of the vIPAG.....101

Figure 5.2 Firing and regression summary.....102

Figure 5.3 Revising the fear circuit.....106

Figure 5.4 Threat timing pilot.....110

Figure 5.2 Revised vIPAG circuitry.....114

ESSENTIAL ABBREVIATIONS

Adaptive Fear is the ability of a rat to appropriately scale fear behavior to a given threat. In the multi-cue Pavlovian fear discrimination procedures discussed in Chapters 2, 3 and 4, this would reflect highest fear to the danger cue, moderate fear to the uncertainty cue and least fear to the safety cue. Any aberration of this (danger > uncertainty > safety) pattern would reflect maladaptive or inaccurate fear. Maladaptive fear is clinically implicated in fear and anxiety disorders.

CeA refers to the central nucleus of the amygdala: lateral and medial subdivisions. Both components send direct GABAergic projections to the vIPAG (Tovote et al., 2016). Despite previous evidence implicating the lateral component in the acquisition of conditioned fear and the medial component being required for the expression of conditioned fear (Cicchi et al., 2010).

cSN refers to the caudal substantia nigra, between Bregma levels -5.54 and -6.72 mm (Paxinos & Watson, 2007). This is the area of interest optogenetically inhibited in Chapter 4, including both the pars compacta and pars reticulata.

eNpHR refers to the active viral construct AAV-hSyn-eNpHR3.0-EYFP, bilaterally infused into caudal substantia nigra neurons in Chapter 4. Laser illumination of neurons transfected with this virus will result in silencing of endogenous cSN activity.

PAG refers to all subdivisions of the periaqueductal gray: dorsal PAG, dorsolateral PAG, lateral PAG, and ventrolateral PAG. Note: recent evidence suggests the dorsal raphe should be included in the periaqueductal complex as an additional component of the most caudal control centers of not only defensive, but also appetitive responding (Silva & McNaughton, 2019)

SN refers to the entire rostrocaudal and mediolateral extent of the substantia nigra pars compacta and reticulata.

vIPAG except in introductions where literature references of a role for the vIPAG in defensive behavior are provided, refers to the caudal portion of the vIPAG between Bregma levels -7.56 and -8.04mm; the area from which neural activity was recorded in Chapters 2 and 3.

YFP refers to the inactive (control) viral construct AAV-hSyn-EYFP, bilaterally infused into caudal substantia nigra neurons in Chapter 4. Laser illumination of neurons transfected with this virus will result in no silencing of endogenous cSN activity.

GLOSSARY OF KEY TERMS

Differential Firing refers to significant differences in excitatory or inhibitory cued firing, between pairs (danger vs. uncertainty or uncertainty vs. safety). Neural activity may be significantly higher to a danger cue than a safety cue.

Fear Expression is the behavioral manifestation of fear. In Chapters 2, 3 and 4, this behavior is measured using conditioned suppression of nose poking, highly correlated with freezing behavior.

Fear Output is a regressor constructed from nose poke suppression ratio data, used to evaluate the information contained in awake, behaving neural recordings of the vIPAG during multi-cue Pavlovian discrimination in Chapters 2 and 3.

Threat Probability is a regressor constructed from the actual probability of an aversive shock during multi-cue Pavlovian discrimination in Chapters 2 and 3. This regressor is used to evaluate the information contained in awake, behaving neural recordings of the vIPAG, and determine whether vIPAG activity is better captured by threat probability or fear output.

**CHAPTER 1: Introduction to the Ventrolateral Periaqueductal Gray
and Defensive Behavior**

1.1 Adaptive Fear

When confronted with potential harm, an estimate of threat probability must be made, and followed by an appropriate fear response. Fear acquisition and the ability to discriminate between levels of potential threat are critical to executing adaptive, threat-evoked defensive behaviors. Disruptions of neural circuits supporting these functions are maladaptive, and clinically implicated in fear and anxiety disorders (Glitzbach-Schoon et al., 2013; Johansen et al., 2011; Milad et al., 2008). In post-traumatic stress disorder (PTSD), the only major mental disorder with known etiology (Pitman et al., 2012), pathological fear is often comorbid with alcohol use disorder (Neupane et al., 2017). This combination intensifies societal impact and further disrupts neural circuits of fear. In support, evidence from our lab suggests that early life adversity and heavy alcohol drinking have the potential to hijack neural circuits supporting adaptive fear behavior (Wright et al., 2015; DiLeo et al., 2016). Current strongly recommended treatments for PTSD are limited to variations of cognitive behavioral therapy (*Clinical Practice Guideline for the Treatment of Posttraumatic Stress Disorder (PTSD) in Adults*, 2017). Fortunately, interest in examining the neural underpinnings of fear is immense and critical to improving therapeutic interventions for fear and anxiety disorders (Giustino & Maren, 2015; Silva & McNaughton, 2019). This dissertation aims to expand on previous neural investigations by refining our current understanding of a brain region canonically associated with fear, and proposing the incorporation of a novel node into what is most certainly a larger fear circuit.

1.2 Periaqueductal Gray

The periaqueductal gray (PAG) is an expansive, evolutionarily conserved (Silva & McNaughton, 2019), midbrain, gray matter area composed of four longitudinal rostrocaudal neuronal columns that border the central aqueduct: dorsomedial, dorsolateral, lateral and ventrolateral. In rats, far rostral portions of the PAG begin at Bregma -4.20 mm (p1, periaqueductal gray) with initial columnar differentiation at Bregma -5.28 mm, in the same coronal plane as the parvocellular red nucleus (Paxinos & Watson, 2007). Extreme caudal portions of this structure extend as far as Bregma -8.76 mm, in the same coronal plane as the caudal raphe nucleus (Paxinos & Watson, 2007).

In humans, blood oxygenation level-dependent functional MRI responses of the PAG are implicated in a defense mode promoting immobility or freezing-like behavior (Hermans et al., 2013), and structural and biochemical abnormalities of the PAG have been observed in patients with panic disorder (Del-Ben & Graeff, 2009). In animals models, the PAG has long been implicated in defensive behavior (Fanselow, 1994; LeDoux et al., 1988), as well as autonomic regulation in response to threat (Bandler, Carrive, & Zhang, 1991; Carrive, 1993), and more recently, predictive fear learning (Cole & McNally, 2009; Walker et al., 2019). Microinjections of excitatory amino acids that depolarize cell bodies within the PAG elicit an array of defensive behaviors (Bandler et al., 1985), whereas electrical stimulation of discreet PAG subdivisions can specifically induce freezing (D. M. L. Vianna et al., 2001). However, more contemporary neuroscience approaches like optogenetic manipulations (Assareh et al., 2016, 2017; Tovote et al., 2016) have also been used to examine the PAG as the final common output of defensive behavior expression.

Routinely, this connection is investigated by measuring freezing induced by fear conditioning.

1.3 Fear Conditioning

In a standard fear conditioning procedure, a neutral auditory cue is paired with an aversive foot shock. Prior to conditioning, exposure to the foot shock results in freezing: expression of defensive behavior in response to a threat. Freezing is a measurable defensive behavior expressed by rodents in response to threat. Over the course of multiple cue-foot shock pairings, the previously neutral auditory cue becomes associated with the aversive outcome; fear conditioned animals will freeze to cue exposure in the absence of foot shock. Variations of procedures like the one just described are incredibly useful for examining how fear behavior is acquired and expressed. Combined with neuroscience techniques, fear conditioning is an ideal tool for investigating roles for particular brain regions and their subdivisions, in fear processes.

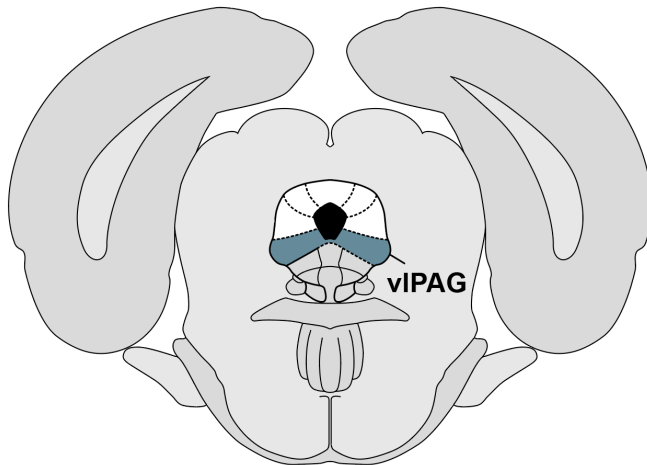


Figure 1.1 Diagram of caudal periaqueductal gray

Bregma -7.68mm with caudal ventrolateral periaqueductal gray indicated in teal. Additional subdivisions of the PAG are indicated in white, with dotted black line boundaries. Adapted from Paxinos & Watson, 2007.

1.4 Ventrolateral periaqueductal gray

A role for the PAG in fear expression is primarily associated with activity in the caudal portion of the ventrolateral column depicted in Figure 1.1 (Carrive et al., 1997). In support, robust increases in c-fos, a marker for neuronal activity, were observed in the caudal ventrolateral periaqueductal gray (vIPAG) following post-conditioning re-exposure to conditioning chambers. In contrast, nearby lateral PAG c-fos expression was sparse and limited to its border with the vIPAG. Despite similar projections between the central amygdala (CeA) and both subdivisions of the PAG, the vIPAG is better suited to support behavioral expression of fear via this functional and anatomical connection (Beitz, 1982; Paredes et al., 2000). However, it is important to acknowledge the limitations of this particular design. Functional activity could be represented by immediate early genes other than c-fos. Additionally, controls were not in place to detect a potential inhibitory link (decreased c-fos) between vIPAG activity and fear expression. Nevertheless, a role for the vIPAG in freezing has been further corroborated by evidence of decreases in freezing

associated with vIPAG electrolytic lesions (Farook et al., 2004), transient increases in freezing associated with discrete vIPAG electrical stimulation (D. M. L. Vianna et al., 2001), and freezing induced by intra-vIPAG optogenetic excitation (Assareh et al., 2016).

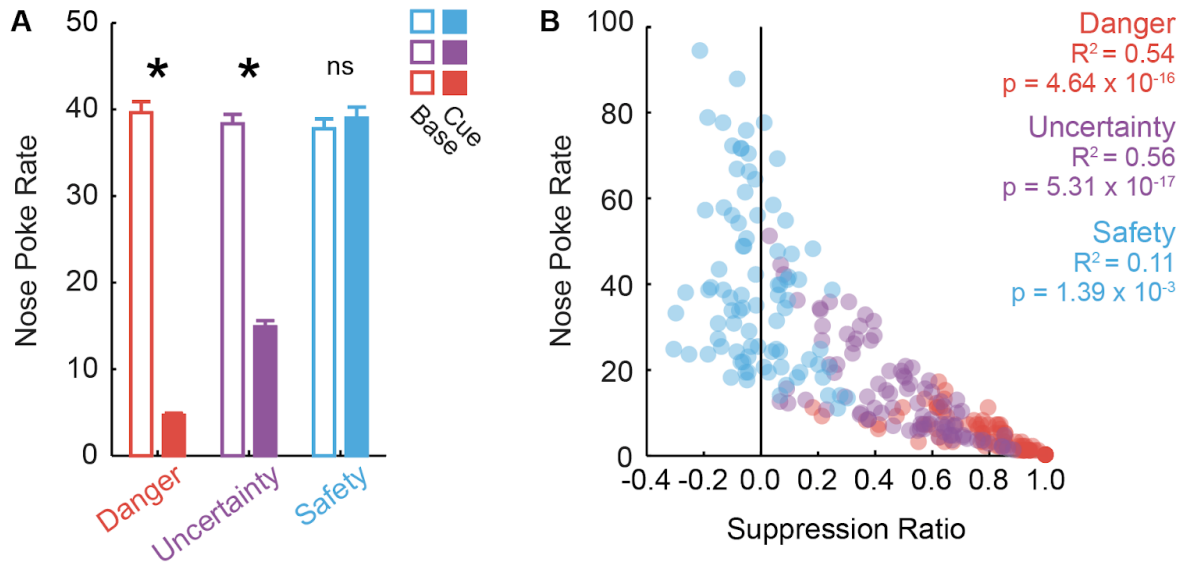


Figure 1.2 Fear discrimination measured by nose poke rate

(A) Mean + SEM nose poke during baseline (open bars) and cue (filled bars) plotted for each trial type, for all 88 recording sessions. Asterisks indicate a significant difference between baseline and cue (paired samples t-test, $p < 0.05$). Baseline nose poke rates did not differ between trial types and rats showed significant reductions in poking to danger and uncertainty, but not safety. (B) Relationship between suppression ratio and nose poke rate for each cue (3) and session (88) is shown. The two measures were significantly correlated, particularly for danger and uncertainty. Data derived from experiments detailed in Chapters 2 and 3.

1.5 Conditioned suppression as a measure of fear

Although most demonstrations of the link between vIPAG activity and fear expression depend on freezing as a measure of fear, further work using conditioned suppression has

provided additional support for the caudal vIPAG in this function (Arico et al., 2017). Conditioned suppression is an established measure of fear (Estes & Skinner, 1941; Rescorla, 1968; Wright et al., 2015; DiLeo et al., 2016; R. A. Walker et al., 2018), highly correlated with freezing behavior (Bouton & Bolles, 1980). In this preparation, rats are trained to nose poke or lever press for a food reward in a fear conditioning chamber. Nose poking is a consistent, rapid and measurable behavior motivated by mild food restriction. Baseline levels of nose poking are established prior to conditioning and rewarded on a schedule completely independent of any cues or shocks. As in fear conditioning, defensive behavior to cues is acquired over the course repeatedly pairing a cue with an aversive outcome. Critically, in response to threat (an auditory cue associated with shock), appetitive responding is suppressed while defensive behavior is engaged to address the threat (i.e., freezing, a motor program incompatible with nose poking). Once the threat resolves, rats rapidly resume appetitive responding. Thus, nose poke suppression is tightly and temporally linked to defensive behavior expression, providing a reliable indirect measure of fear expression. However, the utility of this design extends beyond this simple example; conditioned suppression is sensitive to different levels of uncertain or certain threat.

Nose poke suppression can be graded (low, medium, or high) depending on the level of threat associated with an auditory cue (Figure 1.2 A). In this procedure, rats are conditioned to discriminate between three auditory cues: foot shock is always associated with the danger cue (probability = 1.00), never associated with the safety cue ($p = 0.00$) and unpredictably associated with the uncertainty cue on 37.5% of trials ($p = 0.375$). A

similar discriminative pattern can be achieved when the probability of shock associated with the uncertainty cue is 25% or $p = 0.25$ (Wright et al., 2015; DiLeo et al., 2016; Ray et al., 2020; Strickland et al., 2021). Following conditioning, significant reductions in nose poke rate to aversive danger and uncertainty cues are observed (Figure 1.2 A, solid red and purple bars). By contrast, decreases in nose poking are not observed to the safety cue, which does not mount a defensive response that competes with appetitive responding. Nose poke suppression is typically reported in the form of a suppression ratio, where a value of 1.00 indicates complete suppression (high fear), a value of 0.00 indicates no suppression (no fear), and intermediate levels of fear correspond to values in between these extremes. Suppression ratios are constructed from nose poke rates during each cue relative to baseline nose poking outside of cue presentation, and should reflect a pattern similar to Figure 1.2 A. In support, nose poke rates are positively correlated with suppression ratios $[(\text{baseline nose poke rate} - \text{cue nose poke rate}) / (\text{baseline nose poke rate} + \text{cue nose poke rate})]$, which standardize measures of suppression across animals (Figure 1.2 B).

Unlike freezing, conditioned suppression can be used to measure fear expression on sub-second timescales (DiLeo et al., 2016). Not confounded by freezing, conditioned suppression can remain intact even when freezing is disrupted (Amorapanth et al., 1999). Combined with in vivo electrophysiological recording, this multi-cue procedure allows for assessment of neural activity highly correlated with - but not dependent on - freezing behavior, and provides a framework for investigating whether neural activity in response to threat corresponds to fear expression (suppression ratio) or threat probability ($p = 0.00, 0.25, 0.375$ or 1.00).

1.6 Direct electrophysiological support is lacking

Electrophysiology is a temporally precise tool ideal for examining vIPAG activity in the context of fear expression. Yet, there is limited direct electrophysiological support for the canonical vIPAG and fear expression association (Bear et al., 2016; Carlson & Birkett, 2017). Despite the abundance of evidence linking the vIPAG with fear expression, freezing only partially accounts for previously reported vIPAG activity (Carrive et al., 1997; Vianna et al., 2001; Farook et al., 2004; Assareh et al., 2016; Arico et al., 2017). In theory, a complete neural correlate for fear output could be excitatory or inhibitory, but should begin when a threat is encountered and continue until the threat is resolved. In the laboratory, relationships between vIPAG single-unit activity and freezing have been observed in only a minority of neurons (Tovote et al., 2016), weakly at danger cue onset (Watson et al., 2016), or mixed with activity that purely reflects a danger cue (Ozawa et al., 2017). Further, most of this work has been restricted to recording activity during fear extinction, severely limiting the amount of trials during which simultaneous observations of robust fear and associated neural activity can occur.

Due to technical challenges associated with recording during foot shock, previous electrophysiology studies have relied heavily on recording PAG activity during extinction sessions, instead of directly monitoring activity during ongoing fear conditioning or discrimination (Tovote et al., 2016; Watson et al., 2016; Ozawa et al., 2017). Although this is valuable for examining aberrant extinction which may underlie excessive fear in PTSD (Scott L. Rauch et al., 2006), it fails to capture neural responses to active, ongoing threats. Further, disruptions in fear acquisition, conditioning or discrimination, could all result in similar excessive fear expression (Pitman, 1988). Although the threat estimates

critical to these processes are thought to be generated at the level of the amygdala (Fanselow & LeDoux, 1999; Duvarci & Pare, 2014), it is possible that this computational association is maintained further downstream in the vIPAG. In support, chemogenetic activation of the vIPAG has been associated with impaired fear acquisition (Arico et al., 2017), and preliminary work from our lab demonstrates that rats with pre-conditioning vIPAG dopamine depletions fail to discriminate between danger, uncertainty and safety (Wright et al., 2019).

1.7 Additional weakness in current literature

Technical limitations aside, previous studies utilized procedures in which only a single cue predicted foot shock with certainty (Ozawa et al., 2017; Tovote et al., 2016; Watson et al., 2016), precluding the ability to observe neural activity reflecting a range of threat probabilities and the uncertainty common to realistic threat encounters. The ideal experiment to address previous limitations would capitalize on the temporal precision of in vivo single-unit recording and conditioned suppression, while evaluating vIPAG neural activity during a range of ongoing certain and uncertain threats ($p = 0.00 < 0.375 < 1.00$). Presumably, a design capable of examining relative, graded levels of within-subjects fear could capture whether vIPAG neurons signal amygdala-like threat estimates alongside fear expression, which might be able to explain some of the heterogeneity attributed to previous electrophysiology findings. But, how would a neural correlate for fear expression be distinguished from one for threat probability?

In the conditioned suppression procedure briefly outlined in section 1.5, rats consistently demonstrate adaptive fear via robust discrimination; suppression to danger is high,

uncertainty is moderate, and safety is low. However, suppression non-linearly scales to shock probability; uncertainty produces more suppression than expected given its associated shock probability (Walker et al., 2018; Ray et al., 2018; DiLeo et al., 2016; Wright et al., 2015; Berg et al., 2014). The non-linear relationship between behavior and shock probability is critical to determining if single-unit activity within the vIPAG is better captured by fear output or threat probability. Paired with in vivo optogenetics, this type of multi-cue discrimination is also an ideal tool to investigate brain regions, not typically associated with fear, that may be necessary for fear expression.

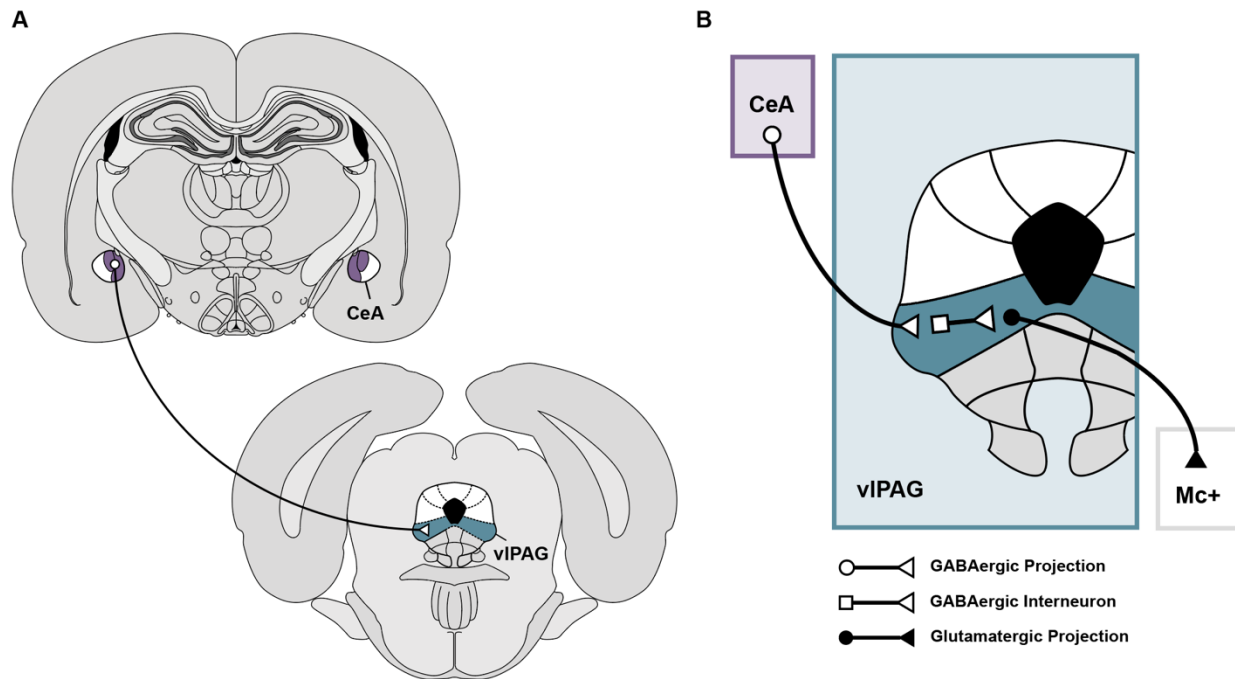


Figure 1.3 Midbrain circuit for defensive behavior

(A) Bregma -2.76mm with lateral and medial central amygdala (CeA) subdivisions in purple (top left), and Bregma -7.68mm with caudal vIPAG indicated in teal (bottom right). Dotted black line boundaries border additional subdivisions of the vIPAG. Additional subdivisions of the CeA and PAG are indicated in white, and not the focus of this

dissertation. (B) Disinhibitory CeA-vIPAG pathway implicated in defensive behavior (Tovote et al., 2016). Diagrams adapted from Paxinos & Watson, 2007.

1.8 A Canonical fear circuit

Despite receiving limited direct sensory input, the PAG is a downstream target of many regions which integrate aspects of threat (Gorka et al., 2018) including the central nucleus of the amygdala (CeA) and the bed nucleus stria terminalis (Shi & Davis, 1999). The PAG also receives afferents from the medial prefrontal cortex, thalamus, hypothalamus, insular cortex, and subthalamic nucleus (Paredes et al., 2000), and projects to regions in the brainstem and spinal cord, which allow it to interact further with sensory and motor information (Keay & Bandler, 2004). As a major point of convergence, the PAG is anatomically well-positioned to coordinate defensive behavior by integrating threat-relevant information from cortical and subcortical brain regions, with sensory information from lower spinal processes.

In the canonical fear circuit, threat probability estimates (the stored associative strength of cue and foot shock) originate in amygdalar nuclei (Davis, 2006; Duvarci & Pare, 2014; Fanselow & LeDoux, 1999; Maren et al., 2013). Amygdalar threat estimates are then sent to the vIPAG, which organizes the behavioral components of fear output, most notably freezing (Figure 1.3 A) (Perusini & Fanselow, 2015; Tovote et al., 2015; Dejean et al., 2015; Koutsikou et al., 2014; Walker et al., 1997). A current disinhibition model further posits that CeA output neurons inhibit local GABAergic neurons in the vIPAG, releasing inhibition of glutamatergic output neurons and initiating fear expression (Figure 1.3 B) (Oka et al., 2008; Tovote et al., 2016). However, this is only one part of what is most certainly a larger circuit for modulating fear behavior.

1.9 Substantia nigra

The ventrolateral periaqueductal gray (vlPAG) has long been implicated in defensive behavior (Arico et al., 2017; Assareh et al., 2017; Bandler et al., 1985; Carrive et al., 1997; Fanselow, 1993; Kim et al., 1993; Liebman et al., 1970; D. M. L. Vianna et al., 2001). By contrast, a role for the substantia nigra (SN) in fear, stands apart from its canonical associations with movement and reward processes (Schultz, 1997; Groenewegen, 2003; Chinta & Andersen, 2005; Bouchet et al., 2018; Sonne et al., 2020). Recently, activation of nigrostriatal dopamine with designer receptors exclusively activated by designer drugs (DREADDs) was associated with improved extinction in fear-conditioned rats (Bouchet et al., 2018). However, activation of this region is insufficient to establish whether SN activity is necessary for fear suppression, and therefore extinction. Further, cell types other than dopamine may contribute to a role for the SN in fear, given the direct monosynaptic GABAergic projection from the SN to the vlPAG (Kirouac et al., 2004). In an effort to expand the canonical fear circuit, I set out to determine if the caudal substantia nigra (cSN) is necessary for fear suppression using optogenetics.

Whereas activation of a brain region examines whether the region has the capacity to drive a particular behavior, inhibition experiments are required to determine if endogenous activity in that region is required for the behavior to occur. Although chemogenetic techniques like DREADDs are valuable for pursuing each of these ends, optogenetic manipulations are required for discrete temporal control over activation or inhibition. For inhibition, a recombinant adeno-associated virus with enhanced halorhodopsin (eNpHR) is infused into the area of interest. Under the human synapsin promoter, all neuron types in the area of interest are transduced with light-gated inward chloride pumps isolated from halobacteria, rendering them silenced in response to light

illumination. Using this approach, neural activity of the cSN can be silenced during active ongoing threats in a multi-cue discrimination procedure. An ideal design to determine not only whether cSN activity relevant is required for fear suppression, but also whether there is a meaningful place for the cSN in a larger fear circuit.

1.10 Summary

In order to refine and expand the canonical fear expression circuit, this dissertation will test whether vIPAG activity may be better captured by threat probability, and to determine if cSN activity is necessary for fear suppression. Both of these goals will require the multi-cue Pavlovian discrimination procedure outlined Section 1.5, which measures fear using conditioned suppression. However, Chapters 2 and 3 of this dissertation will evaluate vIPAG neural activity during ongoing discrimination using awake, behaving single-unit recording, whereas Chapter 4 will combine multi-cue discrimination with awake, behaving optogenetic inhibition of the cSN.

**CHAPTER 2: Do cue-excited vIPAG single-units signal
threat probability or fear output?**

Portions of this chapter have been published in the following research article:

Wright, K.M. & McDannald, M.A., (2019). Ventrolateral periaqueductal gray neurons prioritize threat probability over fear output. *eLife*, 8: e45013. *Dataset available at <http://crcns.org/data-sets/brainstem/pag-1/about-pag-1>*

2.1 Introduction

A series of studies have uncovered a vIPAG population showing short-latency increases in firing to a certain danger cue. This characteristic would be expected of neurons organizing fear output. Yet, robust relationships between vIPAG single-unit activity and freezing have yet to be revealed. If not freezing, then what aspect of fear do vIPAG neurons signal? Here I challenge the canonical view of the vIPAG and its intimate link to fear expression, and test the hypothesis that vIPAG neurons instead signal threat probability.

To accomplish this, I recorded vIPAG neural activity during ongoing, three-cue, Pavlovian discrimination with certain and uncertain shocks outlined in Chapter 1: danger ($p = 1.00$), uncertainty ($p = 0.375$) & safety ($p = 0.00$). I measured fear using conditioned suppression of rewarded nose poking during the entirety of each cue presentation. While suppression is strong to danger, intermediate to uncertainty and weak to safety, the uncertainty cue produces more suppression than would be expected given its shock probability (Berg et al., 2014; Wright et al., 2015; DiLeo et al., 2016; R. A. Walker et al., 2018; M. H. Ray et al., 2018). The vIPAG could signal fear expression via conditioned suppression of reward seeking (Arico et al., 2017): a long-established measure of fear (Estes and Skinner, 1941) highly correlated with freezing behavior (Bouton and Bolles, 1980). However, the nonlinearity of this procedure allows us to determine whether vIPAG single-unit activity is better captured by threat probability.

Previous studies identified a population of vIPAG neurons showing short-latency firing increases to auditory cues paired with foot shock (Ozawa et al., 2017; Tovote et al., 2016; Watson et al., 2016). Thus, this chapter will focus on scrutinizing an expected population

of cue-excited single-units in the vIPAG. A complete neural correlate for fear expression should be supported by cue-excited neurons that increase firing at the beginning of a threat (cue onset) and maintain firing throughout the duration of a threat encounter (cue duration). Further, firing of these neurons will directly reflect trial-by-trial behavior. By contrast, cue-excited neurons encoding threat probability will linearly increase firing according to threat probability (shock probability), irrespective of behavior.

2.2 Methods

2.2.1 Subjects

Ten adult male rats at postnatal day 55 (P55) were obtained from Charles River Laboratories in Raleigh, NC. On arrival, rats were single-housed on a 12 hr light cycle (lights off at 6:00pm) and allowed three acclimation days with *ad libitum* access to water and standard chow (18% Protein Rodent Diet #2018, Harlan Teklad Global Diets, Madison, WI) prior to surgery. Rats were implanted with drivable, sixteen-wire microelectrode bundles. Each animal received between eleven and sixteen days to recover from surgery with *ad libitum* access to water and standard chow. Throughout the experiment, rats had *ad libitum* access to water; however, to generate motivation for a food-reward, standard chow was restricted to maintain rats at 85% of their free-feeding body weight. Three rats were eliminated from the study because electrodes failed to register single-unit activity and one rat was eliminated due to incorrect electrode placement. Reported data are from the remaining six individuals. All protocols were approved by the Boston College Animal Care and Use Committee and all experiments were carried out in accordance with the NIH guidelines regarding the care and use of rats for experimental procedures.

2.2.2 Electrode Assembly

Microelectrodes were constructed on site and consisted of a drivable bundle of sixteen Formvar-Insulated Nichrome wires (25.4 μm diameter: 761500, A-M Systems, Carlsborg, WA) within a 27-gauge cannula (B000FN3M7K, Amazon Supply). The cannula bundle was attached to a manually operated microdrive calibrated to permit ~ 0.042 mm advancement increments. Two free-hanging 127 μm diameter PFA-coated stainless-steel ground wires were also part of the assembly (791400, A-M Systems, Carlsborg, WA). All wires were electrically connected to a Nano Strip omnetics connector (A79042-001, Omnetics Connector Corp., Minneapolis, MN) on a custom 24-contact, individually-routed and gold-immersed circuit board (San Francisco Circuits, San Mateo, CA).

2.2.3 Surgery

Aseptic stereotaxic surgery was performed under isoflurane anesthesia (1 to 5% in oxygen). Prior to incision, Rimadyl/Carprofen (024751, Henry Schein Animal Health, s.c. 5 mg/kg) and Ringer's lactate solution (014792, Henry Schein Animal Health, s.c. 2 to 5 mL) were administered subcutaneously to the back, and 2% lidocaine (002468, Henry Schein Animal Health, s.c. 0.25 mL) was administered subcutaneously above the skull. Post-incision, the skull was scoured in a crosshatch pattern with a scalpel blade to strengthen implant adhesion. Five screws (two anterior to Bregma, two between Bregma and lambda: 3 mm medial to the lateral ridges of the skull, and one on the midline: 5 mm posterior of lambda) were installed in the skull to further stabilize the bond between the skull, electrode assembly and protective head cap. A 1.4 mm diameter burr hole was drilled through the skull, centered on the implant site and the underlying dura was removed to expose the cortex. Nichrome recording wires were freshly cut with surgical

scissors to extend approximately 2.0 mm beyond the cannula at a 15° angle. Just before implant, current was delivered to each recording wire in a saline bath, stripping each tip of its formvar insulation. Each omnetics connector contact was stimulated for 2 s using a resistor-equipped lead; current was supplied by a 12 V lantern battery. Machine grease was placed by the cannula and on the microdrive to prevent orthodontic resin from seizing moveable components.

The electrode assembly was slowly advanced at a 20° angle for implantation dorsal to the vIPAG. Coordinates from cortex: anterior-posterior (AP) -8.00 mm, medial-lateral (ML) -2.45 mm, and dorsal-ventral (DV) -5.52 mm. Once in place, stripped ends of both ground wires were wrapped around the posterior midline screw inserted previously. The microdrive base and a protective head cap surrounding the electrode assembly were cemented in place on the skull with orthodontic resin (C 22-05-98, Pearson Dental Supply, Sylmar, CA) at the end of the procedure, and the omnetics connector was affixed to the head cap.

2.2.4 Behavior Apparatus

The apparatus for Pavlovian fear conditioning consisted of two individual behavior chambers with clear acrylic walls and top, and a grid floor with an acrylic waste pan below. Each grid floor bar was electrically connected to an aversive shock generator (Med Associates, St. Albans, VT) through a custom grounding device. This permitted the floor to be grounded at all times except during shock delivery. A nose poke opening equipped with infrared photocells was mounted on a central, acrylic wall panel and an acrylic external food cup was mounted on the same wall panel 3 inches below. Each behavior chamber was enclosed in a separate sound-attenuating shell. Auditory stimuli were

presented through two speakers mounted on the ceiling of the shell, above the behavior chamber.

2.2.5 Behavioral Procedures

2.2.5.1 Pellet Exposure

Each rat was exposed to 5 grams of reward pellets in their home cage on P56 & P57. On P58, all rats received 30 test pellets released (one per minute) in the behavior chamber food cup (F0021, Bio-Serv, Flemington, NJ).

2.2.5.2 Nose Poke Acquisition

On P59, all rats were shaped to nose poke for pellet delivery in the behavior chamber using a fixed ratio (FR1) schedule in which one nose poke yielded one pellet. Shaping sessions lasted 30 min or until approximately 50 nose pokes were completed. On P60, all rats received one variable interval (VI30) session in which nose pokes were reinforced on average every 30 s. On P61-P64 (inclusive) all rats received four variable interval (VI60) sessions in which nose pokes were reinforced on average every 60 s. For the remainder of behavioral testing, nose pokes were reinforced on a VI60 schedule independent of all Pavlovian contingencies.

2.2.5.3 Cue Pre-exposure

On P65 and P66, all rats received one 42 min session of pre-exposure to the three cues to be used in Pavlovian discrimination. Pre-exposure consisted of four presentations of each cue (12 total presentations) with mean inter-trial intervals (ITIs) of 3.5 min. The order of trial type presentation was randomly determined by the behavioral program and differed for each rat during each session. Auditory cues were 10 s in duration and

consisted of repeating motifs of a broadband click, phaser, or trumpet (listen or download: <http://mcdannaldlab.org/resources/ardbark>).

2.2.5.4 Pavlovian Fear Discrimination

Prior to single-unit recording sessions, each rat received eight, 93 min sessions (one per day) of fear discrimination, consisting of 32 cue trials with mean ITIs of 3.5 min. Each 10 s auditory cue was associated with a unique probability of foot shock (0.5 mA, 0.5 s): danger, $p = 1.00$; uncertainty, $p = 0.375$; and safety, $p = 0.00$. Cue identity was counterbalanced across rats. Foot shock was administered 2 s following the termination of the auditory cue on danger and uncertainty shock trials. This was done in order to observe possible neural activity during the delay period not driven by an explicit cue. A single session consisted of six danger trials, ten uncertainty no-shock trials, six uncertainty shock trials, and ten safety trials. The order of trial type presentation was randomly determined by the behavioral program, and differed for each rat during each session. After the eighth discrimination session, rats were given *ad libitum* access to standard rat chow for at least 24 hours, followed by stereotaxic surgery. Following recovery, discrimination (identical to that described above) resumed with single-unit recording. Animals received discrimination every other day with recording. After each discrimination session with recording, electrodes were advanced either 0.042 mm or 0.084 mm to record from new units during the following session.

2.2.6 Histology

Rats were deeply anesthetized using isoflurane and final electrode coordinates were marked by passing current from a 6 V battery through 4 of the 16 nichrome electrode wires. Rats were perfused with 0.9% biological saline and 4% paraformaldehyde in a 0.2

M Potassium Phosphate Buffered Solution. Brains were extracted and post-fixed in a 10% neutral-buffered formalin solution for 24 hr, stored in 10% sucrose/formalin and sectioned via microtome. All brains were processed for light microscopy using anti-tryptophan hydroxylase immunohistochemistry (T8575, Sigma-Aldrich, St. Louis, MO) and a NovaRed chromogen reaction (SK-4800, Vector Laboratories, Burlingame, CA). Sections were mounted, imaged using a light microscope and electrode placement was confirmed (Paxinos & Watson, 2007).

2.2.7 Single-unit Data Acquisition

Sixteen individual recording wires were bundled and soldered to individual channels of an Omnetics connector. The bundle was integrated into a microdrive permitting advancement in ~0.042 mm increments. The microdrive was cemented on top of the skull and the Omnetics connector was affixed to the head cap. During recording sessions, a 1x amplifying head stage connected the Omnetics connector to the commutator via a shielded recording cable (head stage: 40684–020 and Cable: 91809–017, Plexon Inc, Dallas TX). Analog neural activity was digitized and high-pass filtered via amplifier to remove low-frequency artifacts and sent to the Omniplex D acquisition system (Plexon Inc, Dallas TX). Behavioral events (cues, shocks, nose pokes) were controlled and recorded by a computer running Med Associates software. Timestamped events from Med Associates were sent to Omniplex D acquisition system via a dedicated interface module (DIG-716B). The result was a single file (.pl2) containing all time stamps for recording and behavior. Single-units were sorted offline with a template-based spike-sorting algorithm (Offline Sorter V3, Plexon Inc, Dallas TX). Time stamped spikes and events (cues, shocks, nose pokes) were extracted and analyzed with statistical routines

in MATLAB (Natick, MA). Neural activity was recorded throughout the 500 ms shock delivery period. However, we cannot be certain that shock artifacts did not disrupt spike collection, so we do not present activity from this period.

2.2.8 Statistical Analyses

2.2.8.1 Calculating Suppression Ratios

Fear was measured by suppression of rewarded nose poking, calculated as a ratio: $(\text{baseline poke rate} - \text{cue poke rate}) / (\text{baseline poke rate} + \text{cue poke rate})$ (Rescorla, 1968; Pickens et al., 2009; Anglada-Figueroa & Quirk, 2005; Arico & McNally, 2014; Lee et al., 2005; McDannald & Galarce, 2011). A ratio of '1' indicated high fear, '0' low fear, and gradations between intermediate levels of fear. Use of the suppression ratio permitted the objective measure of relative fear in 1 s intervals across the cue, as well as total fear over the entire 10 s cue presentation (Wright et al., 2015).

2.2.8.2 Behavior Analysis

Behavior was analyzed using analysis of variance (ANOVA) with trial type as a factor. ANOVA for behavior contained three trial types (danger, uncertainty and safety). Uncertainty trial types (shock and no-shock) were collapsed because they did not differ for suppression ratio. During cue presentation, rats did not know the current uncertainty trial type. Paired samples t-tests were performed on suppression ratios for each cue pair.

2.2.8.3 K-means Clustering

The following characteristics were determined for each neuron: baseline firing rate, half the duration of the mean waveform and amplitude ratio of the mean waveform. Duration was determined by measuring the time (ms) from peak depolarization to the trough of

after-hyperpolarization and dividing by two. Amplitude ratio was calculated using $(n - p) / (n + p)$, in which p = initial hyperpolarization (in mV) and n = maximal depolarization (in mV). This approach has been used to successfully separate neuron types in the ventral tegmental area (Roesch et al., 2007). K-means clustering used these three firing characteristics to partition the 245 recorded neurons into two clusters ($k = 2$). Two clusters were chosen because previous studies have found that two neuron types, glutamatergic vGluT2 neurons and GABAergic GAD1+ neurons, comprise the majority of vIPAG neurons, and these neurons can be differentiated by baseline firing rate (Tovote et al., 2016). ANOVA for cluster results found that only baseline firing rate contributed to cluster membership ($F_{1,243} = 829, p < 0.001$). Neither amplitude ratio nor duration reached significance ($F_s < 0.2, p_s > 0.6$). All neurons were clustered, with the majority falling in the low firing rate cluster ($n = 199$) and the remaining in the high firing rate cluster ($n = 46$).

2.2.8.4 Identifying Cue-excited vIPAG Neurons

Independent of cluster analysis, all 245 neurons were screened for short-latency, excitatory firing to auditory cue onset. This was achieved using a paired, two-tailed t-test comparing raw firing rate (spikes/s) during a 2 s baseline period just prior to cue onset and during the first, 1 s cue interval. A t-test was performed for each of the three cues (danger, uncertainty and safety), and corrected for multiple comparisons ($p < 0.017$). The remaining neurons were screened for longer-latency, excitatory firing to the later portion of auditory cues using an identical t-test. Only now, firing rate during a 2 s baseline period just prior to cue onset was compared to firing rate during the last, 1 s cue interval.

2.2.8.5 Z-score normalization

For each neuron, and for each trial type, firing rate (spikes/s) was calculated in 100 ms bins from 10 s prior to cue onset to 12 s following cue offset, for a total of 320 bins. Mean firing rate over the 320 bins was calculated by averaging all trials for each trial type. Mean differential firing was calculated for each of the 320 bins by subtracting mean baseline firing rate (2 s prior to cue onset), specific to that trial type, from each bin. Mean differential firing was Z-score normalized across all trial types within a single neuron, such that mean firing = 0, and standard deviation in firing = 1. Z-score normalization was applied to firing across the entirety of the recording epoch, as opposed to only the baseline period, in case neurons showed little/no baseline activity. As a result, periods of phasic, excitatory firing contributed to normalized mean firing rate (0). For this reason, Z-score normalized baseline activity is below zero in Figure 2.2 A & C. Z-score normalized firing during cue (Figure 2.2 A & C) was analyzed with ANOVA using bin and trial-type as factors. F and p values are reported, as well as partial eta squared and observed power.

For post hoc cue firing analyses (Figure 2.2 B & D), and cue regression analyses, it was necessary to calculate normalized firing in 1 s intervals. To do this, differential firing in the interval of interest (for example, first cue 1 s interval) was calculated for each individual of the 32 trials in a single session. Differential firing in this interval was then Z-score transformed. This process was repeated for each interval of interest in order to maximize the distribution of firing within a single interval. Importantly, statistical outcomes were identical if a single Z-score transformation was applied to all intervals at once.

2.2.8.6 Determining Observed and Expected Cue Firing Patterns

The analysis for Onset neurons ($n = 29$) utilized mean normalized firing to each cue (danger, uncertainty and safety) in the first 1 s interval and analysis for Ramping neurons ($n = 14$) utilized firing in the last 1 s interval. Relative firing to the three cues was used to categorize each Onset and Ramping neuron: ($d > u > s$), ($d > s > u$), ($s > u > d$) or ($u > d > s$). Counting the number observed in each category determined the actual number for each population.

2.2.8.7 Population and Single-unit Firing Analyses

Population firing was analyzed using analysis of variance (ANOVA) with trial type and bin (100 ms) as factors. ANOVA for cue firing contained three trial types (danger, uncertainty and safety). Uncertainty trial types were collapsed because they did not differ for either suppression ratio or firing analysis. This was expected, because rats did not know the current uncertainty trial type during cue presentation. F statistic, p value, observed power and partial eta squared are reported for effects and interactions. Interval firing was compared within a population using a two-tailed, dependent samples t-test.

2.2.8.8 Single-unit Linear Regression

Single-unit, linear regression was used to determine the degree to which fear output and/or threat probability explained trial-by-trial variation in firing of single neurons in a specific time interval. The cue analysis used 1 s intervals. For each regression, all 32 trials from a single session were ordered by type. Z-firing was specified for the interval of interest. The fear output regressor was the suppression ratio for the entire 10 s cue, for that specific trial. The probability regressor was the foot shock probability associated with each specific cue (danger, $p = 1.00$; uncertainty, $p = 0.375$; and safety, $p = 0.00$).

Regression (using the regress function in Matlab) required a separate, constant input. To better visualize the organization of the regression input, the complete regression input for first interval firing of an Onset neuron is shown below.

The regression output of greatest interest was the beta coefficient for each regressor (fear output and probability), quantifying the strength (greater distance from zero = stronger) and direction (>0 = positive) of the predictive relationship between each regressor and single-unit firing.

Onset Neuron: Sample Regression Input for Interval One (first 1 s of cue presentation)					
Trial #	Trial Type	Normalized Firing Rate (Z)	Constant	Independent Regressors	
				Probability	Fear Output
1	danger	2.32	1	1	1.00
2	danger	0.51	1	1	1.00
3	danger	0.81	1	1	1.00
4	danger	1.56	1	1	1.00
5	danger	1.41	1	1	0.73
6	danger	2.92	1	1	1.00
7	uncertainty: shock	0.81	1	0.375	1.00
8	uncertainty: shock	-0.40	1	0.375	0.47
9	uncertainty: shock	0.21	1	0.375	0.64
10	uncertainty: shock	-0.70	1	0.375	0.67
11	uncertainty: shock	-0.85	1	0.375	1.00
12	uncertainty: shock	-0.70	1	0.375	0.64
13	uncertainty: no-shock	-0.70	1	0.375	1.00
14	uncertainty: no-shock	-0.70	1	0.375	0.40
15	uncertainty: no-shock	-0.70	1	0.375	0.23
16	uncertainty: no-shock	0.66	1	0.375	1.00
17	uncertainty: no-shock	0.21	1	0.375	1.00
18	uncertainty: no-shock	-0.70	1	0.375	0.71
19	uncertainty: no-shock	-1.00	1	0.375	0.43
20	uncertainty: no-shock	1.11	1	0.375	1.00
21	uncertainty: no-shock	-0.09	1	0.375	0.56
22	uncertainty: no-shock	-0.85	1	0.375	1.00
23	safety	-0.70	1	0	0.06
24	safety	-0.70	1	0	0.27
25	safety	-0.70	1	0	-0.04
26	safety	-0.40	1	0	0.14
27	safety	-0.70	1	0	0.54
28	safety	-0.70	1	0	0.03
29	safety	0.21	1	0	0.47
30	safety	-0.85	1	0	1.00
31	safety	0.06	1	0	0.20
32	safety	-0.70	1	0	-0.14

Beta Coefficient:

-0.14	2.19
-------	------

Table 2.1 Onset neuron sample regression input

A sample of the regression input for an Onset neuron during the first interval (first second) of cue presentation. Trial types are colored as follows: danger (red), uncertainty shock and no-shock (purple), and safety (blue). Regressors are colored as well: threat probability (pink) and fear output (gray). Beta coefficients (regression output) for each regressor are separate (bottom right).

2.2.8.9 Threat Probability Tuning Curve

Single-unit, linear regression was performed using the fear output and probability regressors as above. Only now, nine separate regression analyses were performed in which the uncertainty component of the probability regressor was systematically varied from 0 to 1 in 0.125 increments (0.000, 0.125, 0.250, 0.375, 0.500, 0.625, 0.750, 0.875 and 1.000). The result of primary interest was the mean beta coefficient for the probability regressor from each variant of regression, as plotted in Figure 2.6 D & H.

2.3 Results

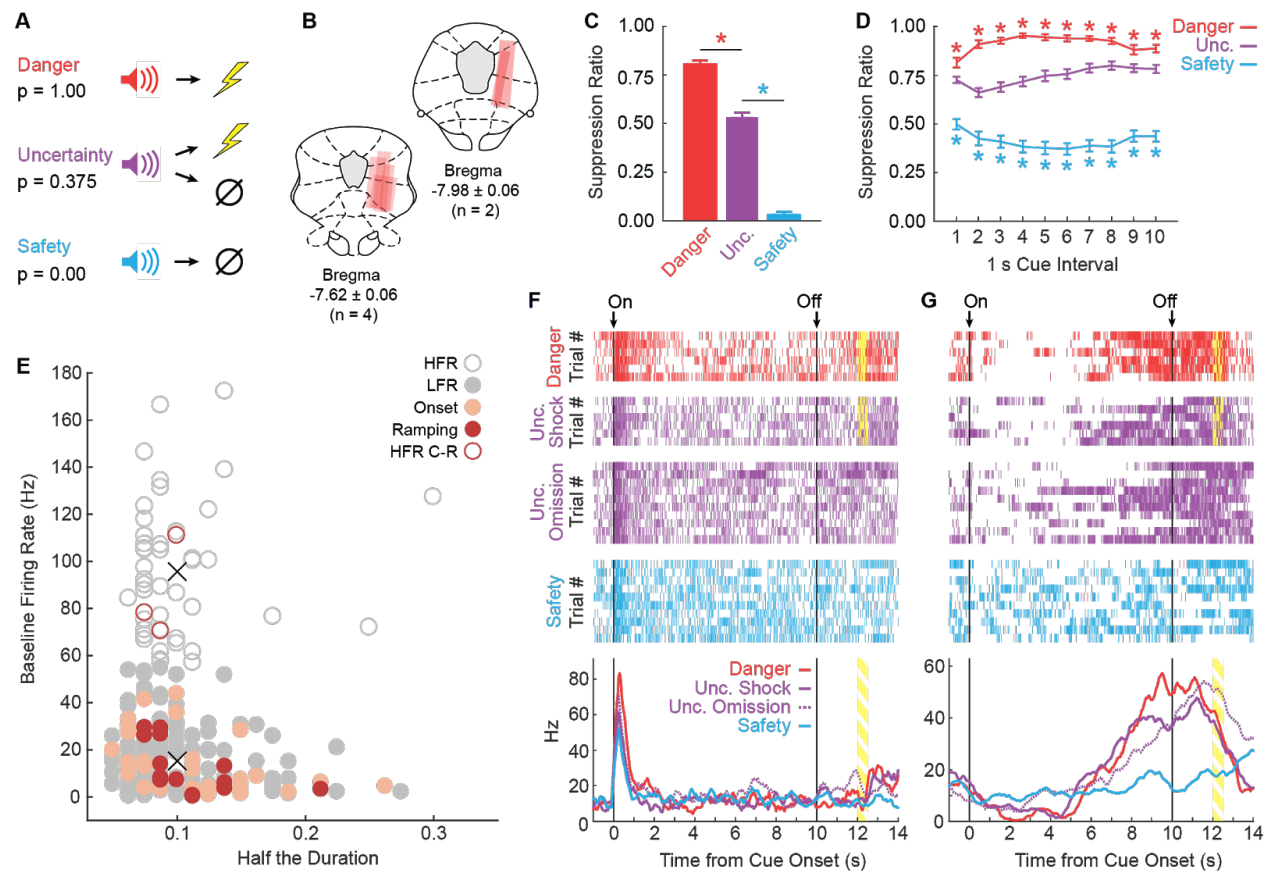


Figure 2.1 Fear Discrimination, Histology, and vIPAG single-unit activity

(A) Pavlovian fear discrimination consisted of three cues, each predicting a unique probability of foot shock: danger, $p = 1.00$ (red); uncertainty, $p = 0.375$ (purple); and safety, $p = 0.00$ (blue). (B) Microelectrode bundle placements for all rats ($n = 6$) and all neurons ($n = 245$) during recording sessions are represented by red bars. (C) Mean \pm SEM suppression ratio during the entire 10 s cue for danger, uncertainty, and safety trials is shown for all sessions in which single-units were recorded ($n = 88$). Discrimination was observed for each cue pair (danger vs. uncertainty, $t_{87} = 12.36$, $p = 7.44 \times 10^{-21}$, red asterisk; uncertainty vs. safety, $t_{87} = 20.85$, $p = 3.50 \times 10^{-35}$, blue asterisk). (D) Mean \pm SEM suppression ratio during each 1 s interval of 10 s cue presentation for danger, uncertainty, and safety trials is shown ($n = 88$). Discrimination was observed during every interval for each cue pair (danger vs. uncertainty, all $t_{87} > 3.00$, all $p < 0.005$ [Bonferroni correction for 10 tests], red asterisks; uncertainty vs. safety, all $t_{87} > 7.00$, all $p < 0.005$, blue asterisks). (E) Scatterplot comparing half the duration of the waveform (x axis) to baseline firing rate (y axis) in all recorded neurons ($n = 245$). Clustering revealed two populations based on baseline firing rate (High Firing Rate (HFR), open circles; Low Firing Rate (LFR), solid gray circles). X symbols indicate cluster centroids. Onset neurons ($n = 29$, peach), Ramping neurons ($n = 14$, wine) and HFR cue-responsive neurons ($n = 3$, wine outline) are indicated. (F and G) Representative single-units from the (F) Onset population and (G) Ramping population. Cue onset (On) and offset (Off) indicated by vertical black lines. Shock delivery indicated by yellow bars. Trial-by-trial firing (top four raster plots), as well as mean firing (bottom, line graphs) are shown for each neuron. Each raster tick represents a spike and each row of spikes reflects one trial [danger ($n = 6$), uncertainty shock ($n = 6$), uncertainty omission ($n = 10$), safety ($n = 10$)]. The bottom row of spikes in each raster plot corresponds to the first cue trial, subsequent trials are above. Line graphs: Mean firing rate (Hz) across all trials for each cue was constructed using 100 ms bins and smoothed, cue boundaries and shock visualization maintained from raster plots above.

Six adult male, Long Evans rats were trained to nose poke in a central port in order to receive a food pellet from a cup below. During fear discrimination (Figure 2.1 A), three distinct auditory cues predicted unique foot shock probabilities: danger ($p = 1.00$), uncertainty ($p = 0.375$) and safety ($p = 0.00$). Trial order was randomized for each rat during each session. Fear was measured with suppression ratio and was calculated by comparing nose poke rates during baseline and cue periods (see Methods). After eight

discrimination sessions, rats were implanted with 16-wire, drivable microelectrode bundles dorsal to the vIPAG (Figure 2.1 B). Following recovery, rats were returned to fear discrimination. Single-units were isolated and held for the duration of each recording session. The electrode bundle was advanced ~40–80 μm between sessions to record from new single-units in subsequent sessions.

Across all 88 recording sessions, all rats demonstrated excellent discriminative fear: high to danger, intermediate to uncertainty, and low to safety (Figure 2.1 C). ANOVA for suppression ratios for the total 10 s cue [within factor: cue (danger vs. uncertainty vs. safety)] found a significant effect of cue ($F_{2,174} = 592.00$, $p = 2.32 \times 10^{-78}$, $\eta p^2 = 0.87$, observed power (op) = 1.00). Paired t-tests confirmed differing ratios for each cue (danger vs. uncertainty, $t_{87} = 12.36$, $p = 7.44 \times 10^{-21}$; uncertainty vs. safety, $t_{87} = 20.85$, $p = 3.50 \times 10^{-35}$). Visualizing nose poke rates to each cue revealed a discrimination pattern matching that for suppression ratio (Figure 1.2). While the foot shock probability associated with uncertainty was closer to safety: danger ($p = 1.00$) \gg uncertainty ($p = 0.375$) $>$ safety ($p = 0.00$); the mean suppression ratio to uncertainty was closer to danger: danger (ratio = 0.80) $>$ uncertainty (ratio = 0.53) \gg safety (ratio = 0.03) (Figure 2.1 C). The non-linear relationship between shock probability and behavior was critical for regression analyses that sought to determine if single-unit firing was better captured by threat probability or fear output.

When the total cue period was divided into 10, 1 s intervals, discrimination was observed in each interval and maintained over cue presentation (Figure 2.1 D). ANOVA for suppression ratios [within factors: cue (danger vs. uncertainty vs. safety) and interval (1-10)] found a significant effect of cue ($F_{2,174} = 489.40$, $p = 3.59 \times 10^{-72}$, $\eta p^2 = 0.85$, op =

1.00) and a cue x interval interaction ($F_{18,1566} = 6.21$, $p = 5.90 \times 10^{-15}$, $\eta p^2 = 0.07$, $op = 1.00$). Suppression ratios are artificially high when calculated in short intervals, making for a poor measure of *absolute* fear. However, this artificial skewing is observed equally to all cues, making suppression ratios in short intervals a valid, *relative* measure of fear.

2.3.1 vIPAG neurons are responsive at cue onset or ramp over cue presentation

I recorded the activity of 245 neurons in six rats over 88 fear discrimination sessions. A previous study optogenetically identified vIPAG glutamate neurons with low baseline firing rates, compared to GABA neurons exhibiting higher baseline firing rates (Tovote et al., 2016). K-means clustering was performed for all 245 neurons using baseline firing rate and waveform characteristics: amplitude ratio and half the duration (Roesch et al., 2007). All neurons separated into one of two clusters purely on the basis of baseline firing rate (Figure 2.1 E), with majority of neurons falling into the low firing rate (LFR) cluster ($n = 199$) and the remaining in the high firing rate (HFR) cluster ($n = 46$).

Independent of cluster membership, the cue-responsiveness of each neuron was determined ($n = 245$). I identified 29 neurons (obtained from 5/6 rats, ~12% of all neurons recorded) with phasic increases in firing to danger, uncertainty, or safety (t-test for firing rate, baseline [2 s prior to cue onset] vs. first 1 s cue interval, $p < 0.017$, Bonferroni correction for three tests). All 29, cue-responsive neurons belonged to the LFR cluster, and were referred to as the Onset population (single-unit example, Figure 2.1 F). Consistent with Ozawa et al., 2017, 17 neurons increased firing to at least one cue during the last 1 s cue interval (interval > baseline, $p < 0.017$). Three of these neurons belonged to the HFR cluster and were likely a unique class of neurons. The remaining 14 cue-responsive neurons (obtained from 4/6 rats, ~6% of all neurons recorded) belonged to

the LFR cluster, and were referred to as the Ramping population (single-unit example, Figure 2.1 G). All further analyses were performed on the 29 Onset neurons and 14 Ramping neurons.

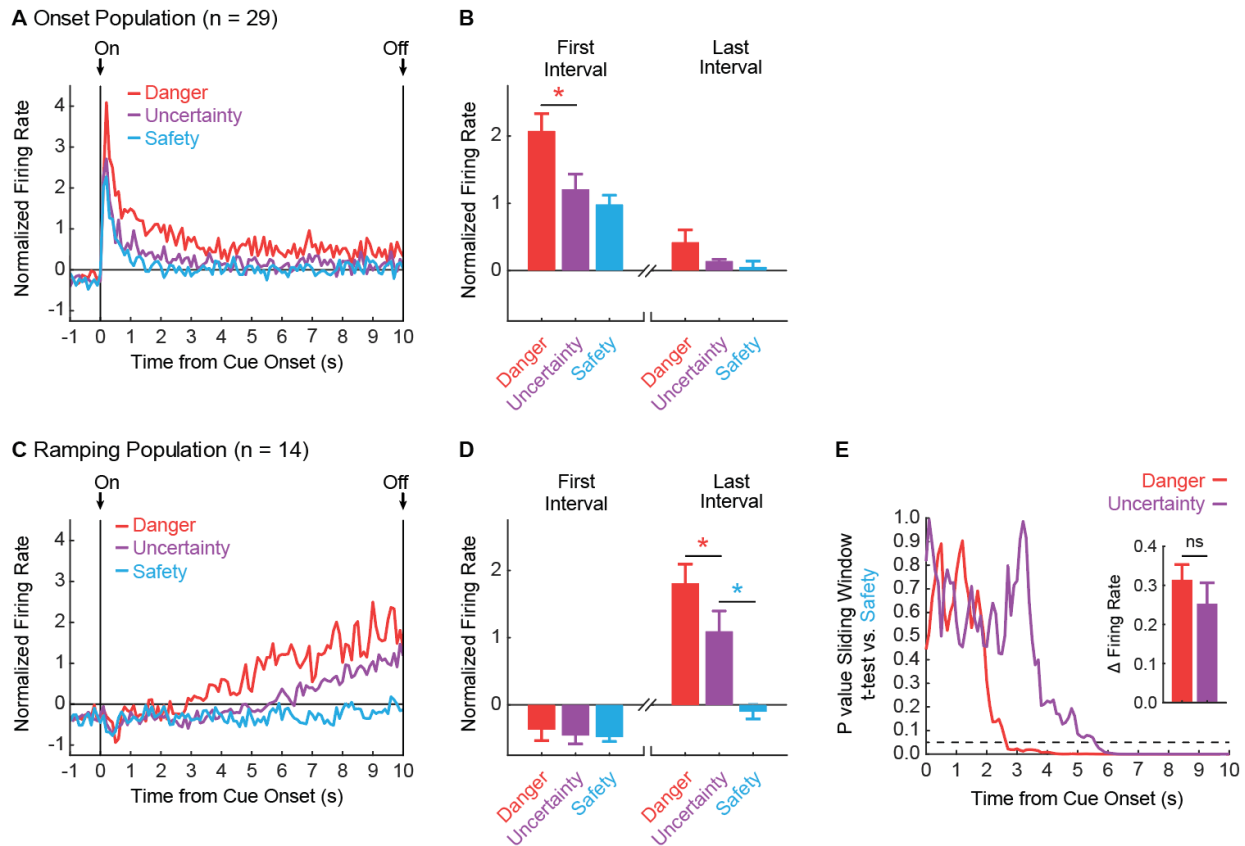


Figure 2.2 vIPAG neurons are responsive to cue onset or ramp over cue presentation

(A) Mean, Z-score normalized firing to danger (red), uncertainty (purple) and safety (blue) is shown for the 1 s pre-cue period and the 10 s cue period for the Onset population (n = 29). Cue onset (On) and offset (Off) are indicated by vertical black lines. (B) Mean + SEM, Z-score normalized firing during the first, 1 s cue interval (left) and the last, 1 s cue interval (right), is shown for each cue. Differential firing was observed for danger vs. uncertainty ($t_{28} = 4.54$, $p = 9.70 \times 10^{-4}$, red asterisk) but not for uncertainty vs. safety ($t_{28} = 1.37$, $p = 0.18$), in the first interval. No differences were observed for danger vs. uncertainty ($t_{28} = 1.69$, $p = 0.10$) or uncertainty vs. safety, ($t_{28} = 0.60$, $p = 0.55$) in the last interval. (C) Normalized firing for the Ramping population (n = 14) plotted as in A. (D) First and last interval firing for the Ramping population (n = 14) plotted as in B. Differential firing was not observed for danger vs. uncertainty ($t_{13} = 0.62$, $p = 0.55$) or uncertainty vs. safety ($t_{13} = 0.24$, $p = 0.82$), in the first interval. By contrast, differential firing was observed for

danger vs. uncertainty ($t_{13} = 3.17$, $p = 7.41 \times 10^{-3}$, red asterisk) and uncertainty vs. safety ($t_{13} = 8.26$, $p = 2.00 \times 10^{-6}$, blue asterisk), in the last interval. (E) A t-test comparing danger (red) and uncertainty (purple) population firing to safety in a 1 s window was slid across the 10 s cue in 100 ms increments. P value of t-test reported on y axis. Dotted line indicates $p=0.05$. Inset: Mean + SEM change in firing rate from the first window of activity departed from safety to the last interval, is shown for danger (red) and uncertainty (purple). ns = no significance of a paired t-test.

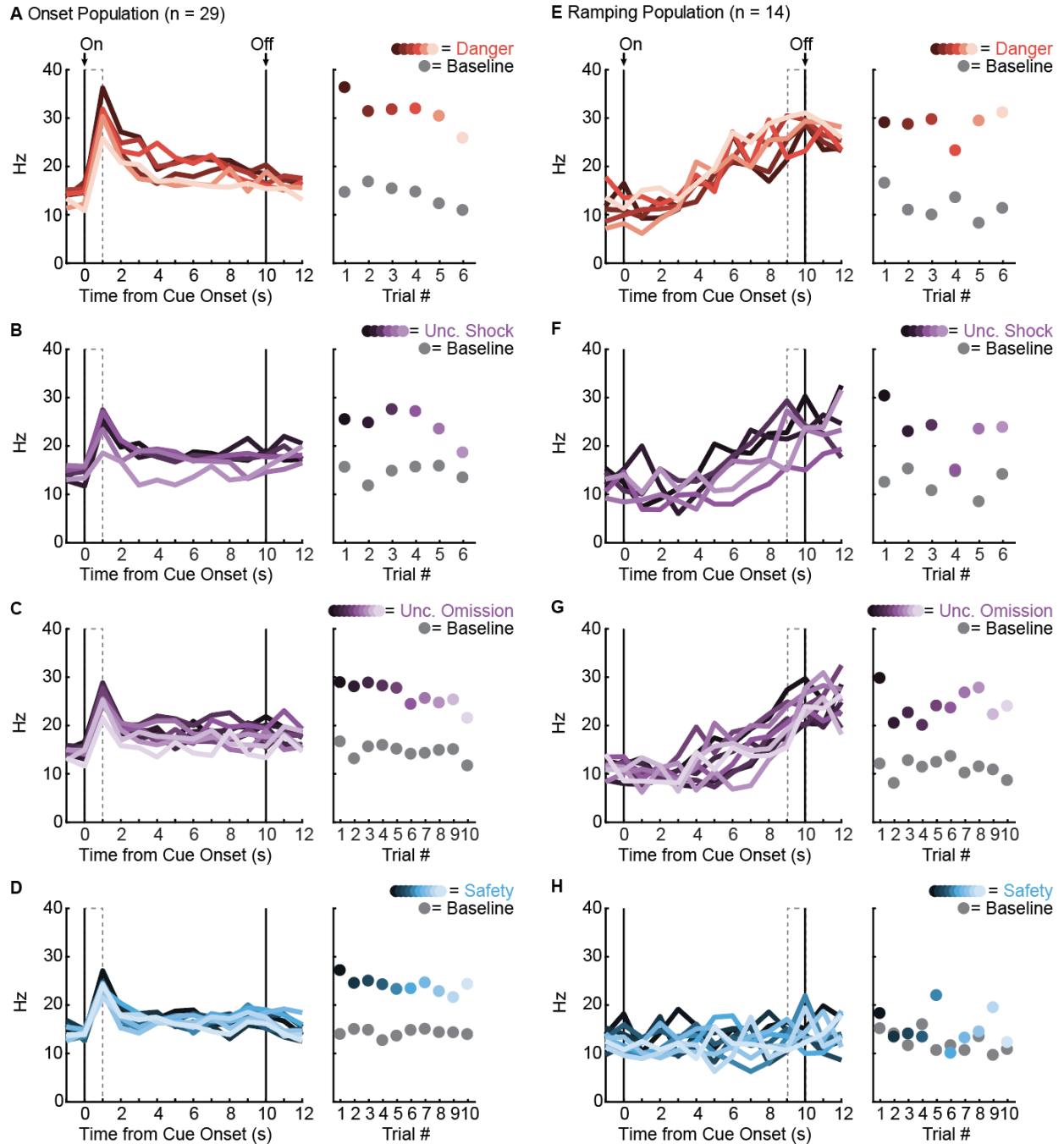


Figure 2.3 Trial by trial firing for Onset and Ramping neurons

(A, left) Raw firing rate (Hz) for the Onset population ($n = 29$) is shown across cue presentation for each of the six danger trials. Trials are color-coded from dark (first trial) to light (last trial) with 'On' indicating cue onset and 'Off' indicating cue offset. (A, right) Population mean firing rate is shown for the first 1 s cue interval (dashed box in A), for each trial. Color scheme maintained from (A, left). Population mean baseline firing (2 s

prior to cue presentation) is shown for each individual trial (gray circles). Identical plots using unique color schemes (uncertainty, purple and safety, blue) were made for each trial type: (B) uncertainty shock, (C) uncertainty omission and (D) safety. Note that increased cue firing over baseline tended to be highest on trial 1, but was observed for every individual trial for all cues. A nearly identical set of plots were made for the Ramping population ($n = 14$, E - H), only now population mean firing rate for each trial (right) is shown for the last 1 s interval of the cue (dashed box on left). Increased cue firing over baseline was consistently observed on danger and uncertainty trials, but not safety trials. Firing patterns observed for the mean of all trials (Figure 2.2 A), (C) were observed at the single trial level for Onset and Ramping populations.

2.3.2 VIPAG neurons show differential firing that is maximal to danger

Despite identifying neurons without regard for relative firing to the three cues, differential firing was observed in Onset neurons at single-unit (Figure 2.1 F) and population (Figure 2.2 A) levels. Onset neurons ($n = 29$) sharply increased activity during the first 1 s cue interval: greatest firing to danger, lesser firing to uncertainty, and least firing to safety (Figure 2.2 B, Left). The differential firing pattern diminished over cue presentation and was completely absent by the last 1 s cue interval (Figure 2.2 B, Right). ANOVA for normalized firing rate (Z-score transformation) for the 29 Onset neurons [data from Figure 2.2 A; within factors: cue (danger vs. uncertainty vs. safety) and bin (100 ms: 1 s prior to cue onset through 10 s cue)] revealed main effects of cue and bin ($F_s > 9$, $p_s < 0.01$, $\eta^2 > 0.20$, $op > 0.95$) but most critically, a cue x bin interaction ($F_{218,6104} = 1.94$, $p < 0.01$, $\eta^2 = 0.06$, $op = 1.00$). Consistent with the ANOVA interaction, Onset neurons showed significantly greater firing to danger compared to uncertainty in the first 1 s cue interval ($t_{28} = 4.54$, $p = 9.70 \times 10^{-5}$). While numerically greater, firing to uncertainty over safety failed to reach significance in the first 1 s interval ($t_{28} = 1.37$, $p = 0.18$). However, ANOVA restricted to uncertainty and safety (100 ms: 1 s prior to cue onset through first 5 s of the cue) revealed a significant cue x bin interaction ($F_{59,1652} = 1.50$, $p = 0.01$, $\eta^2 = 0.051$, op

= 1.00). Differential firing was not observed to danger vs. uncertainty ($t_{28} = 1.69$, $p = 0.10$) or to uncertainty vs. safety ($t_{28} = 0.60$, $p = 0.55$) in the last 1 s cue interval.

Differential firing was observed in Ramping neurons at single-unit (Figure 2.1 G) and population (Figure 2.2 C) levels. Ramping neurons ($n = 14$) did not increase firing to any cue during the first 1 s cue interval (Figure 2.2 D, Left). Instead, activity ramped over cue presentation and greatest firing was observed during the last 1 s cue interval (Figure 2.2 D, Right). Ramping activity was most apparent to danger, intermediate to uncertainty, and absent to safety. The temporal firing pattern (onset \rightarrow offset) was consistent across trials (Figure 2.3). ANOVA for normalized firing rate for the 14 Ramping neurons [data from Figure 2.2 C; within factors: cue (danger vs. uncertainty vs. safety) and bin (100 ms: 1 s prior to cue onset through 10 s cue)] revealed main effects of cue and bin ($F_s > 60$, $p_s < 0.01$, $\eta^2 > 0.40$, $op = 1.00$) and a cue x bin interaction ($F_{218,2834} = 4.33$, $p < 0.01$, $\eta^2 = 0.24$, $op = 1.00$). Illustrative of the ANOVA interaction, Ramping neurons showed no significant differences in firing to danger vs. uncertainty ($t_{13} = 0.62$, $p = 0.55$) or uncertainty vs. safety ($t_{13} = 0.24$, $p = 0.81$) in the first 1 s cue interval. However, differential firing to danger vs. uncertainty ($t_{13} = 3.17$, $p = 7.41 \times 10^{-3}$) and uncertainty vs. safety ($t_{13} = 8.26$, $p = 2.00 \times 10^{-6}$), was observed in the last 1 s cue interval.

Ramping activity to danger and uncertainty could be the product of the *time* at which activity began to increase, or the *rate* of increase. I performed a two-tailed t-test for population firing to danger vs. safety (Figure 2.2 E, red line) and uncertainty vs. safety (Figure 2.2 E, purple line) in 1 s windows, starting with cue onset. I slid the 1 s window across the 10 s cue in 100 ms increments, to reveal the time at which danger and uncertainty population firing departed from safety. I then calculated the rate of firing

increase from the departure window to the last 1 s interval for danger and uncertainty. Differential firing was determined by the time of departure from safety, as opposed to the rate of increase. Ramping activity to danger emerged earlier (Figure 2.2 E red line; 2.8 s following cue onset for $p < 0.05$) than ramping activity to uncertainty (Figure 2.2 E purple line; 5.7 s following cue onset for $p < 0.05$). Change in firing rate from the window of safety departure to the last 1 s cue interval did not differ between danger and uncertainty (Figure 2.2 E, Inset).

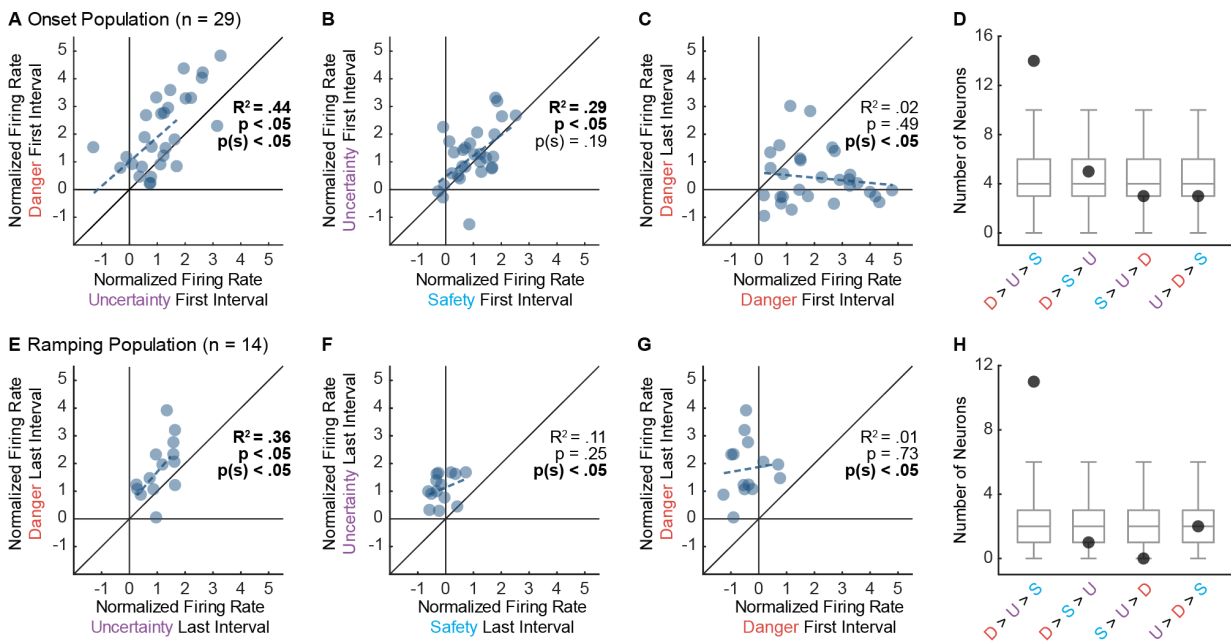


Figure 2.4 Single-unit biases in Onset and Ramping populations

(A) Normalized firing to uncertainty (purple) vs. danger (red) during the first, 1 s cue interval is plotted for all Onset neurons ($n = 29$). Trendline, the square of the Pearson correlation coefficient (R^2) with associated p value (p), and sign test p value $p(s)$ are shown for each plot. (B) Normalized firing to safety (blue) vs. uncertainty (purple) during the first, 1 s cue interval is plotted for Onset neurons ($n = 29$). (C) Normalized firing to danger in the first, 1 s cue interval vs. the last, 1 s cue interval is plotted for Onset neurons ($n = 29$). (D) Number of observed neurons (closed circle) vs shuffled distribution (median, 25th percentile, 75th percentile, lowest/highest non-outliers) shown for four most common firing patterns: danger > uncertainty > safety, danger > safety > uncertainty, safety > uncertainty > danger, and uncertainty > danger > safety. (E) Normalized firing to

uncertainty (purple) vs. danger (red) during the last, 1 s cue interval is plotted for Ramping neurons (n = 14). (F) Normalized firing to safety (blue) vs. uncertainty (purple) during the last, 1 s cue interval is plotted for Ramping neurons (n = 14). (G) Normalized firing to danger in the first, 1 s cue interval vs. the last, 1 s cue interval is plotted for Ramping neurons (n = 14). (H) Number of observed neurons vs shuffled distribution reported as in D.

2.3.3 Population biases are evident in vIPAG single-units

To demonstrate that Onset population activity was the result of a consistent bias across neurons, I directly compared single-unit firing to cue pairs. Danger and uncertainty firing were correlated, and single-units were biased towards greater firing to danger (Figure 2.4 A). Uncertainty and safety firing were also correlated; however, the single-unit bias towards greater firing to uncertainty was not significant (Figure 2.4 B). Underscoring their specificity to cue onset, single-units were biased towards greater firing to danger in the first 1 s cue interval compared to the last interval, and there was no correlation between firing in the two epochs (Figure 2.4 C). Examining relative cue firing for each Onset neuron in the first 1 s interval revealed the most common pattern to be: danger > uncertainty > safety (n = 14). This was the only pattern to contain more units than would be expected than chance (Figure 2.4 D).

The same analysis was performed for the Ramping population, only for the last 1 s interval. Ramping neurons showed a differential firing pattern. A significant correlation between firing to danger and uncertainty was observed, along with a single-unit bias towards greater firing to danger (Figure 2.4 E). Only now, there was no correlation between uncertainty and safety firing, but a consistent bias towards greater uncertainty firing (Figure 2.4 F). Ramping single-units were biased towards danger activity in the last 1 s cue interval, and there was no correlation between firing in the two epochs (Figure 2.4

G). The most common firing pattern in the last 1 s interval was: danger > uncertainty > safety (n = 11). Similar to the Onset population, this was the only pattern to contain more units than expected by chance (Figure 2.4 H).

VIPAG activity is greatest to danger, the cue most strongly suppressing rewarded nose poking. It is therefore possible that Onset and Ramping neurons are simply responsive to nose poke cessation. To examine this possibility, I identified naturally occurring periods of nose poke cessation in inter-trial intervals, when no cues were presented. This analysis found no meaningful changes in Onset or Ramping activity during periods of nose poke cessation, demonstrating activity patterns are specific to cue-induced suppression of nose poking.

At first glance, the firing patterns of Onset and Ramping neurons appear to support the prevailing hypothesis that vIPAG neurons signal fear output. Differential fear (Figure 2.1 C) and differential firing (Figure 2.2 B & D) show the same general pattern: danger > uncertainty > safety. However, closer inspection reveals that relative differences in fear do not match relative differences in firing. Rats showed robust discrimination between uncertainty and safety, regardless of the temporal resolution with which fear was measured (Figure 2.1 C & D). Yet, robust differential firing to uncertainty and safety was modest in the Onset population (Figure 2.2 B, left; Figure 2.4 B). The Ramping population showed stronger differential firing between uncertainty and safety (Figure 2.2 D, right; Figure 2.4 F), but this pattern did not emerge until the end of the cue. Fear discrimination was reliably detected in the first 1 s interval (Figure 2.1 D), indicating that Ramping neurons cannot organize fear output early in cue presentation. While inconsistencies between fear output and neural activity are evident for the Onset and Ramping

populations, further analyses are required to conclusively test the relative contributions of threat probability and fear output to vIPAG single-unit activity.

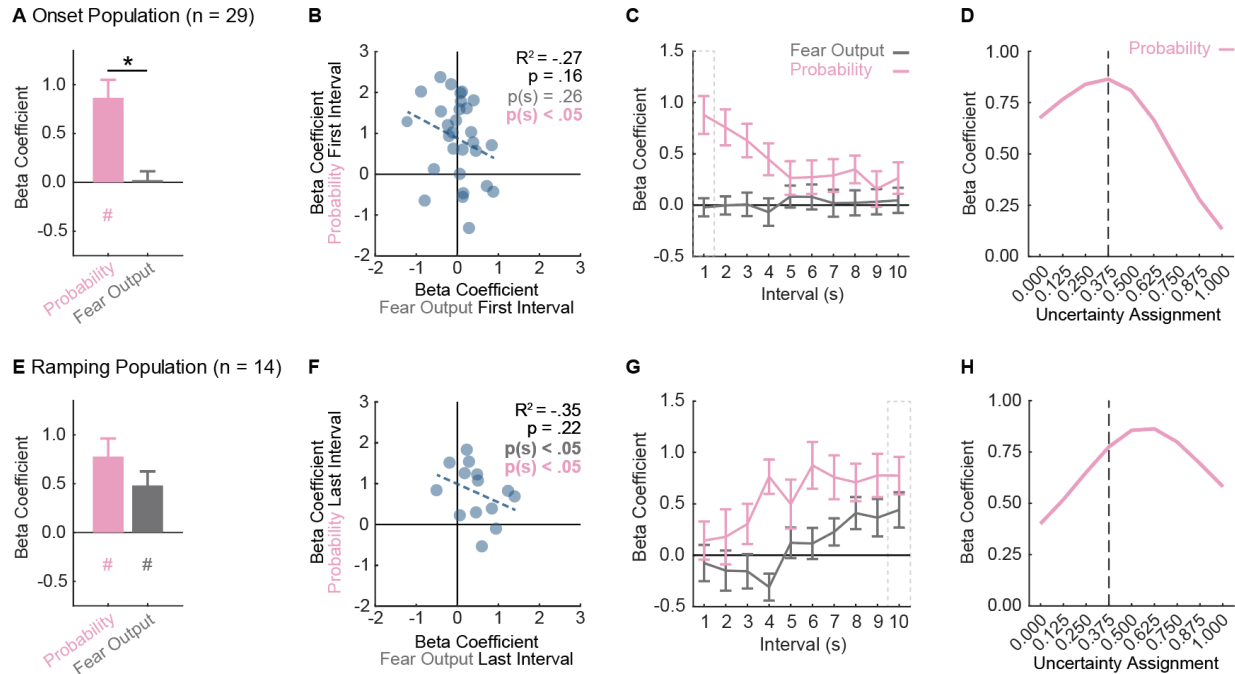


Figure 2.5 vIPAG neurons prioritize threat probability over fear output

(A) Mean + SEM beta coefficient is shown for each regressor, during the first, 1 s cue interval, for the Onset population (n = 29): probability (pink), fear output (dark gray). The beta coefficient for probability was significantly greater than that for fear output (probability vs. fear output, $t_{28} = 3.96$, $p = 4.65 \times 10^{-4}$). *paired samples t-test, $p < 0.05$. #single-sample t-test comparison to zero, $p < 0.05$, color indicates regressor compared to zero. (B) Beta coefficient for fear output (dark gray) vs. probability (pink) during the first, 1 s cue interval is plotted for all Onset neurons (n = 29). Trendline, the square of the Pearson correlation coefficient (R^2) with associated p value, and sign test p value comparing each regressor to zero is shown. (C) Mean \pm SEM beta coefficient is shown for each regressor, during each 1 s cue interval, for the Onset population (n = 29). Dash outlined box indicates interval analyzed in (A). (D) Mean beta coefficient for probability is shown for each of the nine uncertainty assignments for the Onset population (n = 29). Dashed line indicates the actual foot shock probability associated with uncertainty (0.375). (E) Mean + SEM beta coefficient is shown for each regressor, during the last, 1 s cue interval, for the Ramping population (n = 14). The beta coefficient for probability did not differ from fear output (probability vs. fear output, $t_{13} = 1.18$, $p = 0.258$). *paired samples t-test, $p < 0.05$. #single-sample t-test comparison to zero, $p < 0.05$, color indicates regressor compared to zero.

(F) Beta coefficient for fear output (dark gray) vs. probability (pink) during the last, 1 s cue interval is plotted for Ramping neurons ($n = 14$). (G) Mean \pm SEM beta coefficient is shown for each regressor, during each 1 s cue interval, for the Ramping population ($n = 14$). Dash outlined box indicates interval analyzed in (E). (H) Mean beta coefficient for probability is shown for each of the nine uncertainty assignments for the Ramping population ($n = 14$). Dashed line indicates the actual foot shock probability associated with uncertainty (0.375).

2.3.4 Onset neurons signal threat probability

Simultaneous linear regression for single-unit firing was used to formally test the degree to which vIPAG activity is captured by fear output and threat probability (Figure 2.5). Normalized firing rate for each trial was calculated for each single-unit (32 total: six danger, six uncertainty shock, 10 uncertainty omission, and 10 safety), in 1 s bins over the 10 s cue. Fear output was the suppression ratio on that trial. Threat probability was the shock probability associated with the cue: danger: 1.00, uncertainty: 0.375 and safety: 0.00. Fear output and threat probability were used as regressors to explain trial-by-trial variance in single-unit firing. Statistical output was a beta coefficient quantifying the strength ($|\beta| > 0$ = stronger) and direction ($\beta > 0$ = positive) of the predictive relationship between each regressor and single-unit firing. Beta coefficients for single-units comprising the Onset and Ramping populations were subjected to ANOVA with regressor (fear output vs. threat probability) and interval (1 s cue intervals) as factors. This approach was used to determine the relative contribution of fear output and threat probability to single-unit firing over the course of cue presentation.

The results of primary interest for the Onset population came from the first 1 s cue interval, when activity was highest and differential firing was observed. Linear regression unequivocally revealed that Onset single-unit activity was captured by threat probability (Figure 2.5 A). The beta coefficient for threat probability regressor was positive and

significant, exceeding the beta coefficient for fear output, which failed to differ from zero. The population bias was observed across Onset neurons, such that single-unit beta coefficients were positively biased toward threat probability, but not fear output (Figure 2.5 B).

Examining the entirety of cue presentation, threat probability signaling was highest in the first interval, persisted several more seconds and diminished toward the last interval (Figure 2.5 C). Fear output did not account for variance in single-unit firing during any interval. Consistent with this description, ANOVA for beta coefficient with factors of regressor (2 total) and interval (10 total) revealed a main effect of regressor ($F_{1,28} = 6.73$, $p = 0.015$, $\eta p^2 = 0.19$, $op = 0.71$) and a regressor x interval interaction ($F_{9,252} = 2.85$, $p = 0.003$, $\eta p^2 = 0.09$, $op = 0.96$).

The threat probability regressor in the above analyses utilized the actual shock probability assigned to each cue. Of course, the subjects had no *a priori* knowledge of shock probability assignments. It is then possible that vIPAG activity is ‘tuned’ to an alternative shock probability. To examine this, single-unit linear regression for normalized firing in the first 1 s cue interval was performed, maintaining the probabilities for danger (1.00) and safety (0.00), but incrementing the probability assigned to uncertainty from 0 to 1 in 0.125 steps (0.000, 0.125, 0.250, 0.375, 0.500, 0.625, 0.750, 0.875, and 1.000). The mean beta coefficient for each of the nine increments is plotted as a threat-tuning curve for the Onset population (Figure 2.5 D). The beta coefficient resulting from regression using the actual shock probability (uncertainty = 0.375), was the ‘peak’ of the tuning curve. This result is particularly revealing for the analysis in which the uncertainty assignment was 0.000 (first data point on the curve Figure 2.5 D). Onset neurons showed high firing

to danger but lower and more similar firing to uncertainty and safety, leaving open the possibility that Onset neurons signal a more binary output (danger = 1.000) > (uncertainty and safety = 0.000). However, the actual uncertainty assignment (0.375) captured single-unit activity better than the binary assignment (0.000), revealing that Onset activity reflected an estimate of the actual threat probability.

2.3.5 Ramping neurons prioritize threat probability over fear output

Linear regression for the Ramping population in the last 1 s cue interval revealed that single-unit activity was captured by a mixture of threat probability and fear output (Figure 2.5 E). Ramping single-units were biased towards positive beta coefficients for probability and fear output (Figure 2.5 F), but there was no correlation between these regressors. Linear regression for all ten intervals revealed that threat probability signaling was prioritized over fear output (Figure 2.5 G). ANOVA for beta coefficient with factors of regressor (2 total) and interval (10 total) revealed a main effect of regressor ($F_{1,13} = 5.90$, $p = 0.03$, $\eta^2 = 0.31$, $op = 0.61$), but no regressor x interval interaction ($F_{9,117} = 1.12$, $p = 0.37$, $\eta^2 = 0.08$, $op = 0.53$).

If Ramping neurons contain information about threat probability as well as fear output, the tuning curve for ramping neurons should be shifted right of 0.375. This is because the relative weighting of uncertainty differs for threat probability (danger >> uncertainty > safety) and fear output (danger > uncertainty >> safety). I constructed a population threat-tuning curve for normalized firing during the last 1 s interval (Figure 2.5 H, as in Figure 2.5 D). Tuning was shifted right of the actual probability, with a 'peak' of 0.625. This is consistent with mixed signaling of fear output and threat probability during the last 1 s interval by Ramping neurons, rather than a pure threat probability signal.

2.4 Discussion

Chapter 2 set out to scrutinize cue-excited vIPAG neurons and determine if their activity reflected fear output. Consistent with previous reports (Tovote et al., 2016; Watson et al., 2016; Ozawa et al., 2017), I identified a population of Onset neurons with short-latency excitation to danger. Consistent with the most recent report (Ozawa et al., 2017), I found a Ramping population that increased activity over danger presentation. Onset activity reflected an estimate of threat probability, invariant of fear output. Ramping activity reflected threat probability and fear output, though probability emerged earlier and was stronger overall. While vIPAG signals for fear output could potentially emerge at the ensemble level (Jones et al., 2007; Zhou et al., 2018), it appears these multi-unit codes would be composed of cue-excited single-units primarily signaling threat probability. Activity reflecting fear output may be found in other vIPAG populations, such as neurons showing inhibition of firing to cues (Tovote et al., 2015), or single-units that are not cue-responsive (Insanally et al., 2019). Yet, this would still mean that signals for threat probability and fear output co-exist in the vIPAG.

It is important to note that these results are correlative and that Onset neuron activity may not play a causal role in fear output. Previous work has found that short-latency, excitatory responses to danger are largely observed in glutamatergic vIPAG neurons, and that excitation of this population is sufficient to produce freezing (Tovote et al., 2016). Though all Onset neurons fell into the low firing cluster, which could be consistent with glutamatergic firing (Ono et al., 2017). However, we cannot conclude these were glutamatergic neurons. Before further discussing implications, it is important to consider alternative accounts for the observed Onset and Ramping firing patterns.

It is possible that vIPAG neurons signaling fear output are anatomically distinct from those recording in this preparation. However, I intentionally recorded single-unit activity from the caudal portion of the vIPAG, the subdivision of the PAG implicated in conditioned fear expression. Further, vIPAG manipulations that disrupt fear-related behaviors typically include this more caudal region (De Oca et al., 1998), and high-resolution functional magnetic resonance imaging reveals caudal vIPAG activation specific to aversive stimuli in humans (Satpute et al., 2013). I observed threat probability signaling across the entire rostrocaudal extent of these recordings (Bregma -7.56mm through -8.04mm), but the vIPAG stretches $\sim 0.64\text{mm}$ beyond our most caudal recording site. It is therefore possible that neurons signaling fear output are restricted to the extreme caudal vIPAG. Maybe the vIPAG signals fear output, but we did not measure the relevant output?

Previous studies have failed to find robust relationships between vIPAG activity and cued freezing. Here, I used conditioned suppression of rewarded nose poking to provide an objective measure of fear, and to perhaps better capture vIPAG activity. This measure of fear did not capture Onset neuron firing, and only partially captured Ramping neuron firing at the end of cue presentation. Further, Onset and Ramping activity were not merely driven by nose poke cessation. If not freezing, conditioned suppression, or nose poke cessation then perhaps another measure of fear?

Danger cues elicit active fear responses: escape-like behaviors such as darting (Greiner et al., 2019; Gruene et al., 2015). However, darting is prevalent in females, but less so in males. Further, the males used in this study had extensive experience with fear discrimination, and at no point was escape from the foot shock possible. Irrespective of the type of fear measure, most fear behaviors are initiated at cue onset and maintained

until the aversive event occurs. Yet, I did not observe a substantial population of neurons with these temporal firing characteristics, making cue-excited vIPAG activity a poor candidate for sustained fear output.

Neurons responsive toward the end of cue presentation were more heterogeneous, in baseline firing rate and signaling. Ramping neurons prioritized threat probability, but also signaled fear output. However, without sustained fear output signaling, Ramping activity could not drive fear output in full. Further, differential fear expression to safety, uncertainty and danger was observed even in the first second of cue presentation, when Ramping neurons were unresponsive. Ramping neurons may provide a threat probability estimate that increases as threat draws nearer and peaks when threat is imminent. Alternatively, Ramping neurons may help sustain threat estimates in the absence of explicit stimuli, such as in trace conditioning (McEchron et al., 1998; Buchel et al., 1999), or simply estimate more precisely when the noxious event will occur. In support, shifts toward PAG-centric activity are apparent in humans, as capture becomes imminent (Mobbs et al., 2007) or natural threats draw closer (Mobbs et al., 2010); with the caveat that neither of these studies could specify the activated PAG subregion.

If fear output via conditioned suppression is non-linear, and vIPAG activity scales linearly to threat probability, how does the vIPAG fit into fear output? Non-linear fear output may mean that threat systems evolved to avoid predation, not to precisely match the degree of defensive behavior to threat probability. In response to uncertain threats, erring on the side of increased fear may promote survival. Nonetheless, between the Onset and Ramping populations, the vIPAG contains an estimate of threat probability during the entirety of a threat encounter. While cue-excited, vIPAG activity may not signal fear

output, it is rich with information that would inform a variety of fear processes and behaviors.

**CHAPTER 3: Do cue-inhibited vIPAG single-units signal
threat probability or fear output?**

Portions of this chapter have been published in the following research article:

Wright, K.M., Jhou, T.C., Pimpinelli, D. & McDannald, M.A. (2019). Cue-inhibited ventrolateral periaqueductal gray neurons signal fear output and threat probability in male rats. *eLife*, 8:e50054.

3.1 Introduction

In the previous Chapter, I scrutinized an expected population of cue-excited vIPAG units in an effort to reveal a direct neural correlate of fear expression in the vIPAG, and clarify some of the heterogeneity attributed to previous findings. However, I found that cue-excited vIPAG is better captured by threat probability. Although cue-excited single-units have been the focus of a neural substrate for fear output, cue-inhibited vIPAG single-units have also been found (Tovote et al., 2016). Further, optogenetic inhibition of this functional type promotes freezing. Among the vIPAG single-units recorded in Chapter 2, a considerable number inhibited activity on cue presentation (91/245, ~37% of single-units recorded), particularly to danger. Here, I sought to determine if a neural correlate for fear expression may instead reside in cue-inhibited vIPAG neurons; an expected neural correlate, in an unexpected population.

A complete neural correlate for fear expression should be supported by cue-inhibited neurons that decrease firing at the beginning of a threat (cue onset) and maintain decreased firing throughout the duration of a threat encounter (cue duration). Similar to cue-excited neurons, cue-inhibited neurons signaling fear expression will directly reflect trial-by-trial behavior. By contrast, cue-inhibited neurons encoding threat probability should linearly decrease firing according to threat probability (shock probability), irrespective of behavior.

3.2 Methods

With the exception of statistical approaches detailed below, all methods used in Chapter 3 were maintained precisely as established in Chapter 2 (See Chapter 2.2.1 through 2.2.8.1: Subjects, Electrode Assembly, Surgery, Behavior Apparatus, Behavioral

Procedures, Histology, Single-unit Data Acquisition, and Calculating Suppression Ratios for complete details).

3.2.1 Statistical Analyses

3.2.2.1 Behavior Analysis

Suppression ratios were analyzed using analysis of variance (ANOVA) with trial type as a factor. ANOVA for behavior contained three trial types (danger, uncertainty and safety). Uncertainty trial types (shock and no-shock) were collapsed because they did not differ for suppression ratio; during cue presentation, rats did not know the current uncertainty trial type. 95% bootstrap confidence intervals were constructed for differential suppression ratios to determine if discrimination was observed between each cue pair.

3.2.2.2 95% bootstrap confidence intervals

95% bootstrap confidence intervals were constructed using the bootci function in Matlab. For each bootstrap, a distribution was created by sampling the data 1,000 times with replacement. Studentized confidence intervals were constructed with the final outputs being the mean, lower bound and upper bound of the 95% bootstrap confidence interval.

3.2.2.3 Identifying cue-inhibited vIPAG neurons

All 245 neurons were screened for inhibitory firing during the first or last 5 s of danger and uncertainty cue presentation. This was achieved using a paired, two-tailed t-test comparing raw firing rate (spikes/s) during a 10 s baseline period just prior to cue onset with firing during the first or last, 5 s of cue presentation ($p < 0.0125$; Bonferroni corrected for 6 comparisons). Safety-responsive neurons were excluded because few neurons showed significant decreases in firing to safety.

3.2.2.4 Z-Score Normalization

For each neuron, and for each trial, firing rate (spikes/s) was calculated in 100 ms bins from 20 s prior to cue onset to 20 s following cue offset, for a total of 500 bins. Differential firing was calculated for each bin ($n = 500$) by subtracting mean baseline firing rate (2 s prior to cue onset) on that trial. Differential firing for each single-unit was Z-score normalized across all trials such that mean firing = 0, and standard deviation in firing = 1. Z-score normalization was applied to firing across all 500 bins, as opposed to only the bins prior to cue onset, in case neurons showed little/no baseline activity. Z-score normalized firing was analyzed with ANOVA using bin and trial-type as factors (Figure 3.2 A & C). F and p values are reported, as well as partial eta squared and observed power.

3.2.2.5 Identifying Flip and Sustain Neurons

Normalized firing (Z-score) of each cue-inhibited neuron was averaged over the first (early) and last (late) 5 s of danger cue presentation. K-means clustering ($k = 2$) applied to early and late firing of all danger-inhibited neurons ($n = 95$) revealed two clusters of approximately equal size. Neuron identity screening at this stage revealed four neurons previously analyzed in Aim 1. These neurons were removed and did not undergo further analyses. Aim 2 considers 91 cue-inhibited neurons for analysis: Flip neurons ($n = 45$), which were inhibited early but excited late, and Sustain neurons ($n = 46$), which maintained inhibition throughout danger cue presentation.

3.2.2.6 Waveform Analyses

Baseline firing rate, half duration and amplitude ratio of the mean waveform were determined for each Flip and Sustain neuron. Baseline firing rate (spikes/s) was calculated using the 10 s baseline period just prior to cue presentation. Half duration was

determined by measuring the time (ms) from peak depolarization to the trough of after-hyperpolarization and dividing by 2. Amplitude ratio was calculated using $(n - p) / (n + p)$, where p = initial hyperpolarization (in mV) and n = maximal depolarization (in mV).

3.2.2.7 Population Firing Analyses

Flip and Sustain population firing (Figure 3.2) were analyzed using analysis of variance (ANOVA) with trial type and bin (250 ms) as factors. ANOVA for normalized firing contained three trial types: danger, uncertainty and safety. Uncertainty trial types were collapsed because they did not differ for either suppression ratio or firing analysis. This was expected; during cue presentation rats did not know the current uncertainty trial type. F statistic, p value, observed power and partial eta squared are reported for effects and interactions. Bootstrap confidence intervals were performed for mean normalized firing to danger vs. uncertainty and uncertainty vs. safety during the first (early) and last (late) five seconds of cue presentation.

3.2.2.8 Single-unit Linear Regression

As in Chapter 2, single-unit linear regression was used to determine the degree to which fear output and threat probability explained trial-by-trial variation in single-unit firing during specific 1 s cue intervals. The 32 trials composing a single session were ordered by trial type and Z-score normalized firing was specified for each trial and interval. The fear output regressor was the mean suppression ratio for the entire 10 s cue for the specific trial. The probability regressor was the foot shock probability associated with each cue (danger = 1.00, uncertainty = 0.375, safety = 0.00). The regression output of greatest interest is the beta coefficient (β) for each regressor (fear output and threat probability), which quantifies the strength (greater distance from zero = stronger) and direction (>0 = positive, <0 =

negative) of the predictive relationship between each regressor and single-unit firing. ANOVA, bootstrap confidence intervals, sign test and Pearson's correlation coefficient were all used to analyze beta coefficients for Z-score normalized firing.

3.2.2.9 Threat probability tuning curve

Nine separate regression analyses were performed as above. Only now, the value assigned to the uncertainty component of the threat probability regressor was systematically increased from 0 to 1 in 0.125 steps (0.000, 0.125, 0.250, 0.375, 0.500, 0.625, 0.750, 0.875 and 1.000). The first regression used the value of 0.000, second regression 0.125 and so on. Regression was performed for each 1 s interval of the 10 s cue. Beta coefficients for the first 5 s of cue and the last 5 s of cue were averaged to produce early and late threat tuning curves.

3.3 Results

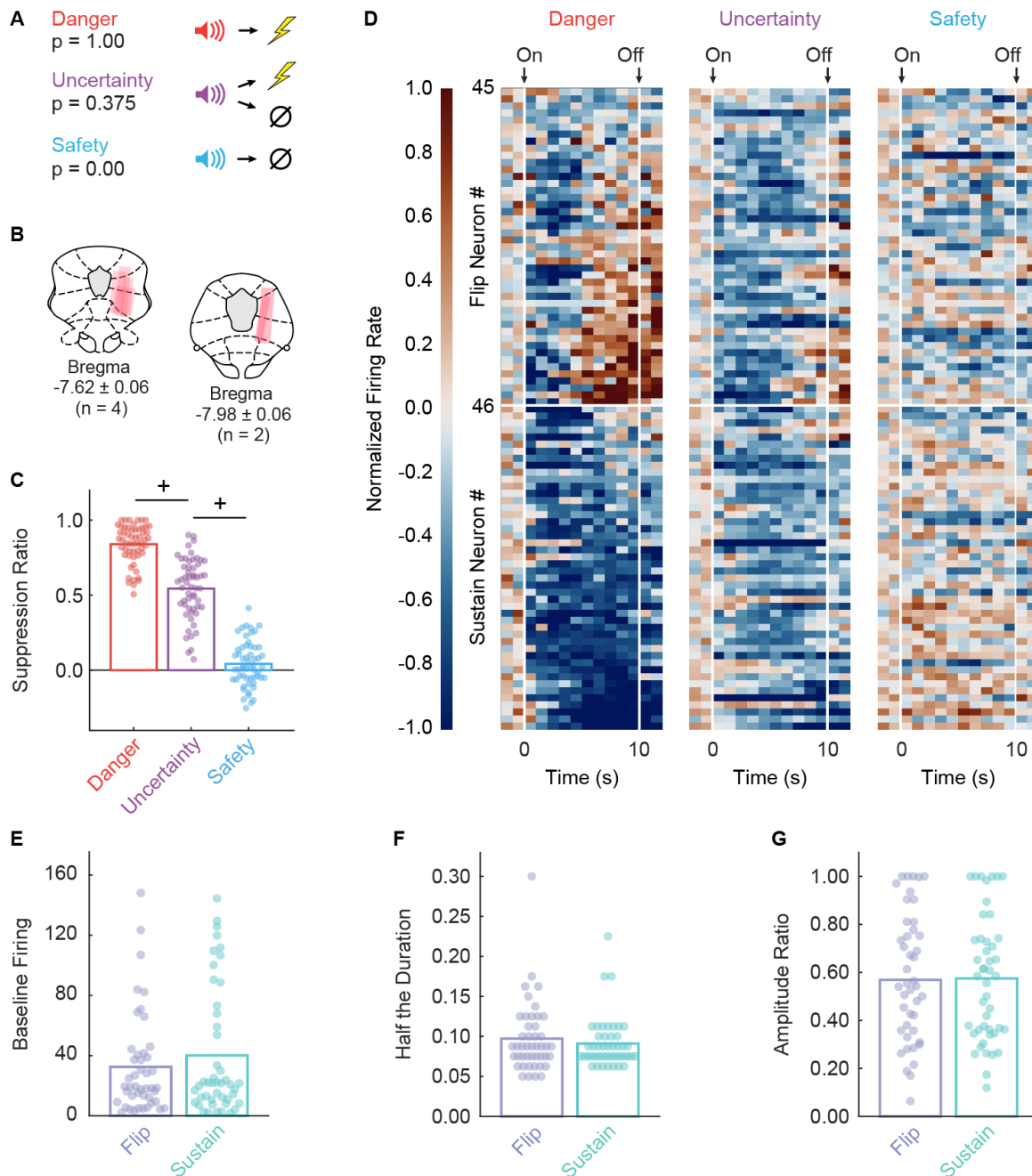


Figure 3.1 Fear discrimination, histology, heat plot and waveform characteristics

(A) Pavlovian fear discrimination consisted of three cues predicting unique foot shock probabilities: danger, $p = 1.00$ (red); uncertainty, $p = 0.375$ (purple); and safety, $p = 0.00$ (blue). (B) Microelectrode bundle placements for all rats ($n = 6$) and all neurons ($n = 245$) during recording sessions are represented by salmon bars. (C) Mean + individual (data

points) suppression ratio for danger, uncertainty, and safety is shown for all recording sessions ($n = 88$). (D) Normalized firing rate in 1 s intervals is shown for each Flip ($n = 45$, top) and Sustain ($n = 46$, bottom) neuron for each trial type (danger, uncertainty and safety). Color scale for normalized firing rate is shown to the right; red indicates high firing and blue low firing. Cue onset and offset are indicated. Single-unit waveform properties of Flip (periwinkle) and Sustain (seafoam) neurons are shown: (E) baseline firing rate, (F) half the duration, and (G) amplitude ratio. +95% bootstrap confidence interval for differential suppression ratio does not contain zero.

Maintained from Chapter 2, rats demonstrated excellent discriminative fear: high to danger, intermediate to uncertainty, and low to safety (Figure 3.1 C). ANOVA for suppression ratios for the total 10 s cue [factor: cue (danger vs. uncertainty vs. safety)] found a significant effect of cue ($F_{2,174} = 592.00$, $p = 2.32 \times 10^{-78}$, $\eta p^2 = 0.87$, observed power (op) = 1.00). This time, 95% bootstrap confidence intervals were constructed for differential suppression ratios to determine if discrimination was observed between each cue pair. Indicative of full cue discrimination, the 95% bootstrap confidence interval did not contain zero for danger vs. uncertainty (Mean = 0.30, 95% CI [(lower bound) 0.24, (upper bound) 0.34]) or uncertainty vs. safety (M = 0.50, 95% CI [0.44, 0.56]) (Figure 3.1 C).

3.3.1 VIPAG neurons flip to excitation or sustain inhibition over cue presentation

Out of 245 recorded neurons in six male Long Evans rats over 88 fear discrimination sessions, I identified 91 neurons (~37% of all neurons recorded) with significant decreases in firing rate to danger or uncertainty. Visualization of all cue-inhibited neurons revealed heterogeneous inhibition of danger firing during the last 5 seconds of cue presentation (Figure 3.1 D, left danger panel). K-means clustering was performed for all cue-inhibited neurons on early (first 5 s) and late (last 5 s) firing to danger, to determine

whether this heterogeneity reflected the activity of two separate populations. The first cluster ($n = 45$) consisted of neurons that were danger-inhibited early, but danger-excited late. These neurons are referred to as the Flip population. The second cluster ($n = 46$) consisted of neurons that were danger-inhibited early and late, and are referred to as the Sustain population. Independent samples t-tests for waveform properties revealed no differences between Flip and Sustain neurons, indicating these populations could only be distinguished by their function (Figure 3.1 E–G): baseline firing, $t_{89} = 0.95$, $p = 0.343$; half the duration, $t_{89} = 0.77$, $p = 0.444$; amplitude ratio $t_{89} = 0.10$, $p = 0.918$.

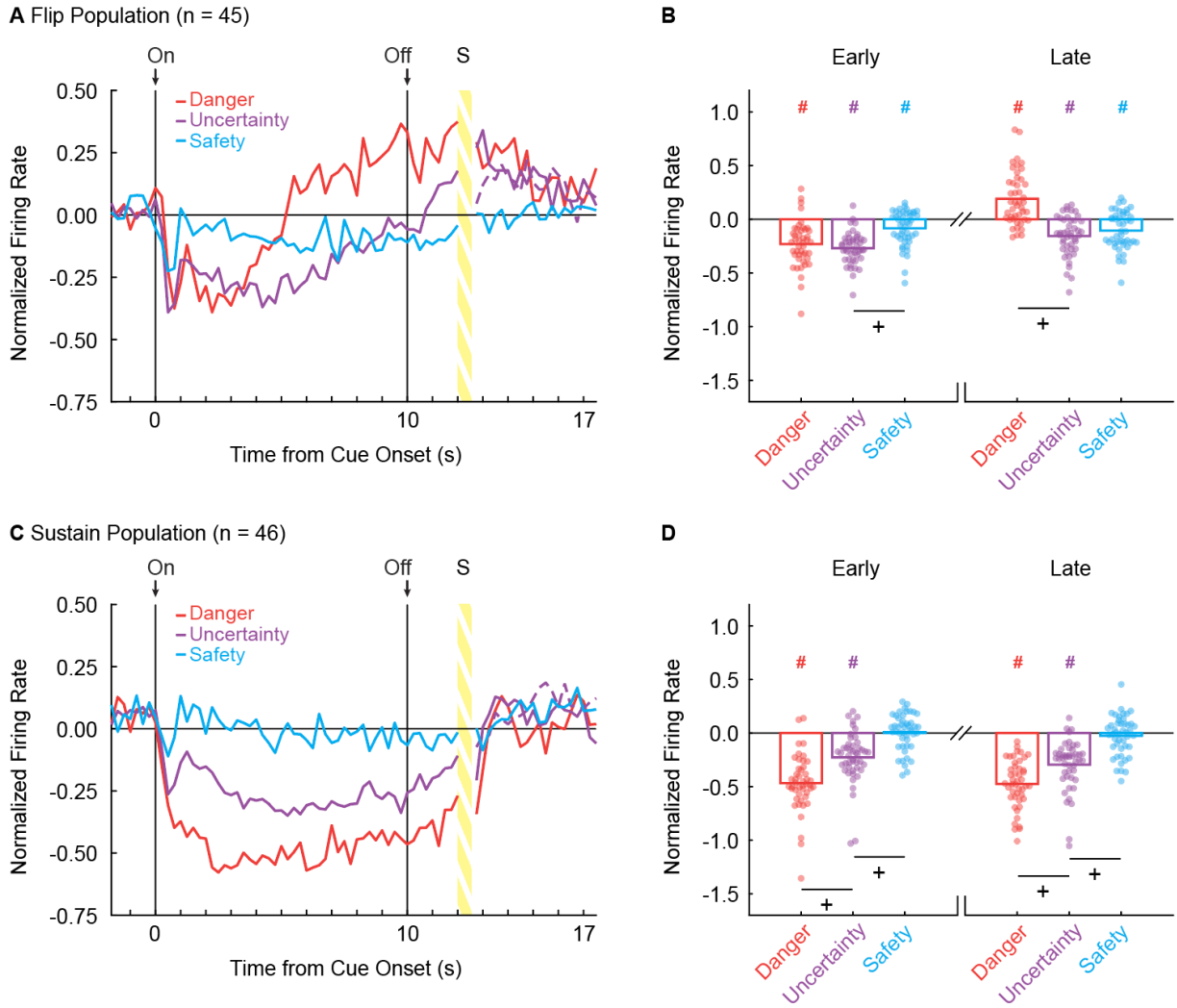


Figure 3.2 vIPAG neurons flip to excitation or sustain inhibition over cue presentation

(A) Mean normalized firing to danger (red), uncertainty (purple) and safety (blue) is shown for the 2 s pre-cue period, 10 s cue period, and 2 s delay period for the Flip population (n = 45). Cue onset (On) and offset (Off) are indicated by vertical black lines. (B) Mean (bar) and individual (data points), normalized firing for Flip neurons during the first 5 s of cue presentation (Early, left) and the last 5 s of cue presentation (Late, right) is shown for each cue. (C) Mean normalized firing for the Sustain population (n = 45), shown as in A. (D) Mean and individual (data points), normalized firing for Sustain neurons, as in B. +95% bootstrap confidence interval for differential firing does not contain zero. #95% bootstrap confidence interval for normalized firing does not contain zero.

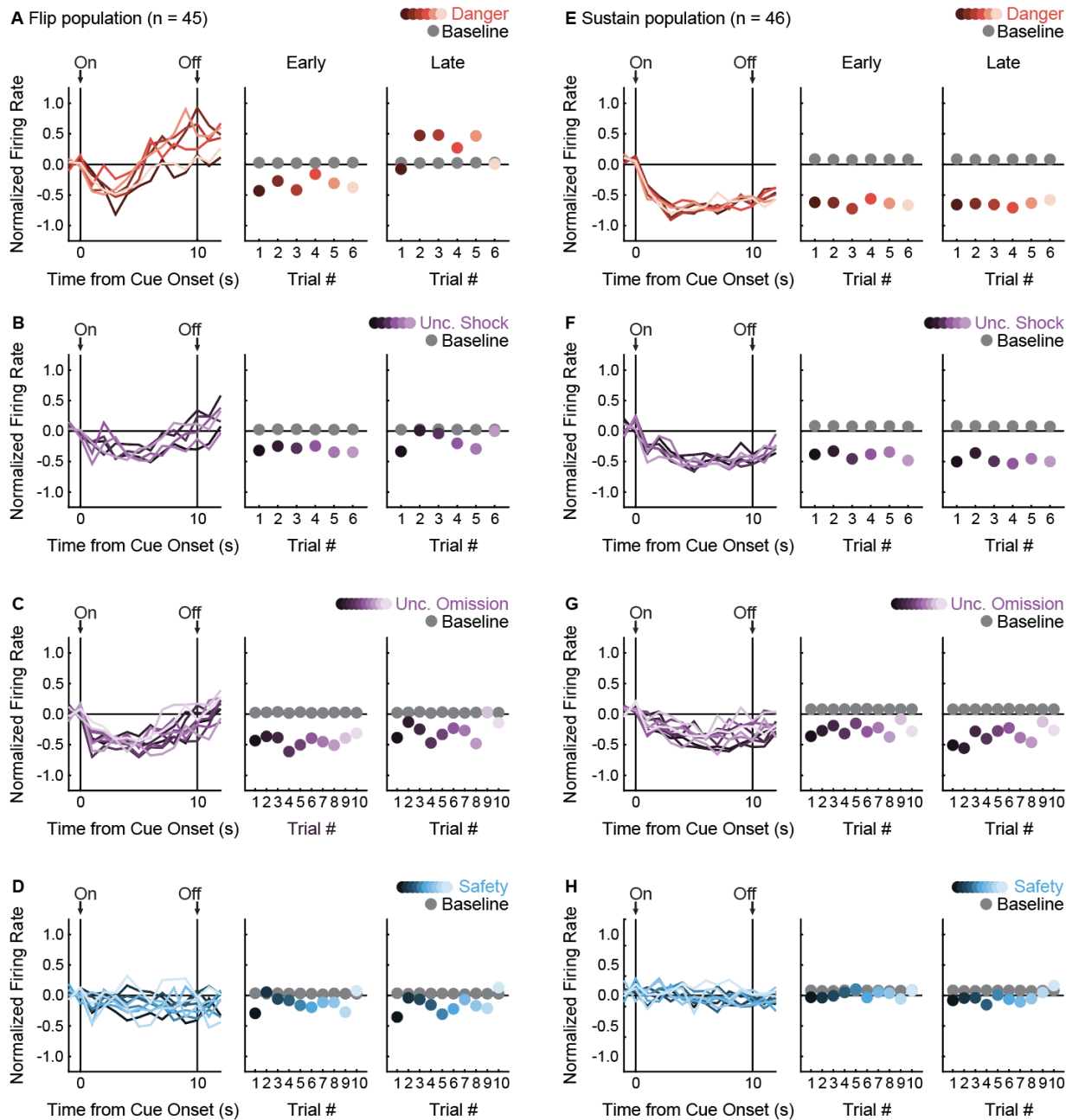


Figure 3.3 Trial by trial firing for Flip and Sustain neurons

(A, left) Normalized firing rate for the Flip population ($n = 45$) is shown across cue presentation for each of the six danger trials. Trials are color-coded from dark (first trial) to light (last trial) with 'On' indicating cue onset and 'Off' indicating cue offset. (A, center) Mean population firing rate for the first 5 s of cue presentation (early) is shown for each trial. Color scheme maintained from A, left. Mean population baseline firing rate (2 s prior to cue presentation) is shown for each trial (gray). (A, right) Firing for the last 5 s of cue presentation (late) shown as in A, center. Identical figures using unique color schemes

were made for each trial type: (B) uncertainty shock, (C) uncertainty omission and (D) safety. An identical set of figures were made for the Sustain population (n = 46; E–H).

3.3.2 Flip and sustain populations show differential cue firing

A vIPAG signal for fear output should begin at cue onset, continue throughout cue presentation, and discriminate between danger, uncertainty and safety. To determine if cue-inhibited vIPAG neurons complied with these requirements, I examined mean population activity over cue presentation for Flip and Sustain neurons. Flip neurons were initially inhibited to uncertainty and danger, but lesser to safety (Figure 3.2 A). As cue presentation continued, inhibition to uncertainty weakened toward safety and firing to danger switched from inhibition to excitation (Figure 3.2 A). ANOVA for normalized firing rate (Z-score) for the 45 Flip neurons [Figure 3.2 A; within factors: trial-type (danger, uncertainty and safety) and bin (250 ms bins encompassing: 2 s baseline, 10 s cue, and 2 s delay)] revealed main effects of cue ($F_{2,88} = 16.58$, $p = 7.74 \times 10^{-7}$, $\eta p^2 = 0.27$, $op = 1.00$) and bin ($F_{55,2420} = 14.83$, $p = 1.03 \times 10^{-114}$, $\eta p^2 = 0.25$, $op = 1.00$), but most critically a cue x bin interaction ($F_{110,4840} = 7.85$, $p = 8.89 \times 10^{-106}$, $\eta p^2 = 0.15$, $op = 1.00$). The population pattern was consistent across individual trials, though late danger excitation was least on the first and last trials (Figure 3.3)

95% bootstrap confidence intervals were constructed to determine if differential firing was observed early and late in cue presentation for Flip neurons. Differential firing was not observed to danger vs. uncertainty early (M = 0.04, 95% CI [-0.05, 0.11]), but was observed late when danger flipped to excitation (M = 0.35, 95% CI [0.26, 0.42]) (Figure 3.2 B, *plus signs). In contrast, differential firing was observed to uncertainty vs. safety early (M = -0.18, 95% CI [-0.26, -0.11]), but not late (M = -0.05, 95% CI [-0.14, 0.05])

(Figure 3.2 B). Furthermore, the 95% bootstrap confidence intervals for normalized firing rate did not contain zero for any cues in either period (Figure 3.2 B, #pound signs), indicating the Flip population was responsive to all cues early and late.

Sustain neurons showed differential inhibition of firing throughout cue presentation: danger < uncertainty < safety (Figure 3.2 C). ANOVA for normalized firing rate [Figure 3.2 C; factors maintained from above] revealed main effects of cue ($F_{2,86} = 72.25$, $p = 3.88 \times 10^{-19}$, $\eta p^2 = 0.63$, $op = 1.00$) and bin ($F_{55,2365} = 14.91$, $p = 6.13 \times 10^{-115}$, $\eta p^2 = 0.26$, $op = 1.00$), as well as a cue x bin interaction ($F_{110,4730} = 5.24$, $p = 1.17 \times 10^{-59}$, $\eta p^2 = 0.11$, $op = 1.00$). Differential firing was observed early and late in cue presentation. In support, the 95% bootstrap confidence interval for differential firing did not contain zero for danger vs. uncertainty (Early: $M = -0.24$, 95% CI [-0.35, -0.14], Late: $M = -0.18$, 95% CI [-0.25, -0.11]) and uncertainty vs. safety (Early: $M = -0.23$, 95% CI [-0.32, -0.15], Late: $M = -0.27$, 95% CI [-0.35, 0.18]) during either cue period (Figure 3.2 D, +plus signs). Even more, the 95% bootstrap confidence interval for normalized firing did not contain zero for danger and uncertainty during both periods, but *did* contain zero for safety during both periods (Figure 3.2 D, #pound signs). Not only was differential firing observed, but Sustain neurons were selectively responsive to danger and uncertainty.

Flip Population (n = 45)

Sustain Population (n = 46)

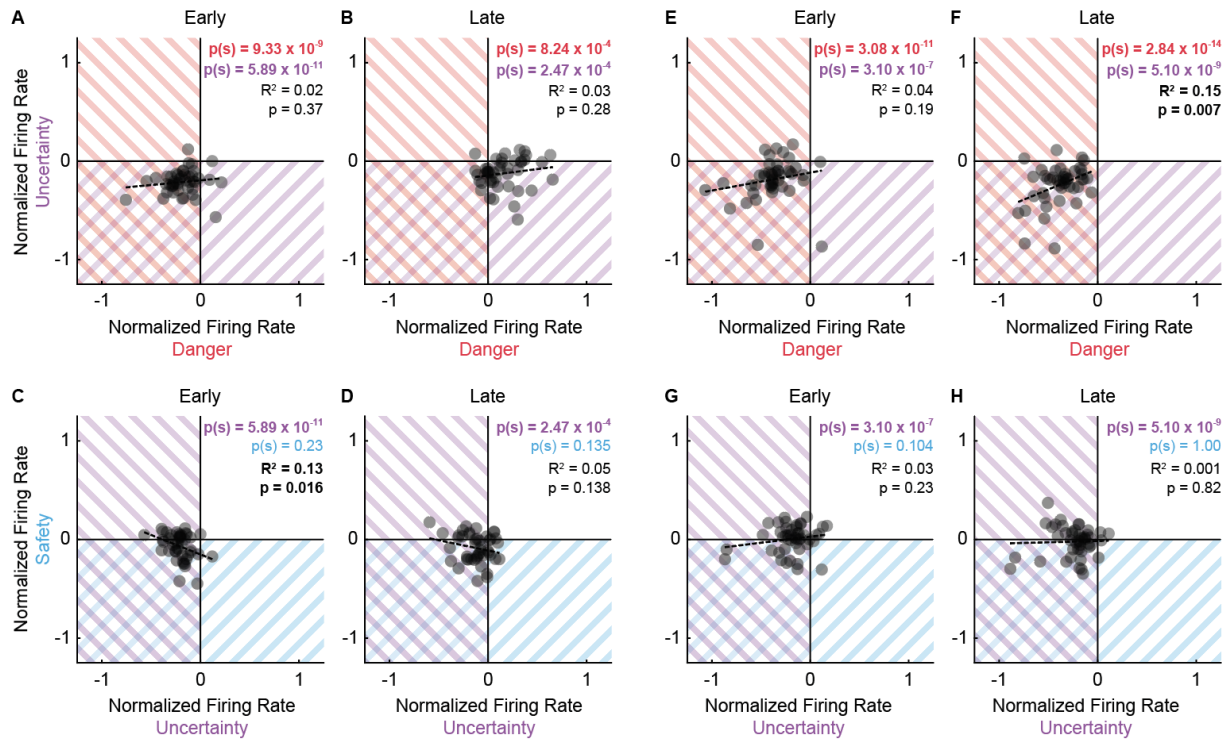


Figure 3.4 Population biases are evident in single-units

(A) Normalized firing to danger (red) vs. uncertainty (purple) during the first 5 s of cue presentation is plotted for all Flip neurons (n = 45). Trendline, the square of the Pearson correlation coefficient (R^2) with associated p value (p), and sign test p value ($p(s)$) are shown for each plot. (B) Normalized firing to danger vs. uncertainty during the last 5 s of cue presentation for all Flip neurons. (C) Normalized firing to uncertainty (purple) vs. safety (blue) during the first 5 s of cue presentation is plotted for all Flip neurons. (D) Normalized firing to uncertainty vs. safety during the last 5 s of cue presentation is plotted for all Flip neurons. All graph properties for E - H are maintained from A - D. (E) Normalized firing to danger (red) vs. uncertainty (purple) during the first 5 s of cue presentation is plotted for all Sustain neurons (n = 46). (F) Normalized firing to danger vs. uncertainty during the last 5 s of cue presentation for all Sustain neurons. (G) Normalized firing to uncertainty (purple) vs. safety (blue) during the first 5 s of cue presentation is plotted for all Sustain neurons. (D) Normalized firing to uncertainty vs. safety during the last 5 s of cue presentation is plotted for all Sustain neurons.

3.3.3 Population biases are evident in single-units

If the vIPAG signals fear output, one would expect population-level signals to be observed at the single-unit level. To examine this, we used sign tests to identify whether single-unit firing was biased away from zero during early and late cue presentation. Flip single-units were biased towards decreased firing to danger [Early: $(p(\text{sign}) = 9.33 \times 10^{-9})$] and uncertainty [Early: $(p(s) = 5.89 \times 10^{-11})$] during early cue presentation (Figure 3.4 A). Strikingly, and consistent with the population response, Flip neurons were biased towards increased firing to danger [Late: $(p(s) = 8.24 \times 10^{-4})$], but decreased firing to uncertainty [Late: $(p(s) = 2.47 \times 10^{-4})$] during late cue presentation (Figure 3.4 B). Contrary to the population result, there was no bias away from zero in single-unit firing to safety early or late (Figure 3.4 C & D). Single-unit biases of Sustain neurons mirrored those observed in the population. Sustain single-units showed a consistent bias toward decreased firing to danger [Early: $p(s) = 3.08 \times 10^{-11}$, Late: $p(s) = 2.84 \times 10^{-14}$] and uncertainty [(Early: $p(s) = 3.10 \times 10^{-7}$, Late: $(p(s) = 5.10 \times 10^{-9})$] throughout cue presentation (Figure 3.4 E & F). Further, Sustain single-units showed no bias in firing to safety in either cue period (Figure 3.4 G & H). Observing fully differential firing by single-units throughout cue presentation further marks Sustain neurons as a candidate for signaling fear output.

3.3.4 Flip neurons switch to threat probability signaling from early to late cue presentation

Descriptive analyses reveal two cue-inhibited populations with distinct temporal activity patterns. However, these analyses do not reveal the information signaled by each population. As in Chapter 2, I used linear regression for single-unit firing to formally test the degree to which Flip and Sustain neurons signaled fear output and threat probability (Figure 3.5). For each single-unit, the normalized firing rate was calculated for each trial (32 total: six danger, six uncertainty shock, 10 uncertainty omission, and 10 safety) in 1 s bins, over the course of cue presentation (14 s total: 2 s pre-cue, 10 s cue, 2 s post-cue). Fear output was the suppression ratio on that trial. Threat probability was the shock probability associated with the cue: danger: 1.00, uncertainty: 0.375 and safety: 0.00. Fear output and threat probability were used as regressors to explain trial-by-trial variance in single-unit firing. The regression output for each single-unit was a beta coefficient quantifying the strength ($|\beta|$ = stronger) and direction ($\beta > 0$ = positive and $\beta < 0$ = negative) of the predictive relationship between the regressor and single-unit firing. Beta coefficients for single-units were subjected to ANOVA with regressor (fear output vs. threat probability) and interval (1 s cue intervals) as factors.

Single-unit regression revealed an early-to-late switch in threat probability signaling in Flip neurons (Figure 3.5 A). ANOVA for beta coefficients with factors of regressor (fear output vs. threat probability) and interval was performed for three periods: baseline (two intervals), cue (10 intervals) and delay (two intervals). The baseline and delay ANOVAs returned no main effects or interactions (all F s < 0.6 , all p s > 0.4). In contrast, the cue ANOVA found significant main effects, but most critically a regressor x interval interaction ($F_{9,396} = 3.56$, $p = 2.85 \times 10^{-4}$, $\eta^2 = 0.075$, $op = 0.990$). The interaction was driven by

negative beta coefficients for fear output and threat probability in two, early cue intervals (95% bootstrap confidence interval did not contain zero, #pound signs), that gave way to positive beta coefficients specific to threat probability in all late cue intervals (95% bootstrap confidence interval did not contain zero, #pound signs; Figure 3.5 A). Further supporting the interaction, beta coefficients for Flip single-units were not biased away from zero for fear output and threat probability during the first 5 s cue period [Probability Early: $p(s) = 0.37$, Fear Output Early: $p(s) = 0.14$] (Figure 3.5 B). However, there was positive bias toward threat probability, but not fear output, during the last 5 s cue period [Probability Late: $p(s) = 2.47 \times 10^{-4}$, Fear Output Late: $p(s) = 0.77$] (Figure 3.5 C). Fear responses are sustained for the cue duration, yet Flip neurons do not consistently signal threat probability or fear output in early cue presentation. The inconsistency in signaling reveals that Flip neurons are not a suitable neural substrate for governing fear output throughout cue presentation.

3.3.5 Sustain neurons signal fear output and threat probability throughout cue presentation

Linear regression revealed consistent signals for fear output and threat probability in Sustain neurons. Beta coefficients were negative at cue onset for each regressor, and maintained negativity throughout cue presentation (Figure 3.5 D). ANOVA for beta coefficients with factors of regressor and interval was performed as before for baseline, cue and delay. The baseline ANOVA returned no main effects or interaction (all $F_s < 1$, all $p_s > 0.3$). The cue ANOVA found only a main effect of bin ($F_{9,405} = 4.23$, $p = 2.90 \times 10^{-5}$, $\eta p^2 = 0.086$, $op = 0.997$), indicating similar signaling of fear output and threat probability. The delay ANOVA found only a main effect of regressor ($F_{1,45} = 7.27$, $p = 0.01$, $\eta p^2 = 0.14$, $op = 0.751$), indicating a difference in signaling of fear output and threat probability

during the delay period. For each regressor over the 10, 1 s cue intervals, the 95% bootstrap confidence interval did not contain zero, indicating that fear output and threat probability signaling were both observed throughout cue presentation. Consistent with equivalent signaling of fear output and probability throughout cue presentation, single-unit beta coefficients for each regressor were biased away from zero for fear output and threat probability during early and late cue presentation [Probability (Early: $p(s) = 1.83 \times 10^{-6}$ and Late: $p(s) = 4.06 \times 10^{-5}$), Fear Output (Early: $p(s) = 0.002$ and Late: $p(s) = 1.56 \times 10^{-4}$)] (Figure 3.5 E & F). Further, single-unit beta coefficients for threat probability and fear output were correlated early and late (Early: $R^2 = 0.41$, $p = 2.38 \times 10^{-6}$ and Late: $R^2 = 0.37$, $p = 9.55 \times 10^{-6}$). The majority of Sustain single-units showed negative beta coefficients for both regressors. However, even the extremes of the distribution showed signaling for both regressors, albeit in opposing directions. Sustain neurons signal fear output *and* threat probability throughout cue presentation.

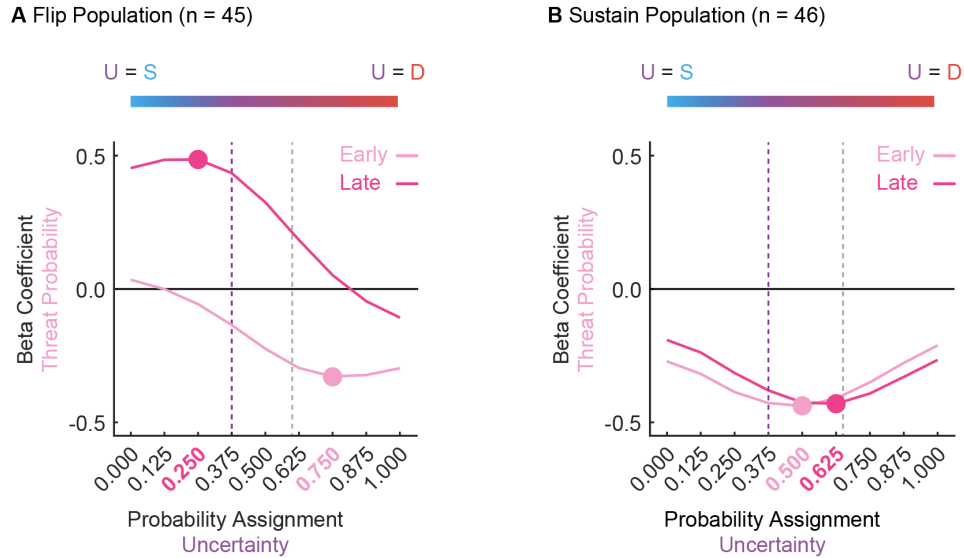


Figure 3.6 Probability tuning

(A) Mean beta coefficient for probability is shown for early (light pink) or late (hot pink) cue presentation for each of nine uncertainty assignments for the Flip population (n = 45). The peak or trough of each curve is indicated by a single point with the corresponding uncertainty assignment highlighted in the same color on the x axis below. Purple dashed line indicates the actual foot shock probability associated with uncertainty ($p = 0.375$). Gray dashed line indicates the mean proportional distance of uncertainty between danger and safety (suppression ratio). The blue-to-red color bar at the top of the figure demonstrates that a leftward shift along the x-axis reflects an uncertainty assignment similar in quality to safety ($p = 0.000$) versus those that would be more similar to a danger cue on the far right ($p = 1.000$). (B) All graph properties maintained from A, but applied to the Sustain population.

3.3.6 Differential threat tuning in flip and sustain neurons

The threat probability regressor in the above analyses utilized the actual shock probability assigned to uncertainty (0.375). Of course, the subjects, and by extension their neurons, had no a priori knowledge of the actual shock probability. Thus, it is possible that Flip and Sustain single-units are ‘tuned’ to alternative shock probabilities. To test this, we performed single-unit linear regression for normalized firing in each 1 s interval as before, maintaining the probabilities for danger (1.00) and safety (0.00), but incrementing the

probability assigned to uncertainty from 0 to 1 in 0.125 steps (0.000, 0.125, 0.250, 0.375, 0.500, 0.625, 0.750, 0.875, and 1.000). Threat probability beta coefficients were averaged over early and late cue presentation. The mean beta coefficient for each uncertainty assignment is plotted as a threat-tuning curve, early and late, for each population (Figure 3.6).

Flip neurons were tuned to alternative foot shock probabilities and this tuning changed from early to late cue presentation. Early threat overestimation (equating uncertainty to danger) gave way to late underestimation (equating uncertainty to safety). The tuning curve trough for early cue presentation occurred at 0.750 (Figure 3.6 A, light pink); overshooting the actual probability of 0.375 (Figure 3.6 A, dashed purple line) and exceeding mean fear output of 0.625 (Figure 3.6 A, dashed gray line). The tuning curve peak for late cue presentation occurred at 0.250 (Figure 3.6 A, dark pink); undershooting the actual probability and mean fear output (Figure 3.6 A, dashed purple line and dashed gray line, respectively). ANOVA for beta coefficient with factors of time (early vs. late) and uncertainty assignment (9) found both main effects and the interaction to be significant (all $F_s > 13$, all $p_s < 0.001$). The relative firing patterns of Flip neurons do not approximate the actual probability of foot shock or the pattern of fear output, and further indicate that these neurons are unlikely to govern fear output.

In contrast, Sustain neuron tuning consistently fell between the bounds of the actual foot shock probability and the mean fear output, changing only subtly over cue presentation (Figure 3.6 B). The trough of the tuning curve occurred at an assignment of 0.500 early and at an assignment of 0.625 late. ANOVA found a main effect of assignment ($F_{8,360} = 5.66$, $p = 8.85 \times 10^{-7}$, $\eta p^2 = 0.112$, $op = 1.00$) and a time x assignment interaction ($F_{8,360} =$

3.25, $p = 0.001$, $\eta p^2 = 0.067$, $op = 0.971$). The stability of Sustain tuning and the bias toward mean fear output further suggests this population as a candidate for fear output.

3.4 Discussion

Chapter 3 set out to scrutinize cue-inhibited vIPAG neurons and determine if their activity reflected fear output. I recorded vIPAG single-unit activity while rats discriminated between danger, uncertainty and safety, found two cue-responsive populations, and revealed a long-awaited complete neural correlate for fear output in the vIPAG. Flip neurons were inhibited to danger early, but excited to danger late. Sustain neurons maintained graded decreases in firing to threat-related cues throughout cue presentation. Flip activity reflected threat probability signaling during the last half of cue presentation. Sustain activity consistently reflected fear output alongside an estimate of threat probability throughout the entirety of cue presentation. Activity reflecting fear output has now been identified in the vIPAG, albeit residing in an unexpected, cue-inhibited population. However, it co-exists with signals for threat probability: within the same population and among other functional populations.

Although Flip neurons are not suitable candidates for signaling fear output, they may help sustain threat estimates in the absence of explicit stimuli (McEchron et al., 1998; Buchel et al., 1999), or simply estimate when a shock will occur. Consistent with this speculation, peak activity of Flip neurons occurred just prior to shock presentation and declined toward baseline shortly after. This finding is in general accord with previous work demonstrating a shift from distal to proximate threats, corresponds to a shift from prefrontal to periaqueductal activity (Mobbs et al., 2007; Mobbs et al., 2010). This may sound similar

to the proposed role for the Ramping population in Chapter 2, which will be addressed in Chapter 5.

By contrast, patterned activity of Sustain neurons complies with basic assumptions of a complete neural correlate for fear output. Sustain neurons decreased firing to threat-related cues, but did not decrease firing to safety. Moreover, neural activity fully discriminated between danger, uncertainty and safety from cue onset through shock presentation, before returning to baseline. Population biases toward fear output and threat probability were maintained at the single-unit level. Interestingly, while threat probability signaling was observed in Sustain single-units, the probability to which neurons were tuned exceeded the actual probability of 0.375, better approximating fear output. Although causal evidence that Sustain neurons drive a discriminative fear response is beyond the scope of these results, a complete neural correlate for fear output in a population of vIPAG neurons has been identified.

An influential theory posits that vIPAG output is achieved through a disinhibition mechanism (Tovote et al., 2016): GABAergic vIPAG interneurons with high baseline firing rates receive inputs from GABAergic CeA projection neurons (Figure 1.3 B). Activation of GABAergic projections from the CeA (increased firing in response to danger cues) inhibits and reduces firing of GABAergic vIPAG interneurons. In turn, this interneuron inhibition releases local inhibition of vIPAG glutamatergic projection neurons, which increase firing to promote freezing through downstream projections. Consistent with a disinhibition mechanism, we observed Sustain neurons that have high baseline firing rates (Figure 3.1 E, purple). However, we observed many Sustain neurons that had low baseline firing rates, including those with baseline rates just above zero. While we cannot conclusively

determine neuron type from baseline firing, it is likely that cue-inhibited neurons are not uniformly GABAergic interneurons. While inconsistent with a pure disinhibition mechanism, our results are consistent with an alternative view in which the vIPAG contains unique output populations that separately convey information via excitation and inhibition (Lau and Vaughan, 2014). Most likely, the vIPAG utilizes disinhibition, as well as independent signaling via cue-excited and cue-inhibited projection populations to inform behavior.

CHAPTER 4: Is endogenous cSN necessary for fear suppression?

4.1 Introduction

Fear is the product of a larger circuit that extends beyond the vIPAG. Whereas a role for the vIPAG in fear is commonplace, a role for the substantia nigra (SN) in fear stands apart from its canonical associations with movement and reward processes (Schultz, 1997; Groenewegen, 2003; Chinta & Andersen, 2005; Bouchet et al., 2018; Sonne et al., 2020). However, new interest in examining the substantia nigra through a fear lens, by way of its dopamine population, is beginning to surface. Dopamine is a widely examined neuromodulator with distinct neural populations scattered throughout the midbrain. Traditionally implicated in movement, reward value and reward prediction error, recent evidence suggests a role for dopamine in mediating aversive functions (Lutas et al., 2019; Robinson et al., 2019).

Previous work has tied dopamine activity to fear extinction (Abraham et al., 2014), but only recently has this association been investigated in nigral dopamine. Specifically, activation of dopamine in the SN has been implicated fear extinction facilitation (Bouchet et al., 2018). In this preparation, Gq-coupled receptors exclusively activated by designer drugs (Gq-DREADDs) were employed to increase phasic activation of a discrete population of dopamine neurons during fear extinction. Rats that received SN Clozapine-N-oxide (SN CNO: active DREADD group) and vehicle (control group) rats both acquired comparable levels of fear extinction during two days of 20 CS presentation. SN CNO rats displayed significantly less freezing versus controls during extinction and demonstrated blocked renewal of fear in a new context. Together, these findings strongly link SN dopamine with fear extinction and renewal. However, there is still much left to uncover. Although a link with fear extinction has been established, a role for the SN in fear conditioning or discrimination remains unknown. Further, chemogenetic activation of the

SN is insufficient to determine whether endogenous SN activity is necessary for fear suppression, and therefore extinction. Finally, cell types other than dopamine may contribute to a role for the SN in fear. Given a direct monosynaptic GABAergic projection from the SN to the vIPAG (Kirouac et al., 2004), at the very least, the SN has the ability to interact with downstream signals for threat probability and fear output.

To expand on previous work connecting the SN and fear, I paired a similar version of the fear discrimination procedure from chapters 2 and 3 with bilateral optogenetic inhibition of the caudal substantia nigra to investigate whether endogenous cSN activity is necessary for suppression of defensive behavior. In this procedure, three auditory cues predict unique foot shock probabilities as before: danger ($p = 1.00$), uncertainty ($p = 0.25$) and safety ($p = 0.00$). However, a foot shock probability of $p = 0.25$ was assigned to the uncertainty cue. A lower probability of shock was utilized in this preparation because there are far fewer trials required for optogenetic experiments versus in vivo recordings, and a shock probability of 0.25 is sufficient to achieve complete discrimination (danger > uncertainty > safety) on a shorter experimental timeline.

4.2 Methods

4.2.1 Subjects

Subjects were 17 male Long Evans rats approximately 60 days old on arrival, obtained from Charles River Laboratories, and maintained on a 12-hr light cycle (lights off at 6:00 PM). Upon arrival, rats were individually housed and acclimated to the animal facility with food and water freely available for three days. Following acclimation, rats were restricted to and maintained at 85% of their free-feeding body weight. All rats were returned to ad libitum food, received surgery, recovered, and were once again maintained at 85% of

their free-feeding body weight for the duration of behavioral testing. All protocols were approved by the Boston College Animal Care and Use Committee and all experiments were carried out in accordance with the NIH guidelines regarding the care and use of rats for experimental procedures.

4.2.2 Optogenetic Ferrule and Fiber Optic Cable Assembly

Optical ferrules were constructed using 2.5mm Ceramic Dome Ferrule Assemblies: 230um ID, bore tolerance: -0/+10um, Concentricity < 20um (MM-FER2002S15-2300: Precision Fiber Products, Chula Vista, CA) paired with multimode optical fiber, 0.22 NA, High-OH, Ø200 µm Core for 250 - 1200 nm (FG200UEA: ThorLabs, Newton, NJ). Ferrules were assembled, polished, and inspected for flares. Light output was tested with a Si Sensor Power Meter (PM160: Thorlabs, Newton, NJ) and a 532nm, 500 mW green laser identical to those used for light illumination during behavior testing (Shanghai Laser & Optics Century Co., Ltd., Shanghai, China). Ferrules were polished until 30-40mW of light from the laser source could reliably produce 25mW of light output from an attached ferrule. Source laser mW requirements (to achieve 25mW ferrule output) were matched for each ferrule pair implanted during surgery. This way, the same amount of source laser light would result in equivalent light intensities in each hemisphere. Bilateral behavior cables consisted of a single metal-shielded shaft encompassing two cladded multimode optical fibers, 0.39 NA, High-OH, Ø200 µm Core for 300 - 1200 nm, TECS Clad: ThorLabs, Newton, NJ). A wye splitter at each end separated each fiber from the central shaft to accommodate individual ferrule-to-ferrule connections with implants on the rat's head and multimode FC connections to the 1x2 rotary commutator above the experimental chamber (MM-CON2004-2300 MM FC Connectors with 230um ferrules:

Precision Fiber Products, Chula Vista, CA). Following fabrication, all cables were re-tested prior to each illumination behavior session to ensure that there was a difference of no more than 5 mW of laser output between each side of the cable. Finally, the source laser power was calibrated for each light illumination session, so that the final cable output would pass the amount of light required for paired ferrule implants to permit either 12.5mW or 25mW light delivery into the brain. Detailed Ferrule and Cable Assembly protocols are available for download at: <http://mcdannalldlab.org/resources/optogenetics>.

4.2.3 Surgery

Stereotaxic surgery was performed in aseptic conditions under isoflurane anesthesia (1–5% in oxygen). Rimadyl (subcutaneous, 5 mg/kg), Lidocaine (subcutaneous, 2%), and Lactated Ringer’s solution (~2–5 mL) were administered preoperatively (R - 024751, L - 002468 & LR - 14792: Henry Schein Vet, Waltham, MA). The skull was exposed via midline incision and scoured in a crosshatch pattern with a scalpel blade to increase resin adhesion. Nine holes were drilled: five for screws, two for infusion and two for ferrules. Five screws were installed in the skull to stabilize the connection between the skull, bilateral optical ferrule implants and a protective head cap (screw placements: two anterior to bregma, two between bregma and lambda about ~3 mm medial to the lateral ridges of the skull, and one on the midline ~5 mm posterior of lambda). Infusions were delivered at a rate of ~0.11 μ l/min, using a 2 μ l Neuros syringe (65459-01: Hamilton Company, Reno, NV) controlled by a microsyringe pump (UMP3-2: World Precision Instruments, Sarasota, FL). Rats received bilateral 0.5 μ l infusions of halorhodopsin, AAV5-hSyn-eNpHR3.0-YFP (n = 9) or a control fluorophore AAV5-hSyn-EYFP (n = 8) aimed at the caudal substantia nigra (cSN): AP -7.10mm, ML +/- 1.90mm, DV -7.75mm

(UNC Vector Core, Chapel Hill, NC). Bilateral optical ferrules were implanted dorsal to the cSN at a 15° angle: AP -6.85mm, ML +/- 3.08mm, DV -6.50mm. Ferrule implants were protected by a black, light-occluding head cap made from a modified 50mL falcon tube. The head cap and ferrules were cemented to the skull using orthodontic resin (C 22-05-98: Pearson Dental Supply, Sylmar, CA). Post-surgery, rats received 8-12 days of undisturbed recovery and 14 days of oral Cephalexin (049167: Henry Schein Vet, Waltham, MA) mixed with Froot Loops to encourage consumption. Dust caps protected the ends of optical ferrule implants during recovery and all behavior sessions when fiber optic cables were not in use.

4.2.4 Behavior Apparatus

The apparatus consisted of four individual experimental chambers (internal dimensions: 30.5 cm x 24.1 cm x 29.2 cm) with aluminum front and back walls, clear acrylic sides and top, and a grid floor (0.48 cm diameter bars spaced 1.6 cm apart). Each grid floor bar was electrically connected to an aversive foot shock generator (Med Associates, St. Albans, VT). An external food cup was present at the center of one wall 2.5 cm above the grid floor. A central panel nose poke opening, equipped with infrared photocells (sampled at approximately 1 kHz), was centered 8.5 cm above the food cup. Each experimental chamber was enclosed in a sound-attenuating shell. Green lasers (532nm) were used to illuminate the caudal substantia nigra. A 5-inch diameter hole in the chamber ceiling funneled to a ~1.5 inch whole just below the commutator, permitting fiber optic cables to be threaded into the experimental chamber from above, and allowed them to move freely with each animal during optogenetic behavior sessions. Fiber optic cables were suspended from a 1 x 2 fiber optic rotary commutator (Doric: Quebec, Canada) mounted

to the shell ceiling. Two speakers were mounted 20 cm apart on the shell ceiling. Chambers were illuminated with a small strip of red LED lights mounted on the shell ceiling.

4.2.5 Behavioral procedures

4.2.5.1 Pellet Exposure

Each rat was exposed to 4 grams of reward pellets in their home cage on two days, followed by one day of automatic pellet delivery to the food cup inside the experimental chamber (F0021, Bio-Serv Flemington, NJ).

4.2.5.2 Nose Poke Acquisition

Each rat was shaped to nose poke for pellet delivery using a fixed ratio schedule in which one nose poke yielded one pellet. Nose poke acquisition sessions lasted for 30 minutes or until approximately 50 nose pokes were completed. Rats moved on to variable interval (VI) schedules in which nose pokes were reinforced on average every 30 s (day 1), or 60 s (days 2-5). For the remainder of behavioral testing, nose pokes were reinforced on a VI-60 schedule independent of all Pavlovian contingencies.

4.2.5.3 Cue Pre-exposure

Each rat was pre-exposed to the three auditory cues to be used in Pavlovian discrimination in two, 42-minute sessions. The 10 s auditory cues were repeating, 500 ms motifs of a horn, siren or broadband click and can be heard as .wav files here: <http://mcdannaldlab.org/resources/ardbark>. Previous studies have found these cues to be equally salient, yet readily discriminable (Wright et al., 2015; DiLeo et al., 2016). Sessions consisted of four presentations of each cue (12 total presentations) with a mean

inter-trial interval of 3.5 min. The order of trial type presentation was randomly determined by the behavioral program, and differed for each rat during each session.

4.2.5.4 Pavlovian Fear Discrimination

Following pre-exposure, all rats received 8, 64-minute behavior-only discrimination sessions. A single session consisted of 18 cue trials: four danger trials, six uncertainty no-shock trials, two uncertainty shock trials, and six safety trials, with a mean inter-trial interval of 3.5 min. Each auditory cue was associated with a different probability of foot shock (0.5 mA, 0.5 s): danger, $p = 1.00$; uncertainty, $p = 0.25$; and safety, $p = 0.00$. The physical identities of the cues were counterbalanced, so that the same sound was associated with different probabilities of foot shock across rats. Foot shock was administered two seconds following the termination of the auditory cue.

4.2.6 Light Illumination

The remaining 10 discrimination sessions were divided into 5, 2-session blocks. All rats were habituated to optogenetic cables in the first 2-session block. For one group of rats [(eNpHR ($n = 3$), YFP ($n = 4$))], the next 8 sessions consisted of 2-session blocks of CUE illumination, no illumination, ITI illumination and no illumination. During CUE illumination sessions, 532 nm green light was delivered bilaterally for the entirety of all 10 s cues. During ITI illumination sessions, light was delivered for 10 s ITI periods between cue trials. No illumination sessions provided measures of Pre and Post illumination fear behavior for comparison to illumination trials, rats were not plugged into behavior cables during block three and block five of no illumination. A second group of rats [(eNpHR ($n=6$), YFP ($n=4$))] received the exact same procedure, only ITI illumination was given first to counterbalance for potential order effects. Due to a programming error, ITI illumination

sessions in each group received one additional 10-second illumination (versus CUE illumination sessions) for a total of 19, 10 s illumination periods.

Increased intensity of laser illumination could result in more firing inhibition and stronger behavioral outcomes. Unsure of which illumination strength would be sufficient and ideal to inhibit cSN activity of transduced neurons, I tested two illumination intensities: a more typical intensity of 12.5mW, and a higher intensity of 25mW. If SN activity is required for fear suppression, 12.5mW of laser illumination may be insufficient to induce a change in behavior. If this were the case, I would expect to see a dose effect: 12.5mW illumination would result in lesser or no behavioral change compared to 25mW illumination. However, if 12.5mW illumination was sufficient to saturate the transduction area and induce behavior change, both illumination intensities would result in equivalent behavioral effects.

To examine the possibility of an effect of dose with respect to laser illumination, animals in each group received either 12.5mW or 25mW of 532nm green laser light during the optogenetic procedure. Of the animals that received CUE illumination first [(eNpHR (n=3), YFP (n=4)], all 4 YFP controls and two of three eNpHR rats received 25mW illumination. Of the animals that received ITI illumination first [(eNpHR (n=6), YFP (n=4)], two YFP controls and two eNpHR rats received 12.5mW bilateral illumination of the cSN; the remaining 2 YFP controls and 4 eNpHR rats received 25mW illumination. Altogether, five animals received 12.5mW illumination and the remaining twelve received 25mW bilateral illumination. Both illumination intensity (12.5mW vs. 25mW) and order of illumination (CUE illumination first vs. ITI illumination first) were included as factors main ANOVA findings.

4.2.7 Histology

Rats were deeply anesthetized using isoflurane, perfused with 0.9% biological saline and 4% paraformaldehyde in a 0.2 M potassium phosphate buffered solution. Brains were extracted, post-fixed in 10% neutral-buffered formalin for 24 hr, stored in 10% sucrose/formalin and sectioned via microtome. All brains were processed for fluorescent microscopy using anti-tyrosine hydroxylase immunohistochemistry (Millipore Sigma AB152 primary paired with Jackson Immuno 711-585-152 pre-conjugated Alexa 594 secondary) and NeuroTrace 435/455 (ThermoFisher N21479).

4.2.8 Statistical Analysis

4.2.8.1 Behavior Analyses

Behavioral data were acquired using Med Associates, Med-PC IV (RRID:SCR_012156) software. Raw data were processed in Matlab (RRID:SCR_001622) to extract time stamps for nose pokes, cues, foot shocks and illumination. Baseline nose poke rate was the mean of the 20 s prior to cue presentation. Cue nose poke rate was the mean of the 10 s cue. Suppression of rewarded nose poking was calculated as a ratio: $(\text{baseline poke rate} - \text{cue poke rate}) / (\text{baseline poke rate} + \text{cue poke rate})$ (Rescorla, 1968; Pickens et al., 2009; Anglada-Figueroa and Quirk, 2005; Arico and McNally, 2014; Lee et al., 2005; McDannald and Galarce, 2011). A ratio of '1.00' indicated high fear and '0.00' indicated low fear. Gradations between these upper and lower bounds indicated intermediate levels of fear. Use of the suppression ratio permitted an objective measure of fear across cue and illumination presentations.

Suppression ratios were analyzed using repeated measures ANOVA in SPSS (RRID:SCR_002865) with between factors: group (eNpHR/YFP), light intensity (12.5 mW

or 25 mW of laser illumination) and order (CUE versus ITI illumination first) and within factors: cue (danger, uncertainty, safety), block (2-session blocks 1 through 5) & Illumination (CUE versus ITI laser illumination). Partial eta squared (ηp^2) and observed power (op) are reported for all ANOVA results as indicators of effect size. 95% bootstrap confidence intervals were constructed to support ANOVA results. Pearson's correlation coefficient (R^2) was used to compare suppression ratios during cue and illumination. For all analyses, $p < 0.05$ is considered significant.

4.3 Results

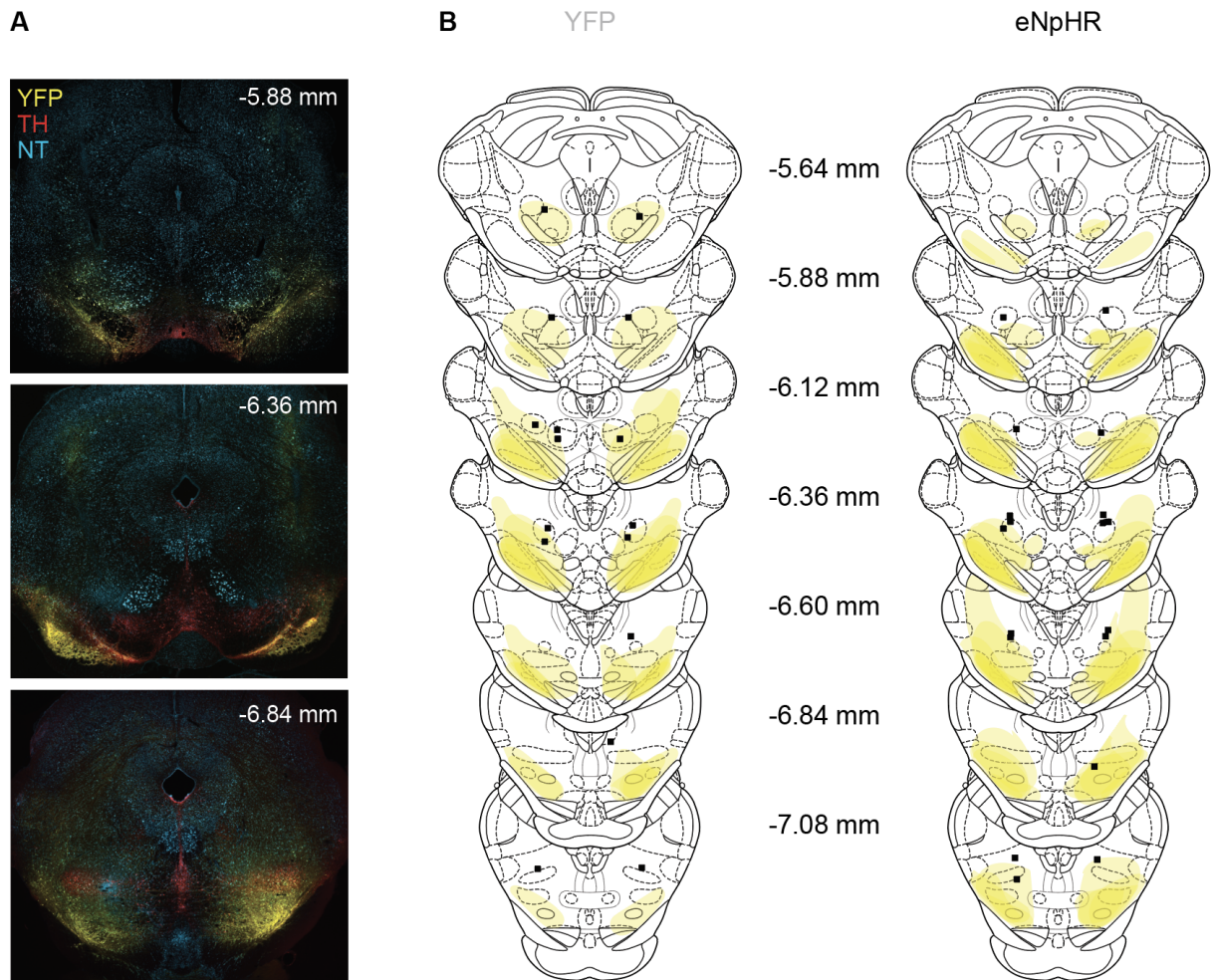


Figure 4.1 Histology and transduction mapping

(A) Representative fluorescent microscopy images of viral transduction from YFP control with bilateral infusions of AAV-hSyn-EYFP (yellow). Fluorescent immunohistochemistry labeling of tyrosine hydroxylase (TH) for rostrocaudal orientation (red), and NeuroTrace (NT) neuron cell body labeling for visualizing overall slice composition (blue). (B) Extent of transduction (yellow) and fibre optic ferrule placements (black squares) plotted for all rats YFP (n = 8, left) and eNpHR (n = 9, right). Atlas images redrawn from (Paxinos & Watson, 2007).

Seventeen adult male, Long Evans rats received bilateral infusions of either enhanced halorhodopsin (eNpHR: AAV-hSyn-eNpHR3.0-EYFP) or a control fluorophore (YFP control: AAV-hSyn-EYFP), and accompanying bilateral optical ferrules dorsal to the caudal substantia nigra (cSN). The cSN was successfully transduced between Bregma levels -5.54 and -6.72 mm, in both YFP controls (n = 8) and eNpHR (n = 9) rats (Paxinos & Watson, 2007). While somewhat diffuse, transduction was concentrated in tyrosine hydroxylase-containing region substantia nigra compacta (dorsal tier) and the reticulata, with each individual showing greater than 90% YFP expression in the cSN at Bregma -6.60 mm. Areas of most consistent transduction for each group of rats are the deepest yellow: between Bregma -6.12 mm and -6.84 mm for YFP controls, or Bregma -5.88 mm and -6.60 mm for eNpHR rats. Ferrule placements were confirmed to be dorsal to the cSN, at Bregma -6.36 mm +/- 0.72 mm. Each rat's complete transduction and ferrule tip placements were drawn from fluorescent slices processed for tyrosine hydroxylase immunohistochemistry and Neurotrace (Figure 4.1 A), made translucent and stacked for visualization (Figure 4.1 B).

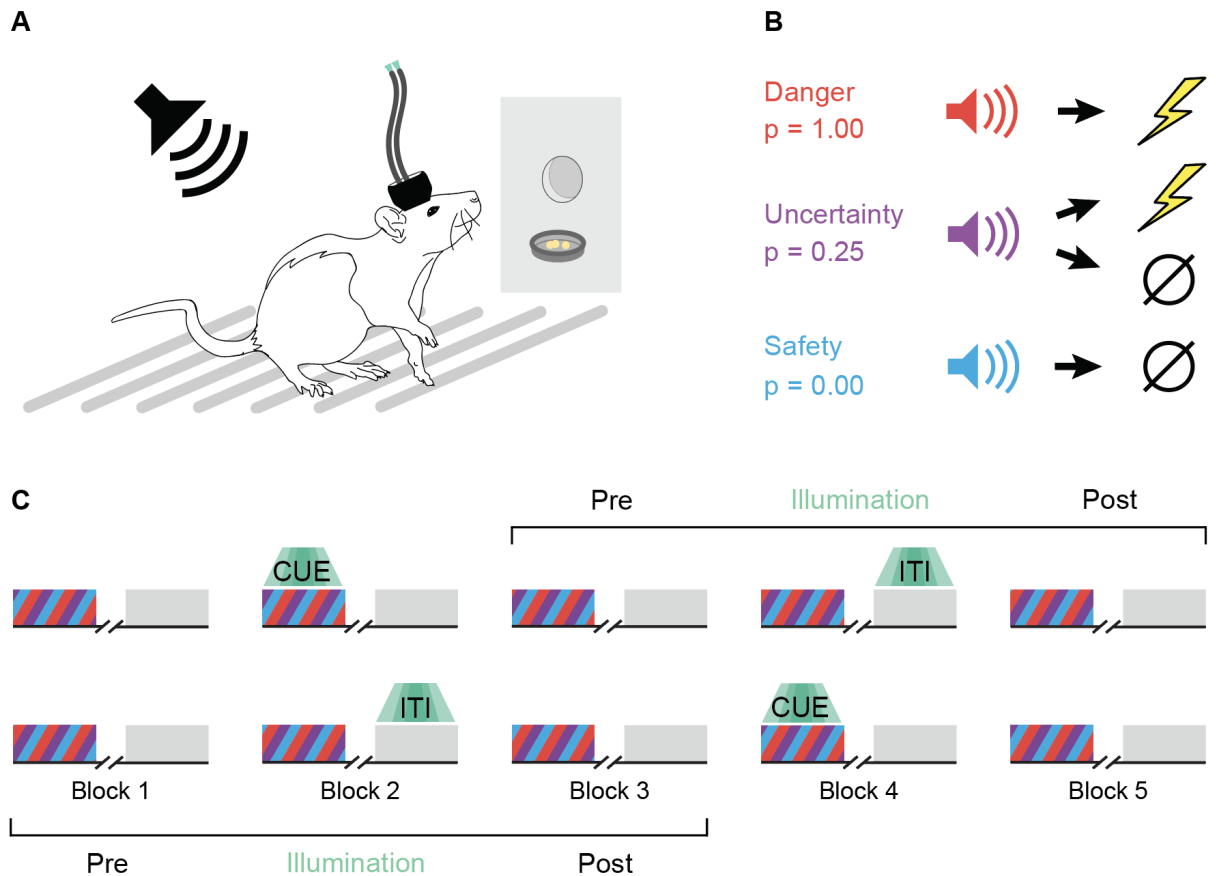


Figure 4.2 Pavlovian discrimination and experiment timeline

(A) Nose poking rat in fear conditioning chamber with light blocking headcap, plugged into bilateral optogenetic cables to permit light delivery. (B) Pavlovian fear discrimination consisted of three auditory cues, each predicting a unique probability of foot shock: danger, $p = 1.00$ (red); uncertainty, $p = 0.25$ (purple); and safety, $p = 0.00$. (C) Laser light was administered for 10 seconds during cue presentation (CUE Illumination) or an equivalent duration intertrial interval (ITI Illumination). Order of illumination CUE first (top) or ITI first (bottom) was counterbalanced. One session of Pavlovian discrimination occurred each day and each block contained two sessions (10 total sessions over 5 blocks).

Following recovery from surgery, all rats were trained to nose poke for a food reward (Figure 4.2 A). During fear discrimination, three distinct auditory cues predicted unique foot shock probabilities: danger ($p = 1.00$), uncertainty ($p = 0.25$) and safety ($p = 0.00$)

(Figure 4.2 B). Trial order was randomized for each rat during each session. Fear was measured with suppression ratio and calculated by comparing nose poke rates during baseline and cue periods (see 4.2 Methods: 4.2.8.1 Behavior Analyses).

After eight discrimination sessions, rats received 10 additional discrimination sessions with and without light illumination (Figure 4.2 C). To minimize the effect of cable attachment on fear behavior, all rats were habituated to optogenetic cables in Block 1 (no illumination). For one group of rats [(eNpHR (n = 3), YFP controls (n = 4)], the next 8 sessions consisted of 2-session blocks: CUE illumination (Block 2) → no illumination (Block 3) → ITI illumination (Block 4) → no illumination (Block 5). A second group of rats [(eNpHR (n=6), YFP controls (n=4)] received the exact same procedure, only ITI illumination was given first to counterbalance potential effects of illumination type order. During CUE illumination sessions, 532 nm green light was delivered bilaterally for all 10 s of each auditory cue (danger = 4, uncertainty = 8, safety = 6). During ITI illumination sessions, light was delivered for 10 s between cue trials. Pre- and Post-illumination fear behavior for all critical comparisons to illumination fear behavior (Blocks 2 & 4) came from no illumination sessions (Blocks 1, 3 & 5).

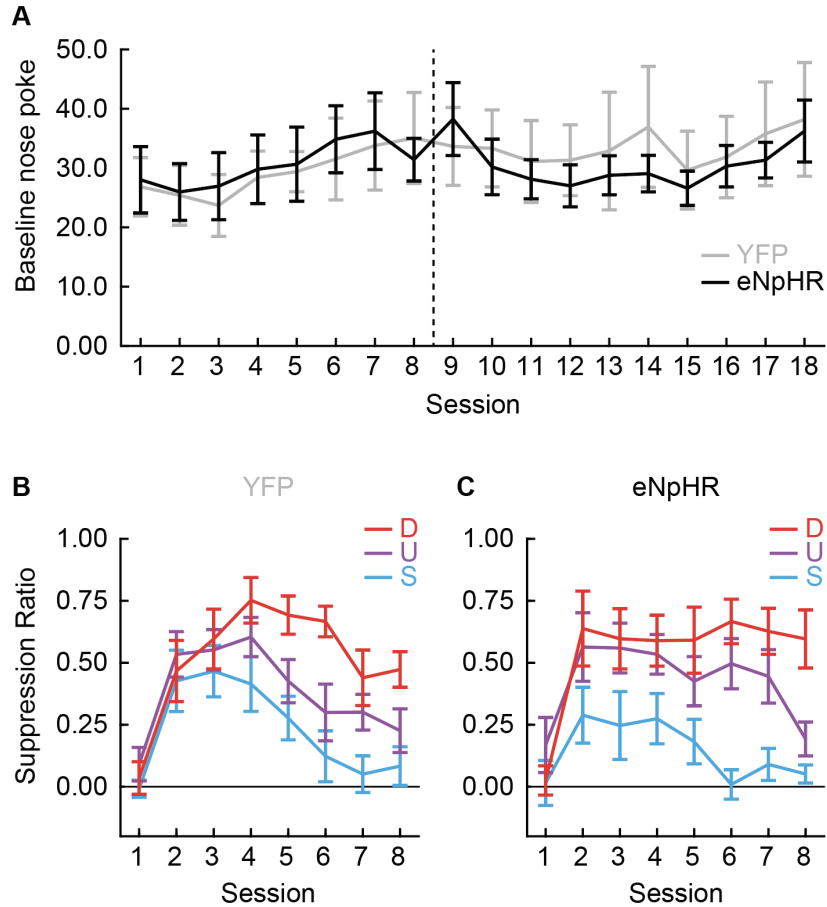


Figure 4.3 Baseline nose poking and pre-illumination discrimination

(A) Baseline nose poking per second for YFP controls (gray) and eNpHR rats (black) throughout behavioral testing. Dotted line indicates division between behavior-only sessions (left sessions, 1-8) and blocked illumination sessions (right sessions, 9-18). (B) Nose poke suppression to danger (red), uncertainty (purple), and safety (blue) cue presentation during the first eight sessions of Pavlovian fear discrimination for YFP controls. (C) Nose poke suppression for eNpHR rats, all graph properties maintained from B.

4.3.1 Baseline nose poking

It is essential that rats in each group demonstrate similar levels of baseline nose poking for nose poke suppression to reflect an accurate measure of fear. The SN is canonically implicated in movement. To ensure our results did not reflect a movement deficit, it was especially important that baseline nose poking was consistent between groups

throughout behavior testing. Critically, YFP controls and eNpHR rats demonstrated equivalent baseline nose poke rates throughout all 18 sessions of discrimination (Figure 4.3 A). In support, ANOVA for baseline nose poke rate [between factors: group (YFP vs. eNpHR), illumination intensity (12.5 mW vs. 25 mW) and illumination order (ITI-CUE vs. CUE-ITI); within factors: session (18)] found a main effect of session ($F_{17,170} = 3.027$, $p = 1.27 \times 10^{-4}$, $\eta^2 = 0.23$, $op = 0.99$), as well as a trend toward significance for a group by session interaction ($F_{17,170} = 1.66$, $p = 0.056$, $\eta^2 = 0.142$, $op = 0.92$). However, this trend may have been due to incorporating excessive additional variance attributed to including illumination intensity and order as factors, which were counterbalanced across groups. ANOVA for baseline nose poke rate excluding illumination intensity and order [between factor: group (YFP vs. eNpHR); within factor: session (18)] found only a main effect of session ($F_{17,255} = 3.027$, $p = 9.00 \times 10^{-6}$, $\eta^2 = 0.19$, $op = 1.00$). Critically, no main effect of group was detected in either ANOVA. These results minimize concerns that group differences observed during fear discrimination result from underlying differences in baseline rewarded nose poking.

4.3.2 Pre-illumination fear discrimination

Consistent with previous studies, suppression ratios were initially high to all cues (Wright et al., 2015; DiLeo et al., 2016; Walker et al., 2018) and full discrimination (danger > uncertainty > safety) was observed by the eighth session. Suppression ratios were high to danger, intermediate to uncertainty, and low to safety (Figure 4.3 B & C). To observe meaningful, differential effects of light illumination in YFP versus eNpHR rats, both groups must demonstrate equivalent fear discrimination prior to light illumination. Critically, YFP controls and eNpHR rats acquired equivalent discrimination prior to light illumination. In

support, ANOVA for suppression ratios [between factor: group (YFP vs. eNpHR); within factors: cue (danger vs. uncertainty vs. safety) & session (8)] found a significant effect of cue ($F_{2,30} = 37.12$, $p = 7.73 \times 10^{-9}$, $\eta^2 = 0.71$, $op = 1.00$), session ($F_{7,105} = 18.07$, $p = 1.41 \times 10^{-15}$, $\eta^2 = 0.55$, $op = 1.00$), and a cue x session interaction ($F_{14,210} = 5.47$, $p = 6.48 \times 10^{-9}$, $\eta^2 = 0.27$, $op = 1.00$). ANOVA revealed no main effect of or interaction with group ($F_s < 1.51$, $p_s > 0.237$). Thus, differences in fear discrimination during illumination blocks cannot be attributed to differences in pre-illumination discrimination.

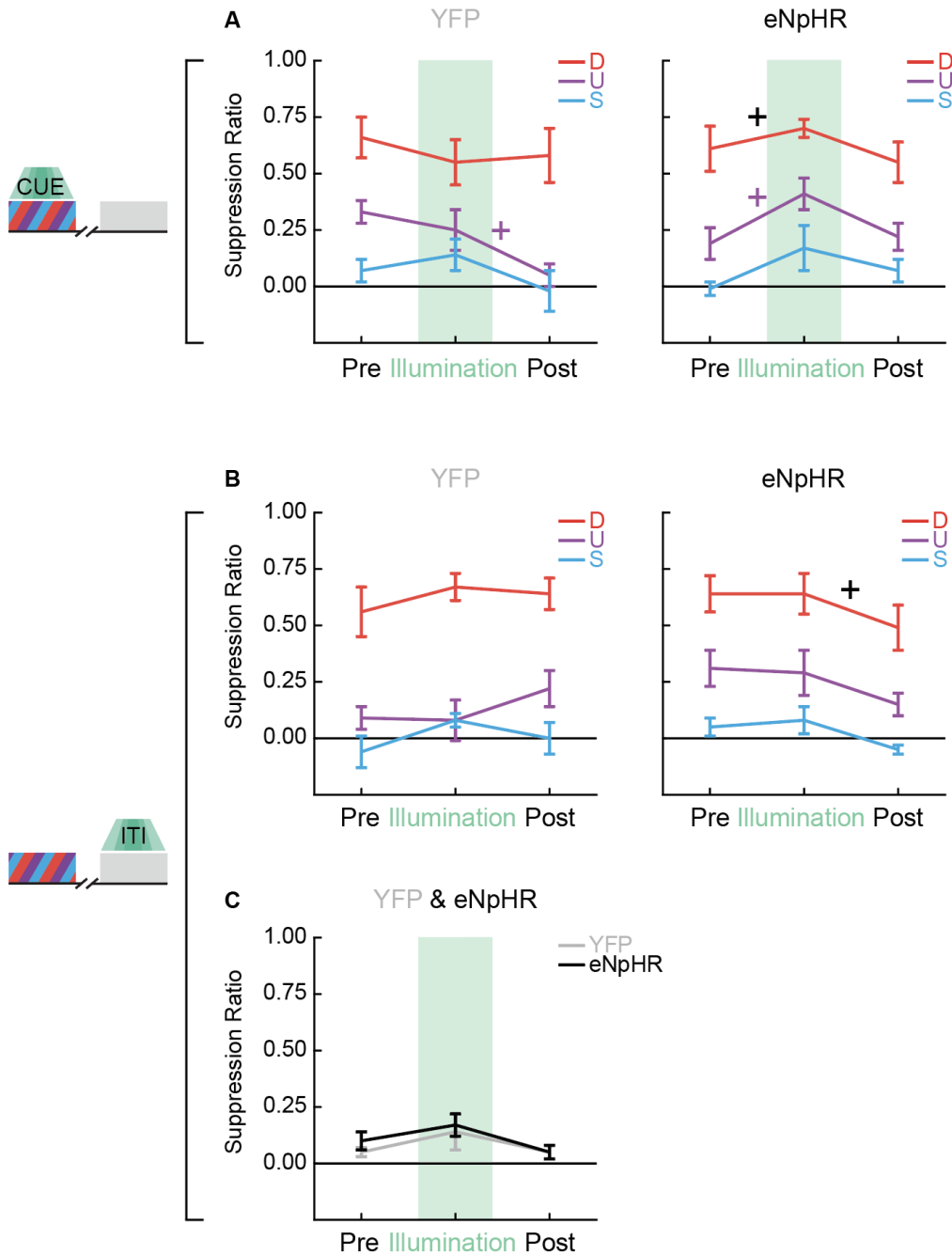


Figure 4.4 cSN inhibition globally inflates fear

(A) Mean + SEM nose poke suppression during 10 s danger (red), uncertainty (purple) and safety (blue) cue presentation for YFP controls (gray/left) and eNpHR rats (black/right) in each two-session block (pre/illumination/post: blocks 1-3 (top) and 3-5 (bottom) in Figure 4.2 C). Green bar background indicates laser illumination during cue presentation (CUE illumination). (B) Mean + SEM nose poke suppression during danger, uncertainty and safety cue presentation for YFP controls and eNpHR rats when 10 s laser

illumination occurred outside of cue presentation (ITI illumination) in each two-session block (pre/illumination/post: blocks 3-5 (top) and 1-3 (bottom) in Figure 4.2 C). Coloring maintained from A. (C) Mean + SEM nose poke suppression during 10 s ITI period for YFP controls (gray) and eNpHR rats (black) for each two-session block when 10 s laser illumination occurred outside of cue presentation. Green bar background indicates laser illumination during ITI period (ITI illumination). Data are from the same blocks represented in panel B. *Black plus signs indicate 95% bootstrap confidence intervals for mean differential suppression ratio (illumination - pre or illumination - post) do not contain zero. *Purple plus signs indicate 95% bootstrap confidence interval for uncertainty differential suppression ratio (illumination - pre or illumination - post) does not contain zero.

Row #	Within-Subjects Effects	F	p	Partial Eta Squared	Observed Power
1	Illumination	7.13	0.024	0.42	0.67
2	Illumination x Group	0.13	0.73	0.01	0.06
3	Illumination x Intensity	0.02	0.89	0.002	0.05
4	Illumination x Order	16.01	0.003	0.62	0.95
5	Illumination x Group x Intensity	1.07	0.33	0.10	0.16
6	Illumination x Group x Order	0.08	0.78	0.01	0.06
7	Illumination x Intensity x Order	0.001	0.98	8.30 x 10 ⁻⁵	0.05
8	Cue	74.68	5.28 x 10⁻¹⁰	0.88	1.00
9	Cue x Group	1.98	0.16	0.17	0.36
10	Cue x Intensity	1.32	0.29	0.12	0.25
11	Cue x Order	0.46	0.64	0.04	0.11
12	Cue x Group x Intensity	1.25	0.31	0.11	0.24
13	Cue x Group x Order	1.17	0.33	0.10	0.23
14	Cue x Intensity x Order	1.50	0.25	0.13	0.28
15	Block	9.54	0.001	0.49	0.96
16	Block x Group	4.42	0.026	0.31	0.69
17	Block x Intensity	6.79	0.006	0.40	0.87
18	Block x Order	3.66	0.044	0.27	0.61
19	Block x Group x Intensity	2.19	0.14	0.18	0.40
20	Block x Group x Order	0.17	0.85	0.02	0.07
21	Block x Intensity x Order	1.40	0.27	0.12	0.27
22	Illumination x Cue	0.12	0.88	0.01	0.07
23	Illumination x Cue x Group	0.91	0.42	0.08	0.19
24	Illumination x Cue x Intensity	4.99	0.02	0.33	0.75
25	Illumination x Cue x Order	1.99	0.16	0.17	0.36
26	Illumination x Cue x Group x Intensity	0.35	0.71	0.03	0.10
27	Illumination x Cue x Group x Order	0.33	0.72	0.03	0.10
28	Illumination x Cue x Intensity x Order	0.99	0.39	0.09	0.20
29	Illumination x Block	0.02	0.98	0.002	0.05
30	Illumination x Block x Group	5.69	0.011	0.36	0.81
31	Illumination x Block x Intensity	4.78	0.020	0.32	0.73
32	Illumination x Block x Order	1.00	0.38	0.09	0.20
33	Illumination x Block x Group x Intensity	0.12	0.89	0.01	0.07
34	Illumination x Block x Group x Order	0.36	0.70	0.04	0.10
35	Illumination x Block x Intensity x Order	2.38	0.12	0.19	0.42
36	Cue x Block	0.84	0.51	0.08	0.24
37	Cue x Block x Group	1.39	0.26	0.12	0.39
38	Cue x Block x Intensity	1.34	0.27	0.12	0.38
39	Cue x Block x Order	2.98	0.03	0.23	0.74
40	Cue x Block x Group x Intensity	1.50	0.22	0.13	0.42
41	Cue x Block x Group x Order	1.47	0.23	0.13	0.41
42	Cue x Block x Intensity x Order	1.15	0.35	0.10	0.33
43	Illumination x Cue x Block	1.23	0.31	0.11	0.35
44	Illumination x Cue x Block x Group	0.74	0.57	0.07	0.22
45	Illumination x Cue x Block x Intensity	0.47	0.76	0.05	0.15
46	Illumination x Cue x Block x Order	0.45	0.77	0.04	0.14
47	Illumination x Cue x Block x Group x Intensity	0.42	0.79	0.04	0.14
48	Illumination x Cue x Block x Group x Order	1.10	0.37	0.10	0.31
49	Illumination x Cue x Block x Intensity x Order	0.23	0.92	0.02	0.10

Table 4.1 Complete ANOVA with all factors

ANOVA table of within-subjects effects with all possible factors [between factors: group (YFP vs. eNpHR), illumination intensity (12.5 mW vs. 25 mW) and counterbalanced procedure order (ITI illumination first - CUE illumination last vs. CUE illumination first - ITI illumination last); within factors: illumination (10 s illumination during CUEs vs. 10 s illumination during ITIs), cue (danger vs. uncertainty vs. safety) & block (3, 2-session blocks: Pre-illumination vs. Illumination vs. Post-illumination)]. F statistic, associated p value, partial eta squared (η^2) and observed power reported for all effects. Significant effects indicated in bold text ($p < 0.05$). Critical and significant three-way, illumination x block x group interaction (green background). Insignificant four-way, illumination x cue x block x group interaction (red background).

4.3.3 Endogenous cSN activity is necessary for fear suppression

A causal role for the cSN in fear suppression requires illumination-dependent increases in fear specific to eNpHR rats during CUE illumination. Following this logic, it is critical that changes in behavior are not due to dose-response illumination effects: whether animals received 12.5mW or 25mW of laser illumination. Or, due to order of illumination presentation: whether animals received CUE illumination or ITI illumination first. In support, no dose-response illumination effects, nor interactions between group and illumination were observed, regardless of intensity or order. Further, collapsing across illumination order and intensity, ANOVA revealed no group x illumination interaction (Table 4.1, Row 2). Complete ANOVA results with all factors are reported in Table 4.1. Changes in suppression ratios during illumination could be driven by responses to any one of the cues: danger, uncertainty or safety. However, increases in suppression driven by the uncertainty cue would be most likely: an aversive cue with room to observe an increase in suppression as it approaches ceiling suppression of 1.00. Increases in suppression driven solely by the uncertainty cue would require a significant *four-way*, illumination x cue x block x group interaction, which we did not find (Table 4.1, Row 44

highlighted in red). Instead, ANOVA for suppression ratio [between factors: group (YFP vs. eNpHR), intensity (12.5 mW vs. 25 mW) and order (ITI-CUE vs. CUE-ITI); within factors: illumination (CUE vs. ITI illumination), cue (danger vs. uncertainty vs. safety) & block (3, 2-session blocks: Pre vs. CUE Illumination vs. Post)] found a significant *three-way*, illumination x block x group interaction ($F_{2,20} = 5.69$, $p = 0.011$, $\eta^2 = 0.36$, $op = 0.81$), indicating the increase in suppression was observed globally, to all cues. It is still possible that changes in cued behavior were driven solely by the uncertainty cue, but that the complete ANOVA was unable to detect the supporting four-way interaction due to the inclusion of extraneous factors.

Eliminating illumination intensity and order, an additional ANOVA for suppression ratio was performed with factors of illumination, group, cue and block. ANOVA revealed a main effect of cue ($F_{2,30} = 96.67$, $p = 8.37 \times 10^{-14}$, $\eta^2 = 0.87$, $op = 1.00$). Although discrimination remained consistent, visual inspection suggested a dominant pattern of increased suppression when the laser was present (Figure 4.4 A). In support, the ANOVA revealed a main effect of block ($F_{2,30} = 8.41$, $p = 0.001$, $\eta^2 = 0.36$, $op = 0.95$). Indeed, rats generally increased suppression during illumination blocks. In agreement with the complete ANOVA, the simplified version also failed to identify a significant *four-way* interaction, but found a significant *three-way*, illumination x group x block interaction ($F_{2,30} = 6.79$, $p = 0.004$, $\eta^2 = 0.31$, $op = 0.89$). Critically, only eNpHR rats in the CUE illumination condition increased suppression to all cues (Figure 4.4 A, right), this pattern was not observed under any other experimental condition (Figure 4.4 A, left and B). In support, the 95% bootstrap CI for differential suppression ratio, for the mean of all cues (mean CUE Illumination - mean CUE Pre illumination) did not contain zero for CUE illumination

sessions in eNpHR rats ($M = 0.16$, 95% CI [0.02, 0.34]) (Figure 4.4 A right, *black plus sign). Moreover, this global increase in suppression was driven mostly, but not solely, by suppression to the uncertainty cue. In support, the 95% bootstrap CI for differential suppression ratio, (uncertainty CUE Illumination - uncertainty CUE Pre illumination) ($M = 0.22$, 95% CI [0.09, 0.43]) also did not contain zero for CUE illumination sessions in eNpHR rats (Figure 4.4 A right, *purple plus sign).

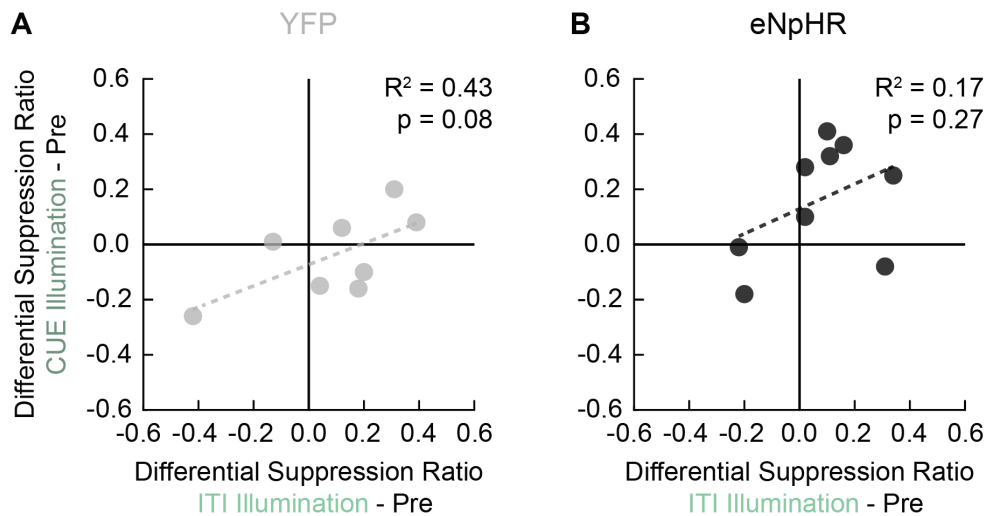


Figure 4.5 Light illumination and suppression

(A) Differential suppression ratios (Illumination - Pre illumination) are plotted for YFP controls (gray). Suppression ratios reflect behavior during cue laser epochs within CUE illumination sessions (dark green, y-axis) vs. differential suppression ratios (Illumination - Pre illumination) during laser-only epochs from ITI illumination (light green, x-axis) sessions. (B) Differential suppression ratios as described in A, plotted for eNpHR rats (black).

4.3.4 Global inflation of fear is specific to cue presentation

The SN is canonically implicated in movement by way of its dopaminergic inputs to the striatum and GABAergic projections to the thalamus (Groenewegen, 2003). Thus, it is possible that inhibition of cSN activity is sufficient to suppress nose poking, a movement, in absence of cue presentation. This interpretation could be consistent with only eNpHR rats demonstrating increased suppression during cue presentation. However, increased suppression would also be observed when laser illumination was delivered alone. Critically, ITI illumination sessions were designed to capture suppression during this exact, laser-only condition. To determine if global inflation of fear was specific cue presentation at the group level, we performed an additional ANOVA for suppression ratio during the laser-only epochs from ITI illumination sessions (Figure 4.4 C). Critically, ANOVA for suppression ratio during ITI I alone [between factor: group (YFP vs. eNpHR) and within factor: block (3, 2-session blocks: Pre vs. ITI Illumination vs. Post)] revealed no main effect of block or group, and no block x group interaction. Although we find no effect of illumination at the group level it is still possible that weaker, laser-only effects could be observed at the level of the individual.

To address this possibility, we asked whether suppression during CUE illumination was related to suppression during laser-only epochs from ITI illumination sessions (Figure 4.5). If laser illumination alone impacted suppression at the individual level, eNpHR rats with large increases in suppression during CUE illumination, should increase suppression similarly during laser-only epochs. Moreover, if these effects were due to inhibition of cSN activity, this relationship should not be observed in YFP rats. No relationships between differential suppression ratios for CUE illumination versus laser-only epochs were found

at the level of the individual. Laser illumination alone was insufficient to induce a change in behavior at the group or individual level. Thus, global increases in suppression, specific to eNpHR rats, were due inhibition of cSN firing during cue presentation. Endogenous SN activity is not only capable of suppressing fear (Bouchet et al., 2018), but also necessary for suppressing fear.

4.4 Discussion

I optogenetically inhibited SN activity during the entirety of cue presentation in male rats while they discriminated between danger, uncertainty and safety. Previous work has demonstrated that dopaminergic neurons in the SN increase their activity in response to not only reward, but also adversity (Frank & Surmeier, 2009). More recently, Bouchet et al., 2018 identified a connection between SN DA activation and improved fear extinction. Although these are important and novel pieces of a larger SN and fear narrative, they do not consider roles for cell types other than dopamine in fear. Nor do they consider potential contributions of the SN to other fear processes, such as discrimination. Extending the current state of this literature, I demonstrated that optogenetically inhibiting endogenous SN activity during fear discrimination globally increases fear to danger, uncertainty and safety.

Before considering further implications of these results, it is necessary to address some limitations. This experiment used only adult male rats, and makes no claims about whether similar global inflation of fear would be observed in biologically female rats. However, sex-specific investigations will be critical going forward. The cSN is necessary for suppression of fear, and activation of dopaminergic SN neurons has the ability to facilitate fear extinction. Many have suggested that PTSD may be a stress-induced

disorder of fear circuitry (Shin & Handwerker, 2009), which could be mediated by excessive fear conditioning or impaired fear extinction (Pitman, 1988). In the United States, the risk of PTSD is twofold higher in women (Breslau, 2002), which may reflect sex differences in underlying aberrant fear circuitry, but certainly reflects a need to consider sex-differences in future experiments. Further investigation of roles for specific cell types within the SN in the context of fear is also necessary.

Our manipulation, under control of the human synapsin promoter, was not cell-type-specific. As such, global inflation I observed could be driven by the optogenetic inhibition of dopaminergic (Bouchet et al., 2018), glutamatergic (Yamaguchi et al., 2013), or GABAergic (Brown et al., 2014) neurons of the cSN. Non-specific manipulation was a great way to begin a causal investigation of the SN in fear. Going forward, cell-type-specific and subdivision-specific manipulations will be necessary to evaluate contributions of the cSN to fear discrimination.

Part of a direct pathway facilitating motor output, the reticular component of the SN is one of two major GABAergic outputs of the basal ganglia (Brown et al., 2014). The validity of the direct and indirect pathway model has come into question (Nambu, 2008). However, in the canonical view, activation of these outputs targets pre-motor areas, 'releasing the brakes' and facilitating motor behavior (Groenewegen, 2003). As part of the nigrostriatal pathway, dopaminergic neurons of the SN compacta are critical inputs to the basal ganglia, classically implicated in movement, and recently implicated in fear extinction. Although we did not observe effects of inhibition specific to movement, our design uniformly inhibited activity in both components of the SN, and contributions of the reticular component to fear have yet to be dismissed.

Chapter 5: Summary of Results and Discussion

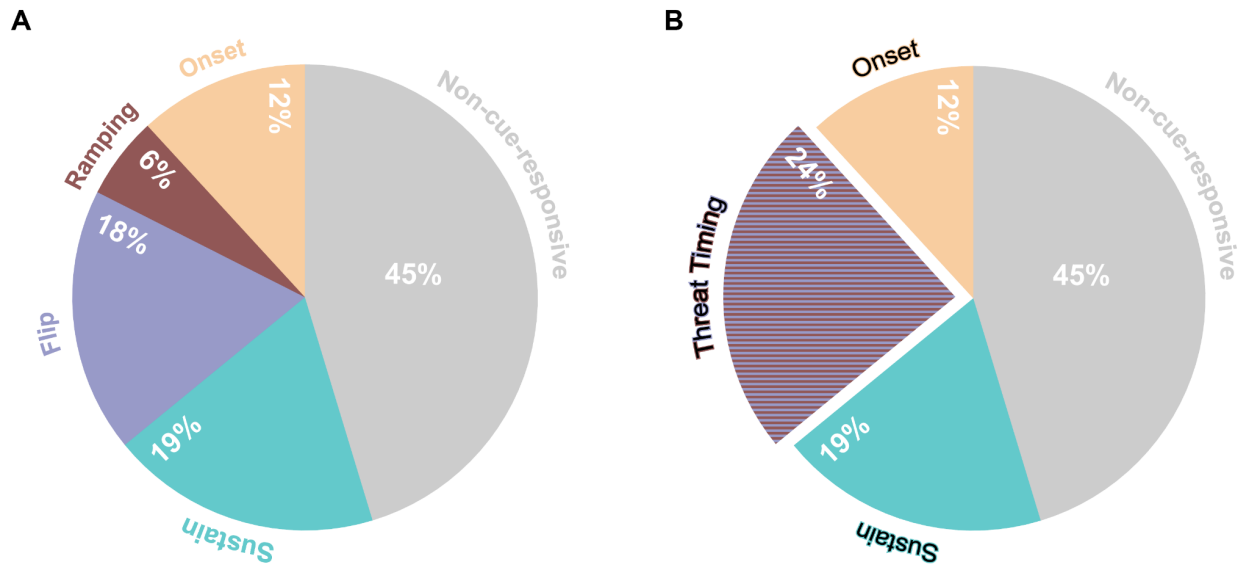


Figure 5.1 Functional Populations of the caudal vIPAG

(A) Four functional populations of the caudal vIPAG identified in Chapters 2 and 3 depicted alongside non-cue-responsive units (gray), the final unanalyzed subdivision of all recorded single-units. Warm tones reflect cue-excited function populations: Onset (peach) & Ramping (wine). Cool tones reflect cue-inhibited populations: Flip (periwinkle) & Sustain (seafoam). (B) Alternative arrangement of function populations, where Flip and Ramping neurons comprise a single population that signals Threat Timing (wine and periwinkle candy stripe).

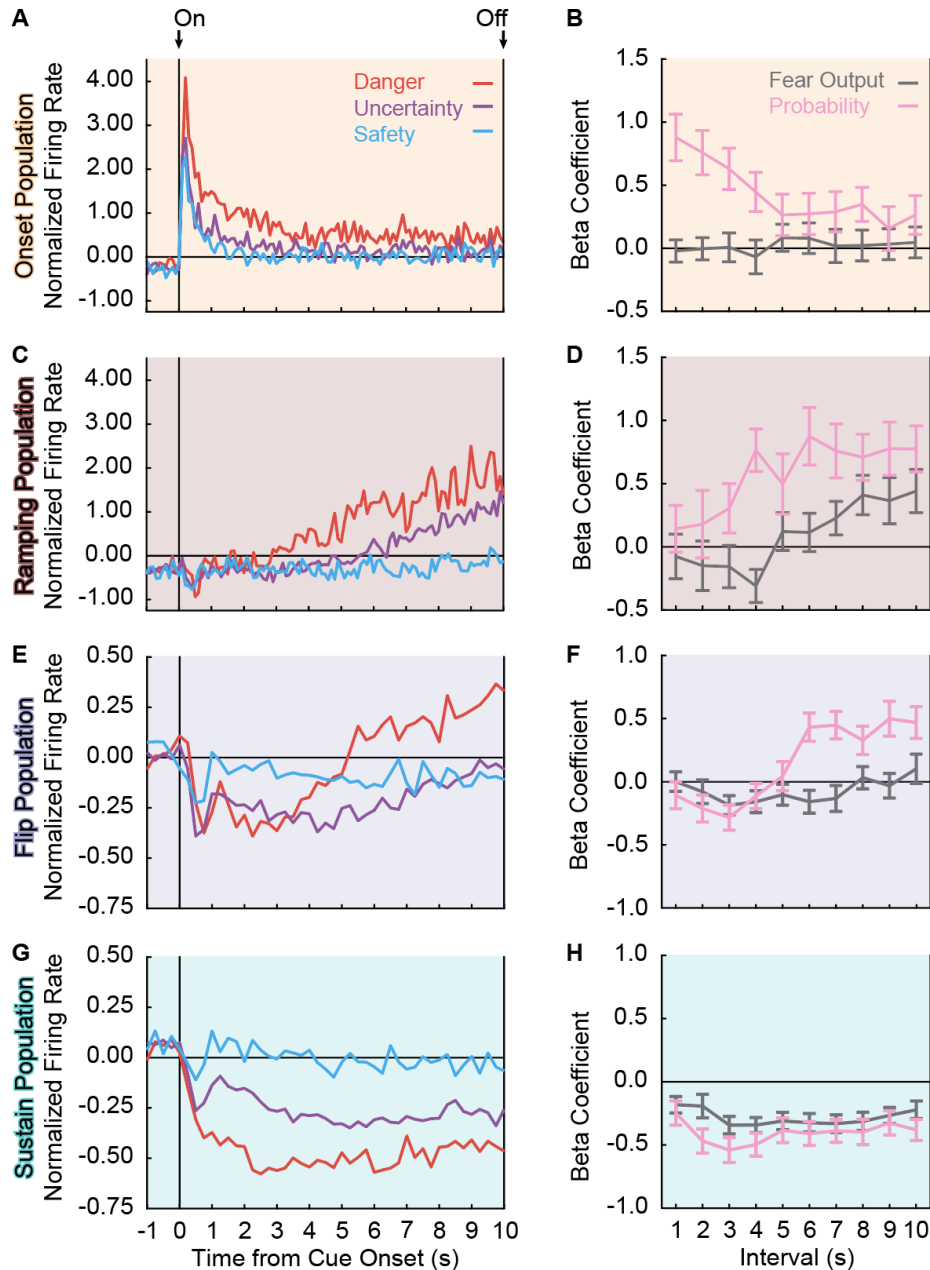


Figure 5.2 Firing and Regression Summary

(A) Mean, Z-score normalized firing to danger (red), uncertainty (purple) and safety (blue) is shown for the 1 s pre-cue period and the 10 s cue period for the Onset population ($n = 29$). (B) Mean \pm SEM beta coefficient is shown for each regressor, in 1 s intervals, for the Onset population: probability (pink), fear output (dark gray). (C) Normalized firing for the Ramping population ($n = 14$) plotted as in A. (D) Mean \pm SEM beta coefficient is shown for each regressor, in 1 s intervals, for the Ramping population. (E) Normalized firing for the Flip population ($n = 45$) plotted as in A. (F) Mean \pm SEM beta coefficients are shown

for each regressor, in 1 s intervals, for the Flip population. (G) Normalized firing for the Sustain population (n = 46) plotted as in A. (H) Mean \pm SEM beta coefficient is shown for each regressor, in 1 s intervals, for the Sustain population. Cue onset (On) and offset (Off) are indicated by vertical black lines for all firing graphs in the left column. Colored backgrounds correspond to Figure 5.1 A.

5.1 Summary of Results

In Chapters 2 and 3, I recorded vIPAG single-unit activity while rats underwent fear discrimination in which three auditory cues predicted unique foot shock probabilities. These findings expanded the functional diversity of vIPAG neurons. Observing robust vIPAG threat-related activity was expected, given its essential role in defensive behavior (Bandler and Depaulis, 1991; Fanselow, 1991; Carrive et al., 1997). However, the diversity of information contained in these signals is surprising (Figure 5.1 A). I identified single-units with short-latency excitation to cue onset (Figure 5.2 A, Onset), longer-latency excitation to cue offset (Figure 5.2 C, Ramping), early cue inhibition which gave rise to late cue danger excitation (Figure 5.2 E, Flip), and sustained scaled inhibition over the course of cue presentation (Figure 5.2 G, Sustain). Altogether, these findings reveal diverse temporal responding and threat signaling in the vIPAG.

Chapter 2 found a cue-excited population that exclusively signaled threat probability (Figure 5.2 B, Onset) as well as a cue-excited population that prioritized threat probability signaling over fear output (Figure 5.2 D, Ramping). Chapter 3 found patterned activity and signaling of neurons resembling that of previously identified Ramping neurons (Figure 5.2 F, Flip), and a population of cue-inhibited neurons containing a complete neural correlate for fear output, but also containing information about threat probability (Figure 5.2 H, Sustain). It is clear that the vIPAG contains a combination of signals that solely reflect threat probability, prioritize threat probability, or signal a combination of fear

output *and* threat probability throughout cue presentation. However, single-units that demonstrate a pure reflection of fear output, in direct accordance with the longstanding hypothesis of vIPAG function, remain elusive.

Activity exclusively reflecting fear output could potentially emerge within the vIPAG at the ensemble level (Jones et al., 2007; Zhou et al., 2018). Yet, this level of activity would still be constructed from neural correlates for threat probability at the single-unit level, unless it could be found in non-cue-responsive single-units (Insanally et al., 2019) (Figure 5.1, gray). Alternatively, it is still possible (although unlikely) that neural activity purely reflecting fear output may reside in neurons in the extreme caudal vIPAG: in the ~0.64mm just beyond our recording site. It is also possible that neural activity purely reflecting fear output, irrespective of threat probability may not be necessary to drive defensive behavior. Nonetheless, signals for threat probability and fear output co-exist in the vIPAG. Although the results presented in Chapters 2 and 3 are purely correlative, these signals could play a causal role in fear expression. Determining the causal, behavioral implications of these functional populations would require identifying the cell type (or types) within each functional population. Then, using transgenic rats, examining the behavioral impact of optogenetically inhibiting each discrete functional type during ongoing behavior. This is particularly challenging in transgenic rat models, which are limited in type compared to mice, and do not express Cre recombinase (the would-be target of a Cre-mediated optogenetic construct) in every region of interest. Moreover, some of the functional types we observed demonstrate widely varied baseline firings rates (Ramping, Flip and Sustain), and may consist of more than one neuron type. If this were the case, a transgenic rodent model designed to target one cell type, would not be able to silence an

entire functional population. Leaving part of the population intact would preclude us from determining whether activity of that population as a whole was necessary to behavior. All of these caveats are beyond the scope of this dissertation. However, a non-cell-type-specific version of this optogenetic procedure is not beyond this document, and was employed in Chapter 4 to evaluate a causal role for the cSN in fear.

I inhibited cSN activity during the entirety of all danger, uncertainty and safety cues to determine whether endogenous cSN activity was necessary for suppression of conditioned fear. CSN Inhibition resulted in global inflation of fear to all cues. Critically, this effect was specific to CUE-Illumination in eNpHR rats. Endogenous cSN activity is not only capable (Bouchet et al., 2018), but also required for fear suppression. It is clear that the cSN should be considered as a novel node in the fear circuit. In fact, cSN activity could modulate some of the functional vIPAG populations revealed in Chapters 2 and 3 via a direct, robust projection from the SN to the vIPAG (Kirouac et al., 2004).

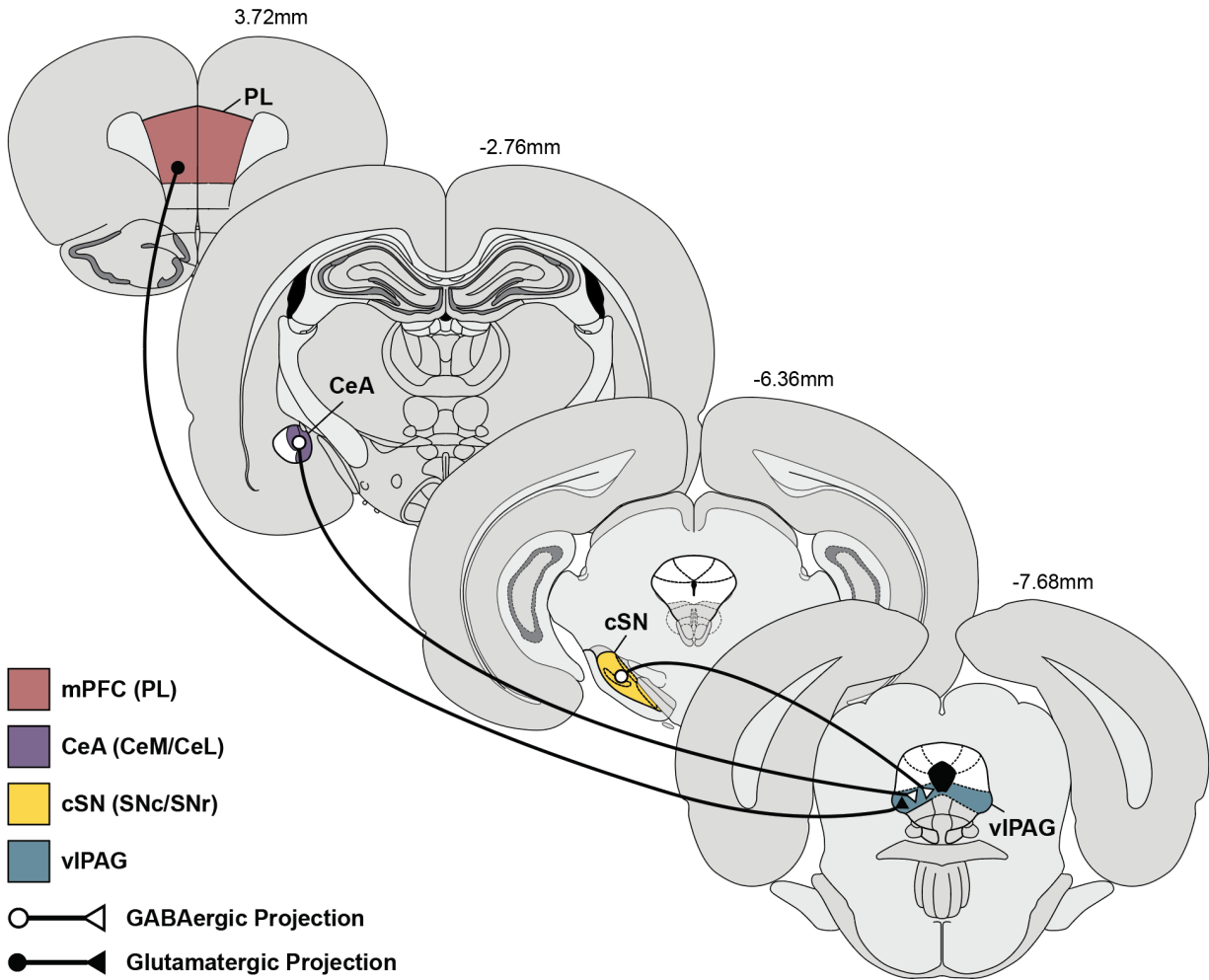


Figure 5.3 Revising the fear circuit

Top left to bottom right: Bregma +3.72mm with prelimbic mPFC (PL) indicated in rust, Bregma -2.76mm with lateral and medial central amygdala (CeA) subdivisions indicated in purple, Bregma -6.36mm with pars compacta and pars reticulata components of the caudal substantia nigra (inhibited in Chapter 4) indicated in marigold, and Bregma -7.68mm with caudal vIPAG (Chapter 2 and 3 recordings) indicated in teal (bottom right). Additional subdivisions of the CeA and PAG are indicated in white, and not the focus of this dissertation. Diagrams adapted from Paxinos & Watson, 2007.

5.2 Discussion

5.2.1 The vIPAG as a site of integration

It is nearly universally accepted that the amygdala is a key node of dysfunction in stress (Rauch et al., 2000) and anxiety disorders (Etkin & Wager, 2007). This may be driven in part by technical considerations: whole-brain functional magnetic resonance imaging (fMRI) can detect amygdala BOLD signals (Johnstone et al., 2005), while detecting subregion-specific PAG BOLD signals requires less common, high-field strength fMRI (Satpute et al., 2013). Perhaps the primary intellectual driver is that the amygdala is theorized to be a privileged site of integration and learning in the fear circuit (Admon et al., 2013; Mahan & Ressler, 2012). The functional populations identified in Chapters 2 and 3 illustrate that the amygdala is not privileged in this regard, and mark the vIPAG as a likely node of dysfunction in psychiatric disorders of fear and anxiety. Appreciation for the vIPAG as a site of integration will hasten mapping of a more complete fear circuit. Moreover, deliberate study of vIPAG function (Arico et al., 2017; Assareh et al., 2017; Rozeske et al., 2018) and dysfunction in psychiatric disease (Yeh et al., 2017), will be essential to developing effective therapies for disorders characterized by exaggerated threat estimation and aberrant fear. In addition to highlighting the vIPAG as a site of integration, the functional populations identified in Chapters 2 and 3 also pose interesting questions about the functional relationship between the vIPAG and the CeA.

5.2.2 Rethinking the functional CeA-vIPAG relationship

VIPAG threat probability signals may be trained up by the CeA, but become CeA-independent with sufficient training (Ozawa et al., 2017). Consistent with this interpretation, the CeA is essential to the acquisition of conditioned suppression with

limited training, but extended training mitigates the effects of CeA lesions (Lee et al., 2005; McDannald, 2010). However, I do not expect the CeA to become inessential following extensive fear discrimination training; threat probability estimates should continue to be updated as needed. In support, the CeA is likely essential to updating vIPAG threat probability signaling (McNally et al., 2011; Ozawa et al., 2017).

5.2.3 Predatory imminence continuum

The findings of Chapters 2 and 3 are best understood through comparison to the account of vIPAG function outlined in the predatory imminence continuum (PIC): a highly influential theory of defensive behavior (Fanselow & Lester, 1988). Organizing features of the PIC are time and degree of threat. As predation becomes more imminent (pre-encounter → post-encounter → circa-strike), the form and intensity of defensive behaviors change. Cued fear is argued to capture post-encounter defenses: immobility elicited when predators are nearby. In the neural instantiation of the PIC, the amygdala integrates information about environmental stimuli (auditory cues here), nociceptive information (foot shock) and time, to produce a signal for degree of threat (Fanselow & Lester, 1988). This amygdala-derived signal is relayed to the vIPAG to organize fear output (Fanselow, 1991, 1994). Implicit in the PIC model, is that the vIPAG does not contain information about time or degree of threat – only the resultant fear output. Yet, I found vIPAG neurons containing detailed information about degree of threat.

Although threat probability signaling was prioritized (Ramping and Flip) and consistent (Sustain) in other functional populations, information solely about degree of threat to challenge the vIPAG PIC model, was specific to Onset neurons. Onset activity may be

used to organize a variety of fear responses, but these neurons do not intrinsically signal fear output. What might that look like?

Onset vIPAG neurons may organize fear responses via projections to the central amygdala (CeA) for fear updating, to the magnocellular nucleus of the medulla (Mc) (Tovote et al., 2016) and rostral ventromedial medulla (RVM) for fear output via freezing (D. M. Vianna et al., 2008). Or, Onset projections to midline/intralaminar thalamus could rapidly relay threat probability estimates to a larger fear network (basolateral amygdala, prelimbic cortex, infralimbic cortex, insular cortex, etc.) (Buchanan & Thompson, 1994; Krout & Loewy, 2000; Sengupta & McNally, 2014; Vertes et al., 2015), promoting a variety of threat-related processes (Faull et al., 2016). Whereas the activity pattern of Onset neurons is distinct and reflects degree of threat, activity patterns of Flip and Ramping neurons are noticeably similar. In fact, Flip and Ramping activity may contain information about threat timing, another element of the canonically amygdala-centric, PIC model.

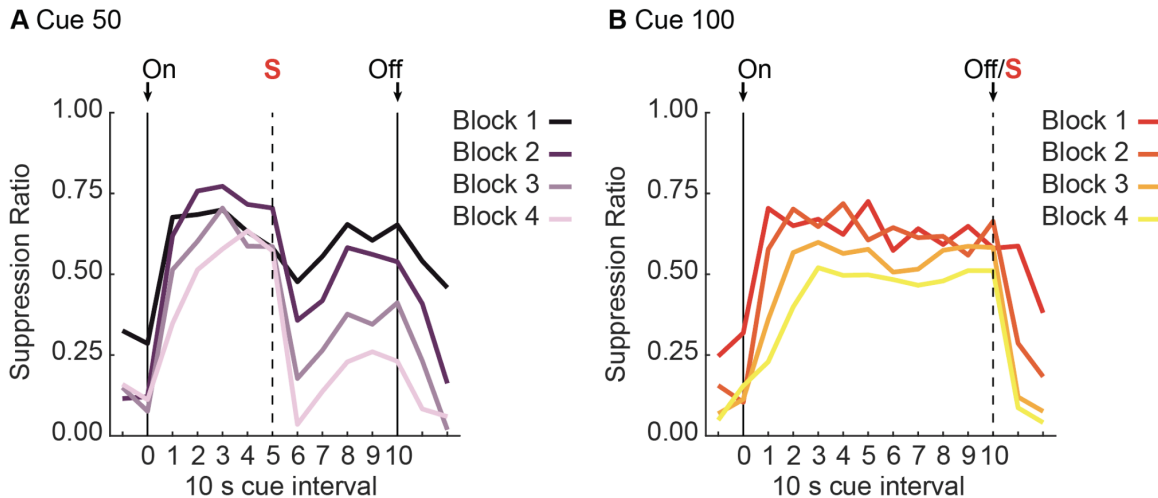


Figure 5.4 Threat timing pilot

(A) Mean \pm SEM suppression ratio to Cue 50 during 14, 10 s intervals (20 s pre-cue, 100 s of cue presentation and 20 s post-cue) is shown for female rats ($n = 8$). Blocks reflect 5 sessions each of 20-session Threat Timing procedure: Cue 50 vs. Cue 100 discrimination. Suppression to Cue 50 ranges from dark purple (Block 1) to light purple (Block 4). Time of cue onset and offset are indicated with 'On' and 'Off' and time of shock is indicated with a dotted vertical line accompanied by a red 'S' atop. (B) Mean \pm SEM suppression ratio of same female rats to Cue 100. Suppression to Cue 100 ranges from red (Block 1) to yellow (Block 4). All other graph properties maintained from A, applied to Cue 100 behavior.

5.2.4 Flip and Ramping neurons likely signal threat timing

There are many similarities between Flip and Ramping neurons. In terms of signaling, Flip and Ramping neurons both prioritize threat probability toward the last half of cue presentation. In terms of firing, Flip and Ramping populations demonstrate brief decreases in activity at the time of cue presentation, that ultimately give way to gradual increases in firing to shock-predictive cues (danger and uncertainty). Like Flip neurons (Figure 3.2 A), Ramping neurons continue firing to shock-predictive cues through a 2 s post-cue delay, and diminish firing just after shock delivery has occurred (Wright et al., 2019; Wright & McDannald, 2019). Indeed, Flip and Ramping neurons may comprise a

single Threat Timing population, critical for timing impending noxious events (Figure 5.1 B). The multi-cue discrimination procedure described in Chapters 2 through 4 was not designed to examine whether vIPAG single-units signal threat timing. So, I drew from a classic temporal discrimination task (Rosas & Alonso, 1996), to devise and pilot a new behavioral procedure, which can be used at a later time to test whether Flip and Ramping neurons actually signal Threat Timing.

5.2.4.1 Investigating threat timing

In the threat timing procedure, rats are trained to nose poke for a food reward and fear is measured using suppression ratio as previously described (Methods: Chapter 2, 3 and 4). Rats are habituated to two, to-be-continued auditory cues, followed by 5, 4-session blocks of discrimination. Unlike previous procedures with 10-second cues and uncertain shocks, threat timing discrimination consists of 100-second cues, always associated with shock. Foot shock occurs halfway through Cue 50 (50 seconds into cue presentation) and at the end of Cue 100 (at the 100th second of cue presentation). Within the first 4-session block, rats are able to discriminate between Cue 50 and Cue 100 (Figure 5.4).

Rats demonstrate increased suppression to Cue 50 between the time of cue onset and foot shock presentation. Suppression diminishes during the 10 seconds following foot shock, before increasing again until cue termination. Pre-shock suppression to Cue 50 is higher than post-shock suppression to Cue 50, and post-shock suppression decreases over each discrimination block (Figure 5.4 A). By contrast, suppression to Cue 100 increases from the time of cue onset, is maintained throughout cue presentation, and diminishes during the 10 seconds following foot shock/cue termination (Figure 5.4 B).

Paired with single-unit recording, signals specific to threat timing can be isolated using this procedure, while threat probability stays the same.

To determine whether Flip and Ramping neurons signal Threat Timing, caudal vIPAG activity will need to be recorded while rats receive threat timing discrimination. What might firing of Threat Timing neurons look like in this procedure? Increases in firing should be observed to Cue 50 and Cue 100, and maximal firing to each cue should be observed just prior to foot shock. Although maximal firing to the two cues should be the same (both shocks are identical), the rate of increased firing toward maximal firing should differ. Specifically, the slope of firing to Cue 50 from the time of cue onset to the time of foot shock, should be exactly double that of Cue 100. This is because there is exactly half the amount of time to reach maximal firing to the Cue 50 cue. Moreover, Threat Timing neurons would fire toward shock delivery, irrespective of behavior. Threat Timing neurons would not be expected to increase firing post-shock, despite increased post-shock fear suppression observed to Cue 50 (Figure 5.4 A, intervals 6 - 10). The range of baseline firing rates within the Ramping and Flip populations suggests there may be GABAergic and glutamatergic neurons in the vIPAG that signal Threat Timing.

5.2.4.2 Threat Timing neurons are likely more than one cell type

In Chapter 2, 17 neurons increased firing to at least one cue during the last, 1 s cue interval. Three of these neurons were outliers, belonged to a separate high firing rate cluster (~70 - 110 Hz), and were excluded from Ramping (~0 - 30 Hz) population analyses. In Chapter 3, Flip neurons, demonstrated a wide range of baseline firing rates (~0 - 150 Hz) and similar patterned activity. Combined, this evidence suggests the previously excluded units should be included in a combined Threat Timing population,

and that the combined population likely consists of more than one cell type on the basis of baseline firing rate: high firing (HF) and low firing (LF). GABAergic and glutamatergic cue-responsive units have been identified in the vIPAG previously. Of the two, GABAergic neurons demonstrated higher baseline firing (Tovote et al., 2016). Although speculative, Threat Timing neurons may be GABAergic (HF) and glutamatergic (LF).

For the remainder of this discussion, I will consider Threat Timing neurons as one of three functional vIPAG populations, alongside the Onset and Sustain populations (as depicted in Figure 5.1 B). Moreover, I will incorporate all of these functional populations into a single, likely model of vIPAG interconnectivity. Combined with considering contributions of novel fear-related inputs to the vIPAG, the remainder of this document serves to revise the role of the ventrolateral periaqueductal gray in the fear circuit.

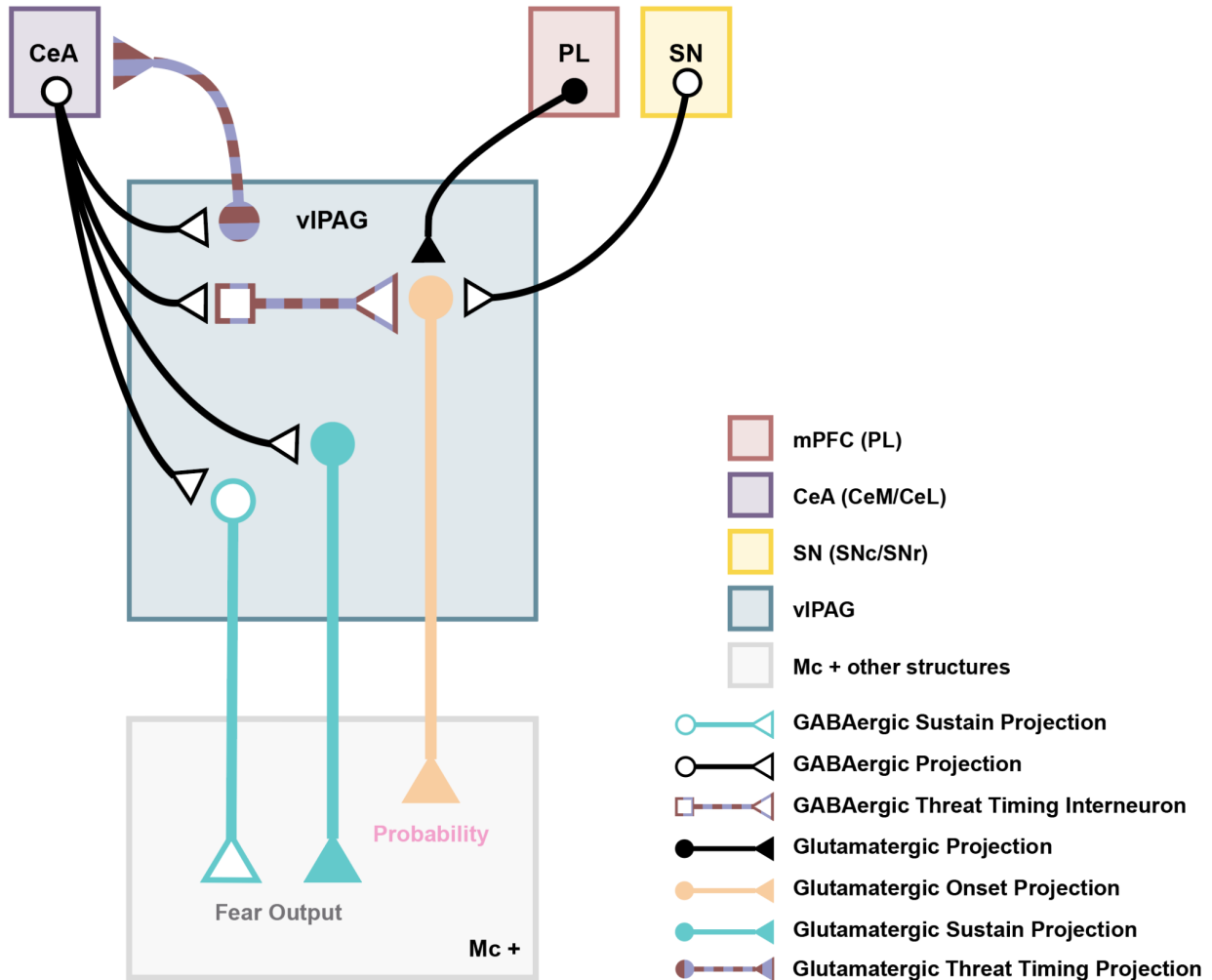


Figure 5.5 Revised vIPAG circuitry

Schematic of revised caudal ventrolateral periaqueductal gray (vIPAG) microcircuitry. Colored neurons refer to functional vIPAG populations according to the alternative arrangement posed in Figure 5.1 B. Black neurons are inputs to the vIPAG. Solid filled neurons are putatively glutamatergic. Colored neurons with white fill are putatively GABAergic. Black neurons with white fill are verified GABAergic projections to the vIPAG. Circle ends indicate projection neurons and squares ends indicate interneurons. Brain regions are color coded blocks: prelimbic medial prefrontal cortex (PL: rust), medial and lateral central amygdala (CeA: purple), caudal substantia nigra pars compacta and pars reticulata (SN: marigold), caudal vIPAG (vIPAG: teal), and magnocellular nucleus of the medulla as one of many structures which could receive functional vIPAG output (Mc+: gray). Fear output (dark gray) and threat probability (pink) signaling of Sustain (seafoam) and Onset (peach) are indicated with colored text. Threat timing neurons are candy striped (periwinkle and wine).

5.2.5 A different type of disinhibition

GABAergic vIPAG neurons demonstrate higher baseline firing. HF Threat Timing neurons may be GABAergic. In the current disinhibition microcircuit, inhibition of GABAergic interneurons leads to activation of glutamatergic vIPAG output neurons which induce freezing (Tovote et al., 2016). HF Threat Timing neurons may be GABAergic interneurons (Figure 5.5, candy stripe white fill). In this way, the brief decrease in Threat Timing firing observed at the beginning of cue presentation, would allow for increased activity in a separate functional population to occur. Which population might that be? Miraculously, the brief decrease in firing observed in Threat Timing neurons is restricted to the first 1 s interval of cue presentation. At that exact time, for that exact duration, a sharp increase in Onset firing is observed (Figure 5.2 A, C and E). Consistent with the disinhibition microcircuit (Figure 1.3), GABAergic CeA inputs would provide the brief inhibition required to disinhibit Onset activity. This would enable Onset firing, and allow Onset signals to inform fear output signals (local to the magnocellular nucleus of the medulla (Mc)) downstream. By contrast, LF Threat Timing neurons may be glutamatergic output neurons of the vIPAG (Figure 5.5, candy stripe solid fill).

In the disinhibition model, this would imply that GABAergic Threat Timing neurons could synapse on glutamatergic Threat Timing neurons. However, a second threat timing signal would be far more valuable as a separate, output projection. Moreover, increased firing is required to observe the actual Threat Timing component (maximal firing just prior to foot shock) of patterned activity, which would not be possible with GABAergic input alone. Although CeA neurons preferentially synapse on GABAergic vIPAG cells, they also project to glutamatergic vIPAG neurons. According to the PIC model, amygdala derived

information about threat timing could proceed to the vIPAG via this direct projection. However, this presents a similar problem: CeA projections to the vIPAG are also GABAergic. If LF Threat Timing neurons received either of these GABAergic projections, they would need additional excitatory input to increase firing as threat draws near.

5.2.6 A glutamatergic vIPAG Input

A source of threat relevant glutamatergic input to the caudal vIPAG unclear. However, the prelimbic medial prefrontal cortex (PL) is part of a triad of brain regions (including the hippocampus and amygdala) implicated in fear expression. Specifically, the PL is thought to exert top-down control over the canonical site of threat integration: the amygdala (Giustino & Maren, 2015). PL to amygdala projections implicated in top-down control of fear are glutamatergic (DeFelipe & Fariñas, 1992). As an additional site of threat integration, it is possible the PL may also exert top-down glutamatergic control over the caudal vIPAG. Indeed, there is a direct projection from the PL to the caudal vIPAG (Beitz, 1982), and some have already suggested the PL may bypass the amygdala to directly influence freezing behavior (Giustino & Maren, 2015). Similar to the amygdalar projection, it would be reasonable to suggest input to the vIPAG from the PL is also glutamatergic (Figure 5.4, solid black projection), and that this input could increase firing of Threat Timing neurons for signaling impending noxious events. If LF Threat Timing neurons are glutamatergic output neurons, where might they project to?

5.2.7 Updating Threat Timing

As a complimentary site of threat timing integration, glutamatergic Threat Timing projections from the vIPAG could return to the amygdala for further processing and updating. Similar to the Onset threat probability signal, vIPAG threat timing (thought to be

part of amygdalar-centric threat integration) signals may be trained up by the CeA, but become CeA-independent with sufficient training. Like Threat Timing neurons, Sustain neurons demonstrate a wide range of baseline firing rates, and likely consist of HF GABAergic and LF glutamatergic neurons.

5.2.8 Sustain neurons are putatively GABAergic and glutamatergic

In line with previously mentioned reports of vIPAG firing rates, HF Sustain neurons are likely GABAergic, whereas LF Sustain neurons are likely glutamatergic. In the canonical circuit, vIPAG fear output signals are sent to the RVM or Mc to influence downstream behavior. Thus, it is sensible to presume that both HF and LF Sustain neurons, encoding fear output, are GABAergic or glutamatergic vIPAG projection neurons (Figure 5.4, white fill and solid seafoam). Sustain neurons are cue-inhibited, and require decreases in firing to signal fear output. Decreases in firing are likely mediated by GABAergic inputs to Sustain neurons.

The SN provides GABAergic input to the vIPAG. However, the results of Chapter 4 strongly suggest this projection does not likely influence the firing of either HF or LF Sustain neurons. Decreases in firing are the hallmark of Sustain neurons and fear output in the vIPAG. Moreover, decreases in Sustain firing are associated with increased fear. In Chapter 4, silencing the cSN would have removed inhibition from Sustain neurons, diminishing the decreased firing required to signal fear output. Increased firing in Sustain neurons (less of a decrease) would give rise to decreased fear. However, I observed global inflation of fear to all cues. Thus, it is more likely the CeA provides GABAergic inhibition to Sustain output neurons (Figure 5.4).

5.2.9 Substantia Nigra and the vIPAG microcircuit

Is there another way the substantia nigra might fit into the vIPAG microcircuit? The recent disinhibition model suggests that GABAergic CeA output neurons synapse on local GABAergic vIPAG interneurons (Tovote et al., 2016). In turn, the inhibition of local vIPAG interneurons in this microcircuit, releases inhibition of glutamatergic vIPAG output neurons and permits fear expression. It is possible that the GABAergic projections from the SN to vIPAG (Kirouac et al., 2004) behave similarly: also synapses on local vIPAG GABAergic interneurons. If this were the case, inhibiting the SN in our manipulation would have had no effect on fear suppression: disinhibition of glutamatergic vIPAG output would not occur if GABAergic SN output to the vIPAG was silenced. I observed a global increase in fear in eNpHR rats (Figure 4.4 A, right). Instead of using a similar disinhibition microcircuit, GABAergic SN output to the vIPAG is more likely to influence a cue-excited population: Onset neurons.

5.2.10 Onset hub of signal integration

Unlike any other functional population, Cue-excited Onset neurons signal threat probability, invariant of fear output. Similar to the amygdala, Onset neurons of the vIPAG are incredibly well-suited to integrate many types of information that can inform fear output and wide range of threat-related processes. In stark contrast to the canonical view of vIPAG function, short-latency cue-excited Onset neurons are not simple fear output relays. They are sophisticated, computational units that likely project to downstream pre-motor targets, and more. Unlike Sustain and Threat Timing neurons, Onset neurons uniformly belong to one putatively glutamatergic (LF) cluster. Like Sustain neurons, and

Threat Timing neurons, in order for threat probability signals to leave the vIPAG, they must project.

In the revised disinhibition circuit, briefly inhibited Threat Timing neurons give rise to peak Onset firing and threat probability signalling. This projection also allows Onset neurons to receive information about Threat Timing which, when varied, could be critical to assessing level of threat, and informing an appropriate defensive response. Onset neurons are also well-suited to receive glutamatergic input from the PL, because their signaling depends on increased firing. In turn, PL activity related to fear expression has the ability to execute top-down control over Onset firing, potentially overriding vIPAG-level computation, to drive fear expression in downstream regions (RVM/Mc). However, that is not all. Activity of GABAergic cSN neurons also has the ability to interact with Onset neurons (Figure 5.5, SN input). Unlike Threat Timing neurons, which only increase firing to aversive cues, Onset firing increases are observed to all cues (danger, uncertainty and safety). Global increases in fear were observed to all cues following cSN inhibition, suggesting a role for the cSN in overall modulation of fear suppression. Interestingly, silencing a GABAergic projection to vIPAG Onset neurons, would release Onset inhibition and likely result in a global firing increase in Onset firing. In absence of cSN inhibition, Onset firing could be driven even higher by glutamatergic PL input, maximizing threat probability output of the vIPAG to Onset neuron targets.

5.2.11 Conclusions

The results of this work have contributed a wealth of information to our understanding of vIPAG function. The vIPAG is a critical site of threat processing that likely uses a combination of direct inhibition, excitation and disinhibition to integrate and distribute a

diverse range of information about fear output, threat probability, and threat timing. Concurrent with these findings, there is increasing evidence that vIPAG dysfunction may contribute to a variety of psychiatric disorders (George et al., 2019). Indeed, further understanding of the factors that determine vIPAG neuron function: cell-type (Li et al., 2016), transcriptome (Okaty et al., 2015; Okaty et al., 2019), connectome (Rozeske et al., 2018) and more (McPherson et al., 2018), will be essential to understanding the neural mechanisms underlying adaptive and maladaptive fear, and informing improved therapeutic interventions for fear and anxiety disorders.

References

- Abraham, A. D., Neve, K. A., & Lattal, K. M. (2014). Dopamine and extinction: A convergence of theory with fear and reward circuitry. *Neurobiology of Learning and Memory*, *108*, 65–77. <https://doi.org/10.1016/j.nlm.2013.11.007>
- Admon, R., Milad, M. R., & Hendler, T. (2013). A causal model of post-traumatic stress disorder: Disentangling predisposed from acquired neural abnormalities. *Trends in Cognitive Sciences*, *17*(7), 337–347. <https://doi.org/10.1016/j.tics.2013.05.005>
- Amorapanth, P., Nader, K., & LeDoux, J. E. (1999). Lesions of periaqueductal gray dissociate-conditioned freezing from conditioned suppression behavior in rats. *Learning & Memory*, *6*(5), 491–499.
- Anglada-Figueroa, D., & Quirk, G. J. (2005). Lesions of the basal amygdala block expression of conditioned fear but not extinction. *Journal of Neuroscience*, *25*(42), 9680–9685. <https://doi.org/10.1523/JNEUROSCI.2600-05.2005>
- Arico, C., Bagley, E. E., Carrive, P., Assareh, N., & McNally, G. P. (2017). Effects of chemogenetic excitation or inhibition of the ventrolateral periaqueductal gray on the acquisition and extinction of Pavlovian fear conditioning. *Neurobiology of Learning and Memory*, *144*, 186–197. <https://doi.org/10.1016/j.nlm.2017.07.006>
- Arico, C., & McNally, G. P. (2014). Opioid receptors regulate blocking and overexpectation of fear learning in conditioned suppression. *Behav Neurosci*, *128*(2), 199–206. <https://doi.org/10.1037/a0036133>
- Assareh, N., Bagley, E. E., Carrive, P., & McNally, G. P. (2017). Brief optogenetic inhibition of rat lateral or ventrolateral periaqueductal gray augments the acquisition of Pavlovian fear conditioning. *Behav Neurosci*, *131*(6), 454–459. <https://doi.org/10.1037/bne0000217>
- Assareh, N., Sarrami, M., Carrive, P., & McNally, G. P. (2016). The Organization of Defensive Behavior Elicited by Optogenetic Excitation of Rat Lateral or Ventrolateral

- Periaqueductal Gray. *Behavioral Neuroscience*, 130(4), 406–414.
<https://doi.org/10.1037/bne0000151>
- Bandler, R., Depaulis, A., & Vergnes, M. (1985). Identification of midbrain neurones mediating defensive behaviour in the rat by microinjections of excitatory amino acids. *Behav Brain Res*, 15(2), 107–119.
- Bear, M. F., Connors, B. W., & Paradiso, M. A. (2016). *Neuroscience: Exploring the brain* (18396629; Fourth edition.). Wolters Kluwer.
- Beitz, A. J. (1982). The organization of afferent projections to the midbrain periaqueductal gray of the rat. *Neuroscience*, 7(1), 133–159.
- Berg, B. A., Schoenbaum, G., & McDannald, M. A. (2014). The dorsal raphe nucleus is integral to negative prediction errors in Pavlovian fear. *European Journal of Neuroscience*, 40(7), 3096–3101.
- Bouchet, C. A., Miner, M. A., Loetz, E. C., Rosberg, A. J., Hake, H. S., Farmer, C. E., Ostrovskyy, M., Gray, N., & Greenwood, B. N. (2018). Activation of Nigrostriatal Dopamine Neurons during Fear Extinction Prevents the Renewal of Fear. *Neuropsychopharmacology*, 43(3), 665–672. <https://doi.org/10.1038/npp.2017.235>
- Bouton, M. E., & Bolles, R. C. (1980). Conditioned fear assessed by freezing and by the suppression of three different baselines. *Animal Learning & Behavior*, 8(3), 429–434.
- Breslau, N. (2002). Gender differences in trauma and posttraumatic stress disorder. *The Journal of Gender-Specific Medicine : JGSM : The Official Journal of the Partnership for Women's Health at Columbia*, 5(1), 34–40.
- Brown, J., Pan, W.-X., & Dudman, J. T. (2014). The inhibitory microcircuit of the substantia nigra provides feedback gain control of the basal ganglia output. *ELife*, 3, e02397.
<https://doi.org/10.7554/eLife.02397>
- Buchanan, S. L., & Thompson, R. H. (1994). Neuronal-Activity in the Midline Thalamic Nuclei during Pavlovian Heart-Rate Conditioning. *Brain Research Bulletin*, 35(3), 237–240.

[https://doi.org/10.1016/0361-9230\(94\)90128-7](https://doi.org/10.1016/0361-9230(94)90128-7)

- Buchel, C., Dolan, R. J., Armony, J. L., & Friston, K. J. (1999). Amygdala-hippocampal involvement in human aversive trace conditioning revealed through event-related functional magnetic resonance imaging. *Journal of Neuroscience*, *19*(24), 10869–10876.
- Carlson, N. R., & Birkett, M. A. (2017). *Physiology of Behavior* (12th ed.).
- Carrive, P., Leung, P., Harris, J., & Paxinos, G. (1997). Conditioned fear to context is associated with increased fos expression in the caudal ventrolateral region of the midbrain periaqueductal gray. *Neuroscience*, *78*(1), 165–177. [https://doi.org/10.1016/S0306-4522\(97\)83047-3](https://doi.org/10.1016/S0306-4522(97)83047-3)
- Chinta, S. J., & Andersen, J. K. (2005). Dopaminergic neurons. *The International Journal of Biochemistry & Cell Biology*, *37*(5), 942–946.
<https://doi.org/10.1016/j.biocel.2004.09.009>
- Ciocchi, S., Herry, C., Grenier, F., Wolff, S. B. E., Letzkus, J. J., Vlachos, I., Ehrlich, I., Sprengel, R., Deisseroth, K., Stadler, M. B., Müller, C., & Lüthi, A. (2010). Encoding of conditioned fear in central amygdala inhibitory circuits. *Nature*, *468*(7321), 277–282.
<https://doi.org/10.1038/nature09559>
- Clinical Practice Guideline for the Treatment of Posttraumatic Stress Disorder (PTSD) in Adults: (501872017-001)*. (2017). [Data set]. American Psychological Association.
<https://doi.org/10.1037/e501872017-001>
- Cole, S., & McNally, G. P. (2009). Complementary roles for amygdala and periaqueductal gray in temporal-difference fear learning. *Learn Mem*, *16*(1), 1–7.
<https://doi.org/10.1101/lm.1120509>
- Davis, M. (2006). Neural systems involved in fear and anxiety measured with fear-potentiated startle. *Am Psychol*, *61*(8), 741–756.
- De Oca, B. M., DeCola, J. P., Maren, S., & Fanselow, M. S. (1998). Distinct regions of the periaqueductal gray are involved in the acquisition and expression of defensive

- responses. *Journal of Neuroscience*, 18(9), 3426–3432.
- DeFelipe, J., & Fariñas, I. (1992). The pyramidal neuron of the cerebral cortex: Morphological and chemical characteristics of the synaptic inputs. *Progress in Neurobiology*, 39(6), 563–607. [https://doi.org/10.1016/0301-0082\(92\)90015-7](https://doi.org/10.1016/0301-0082(92)90015-7)
- Dejean, C., Courtin, J., Rozeske, R. R., Bonnet, M. C., Dousset, V., Michelet, T., & Herry, C. (2015). Neuronal Circuits for Fear Expression and Recovery: Recent Advances and Potential Therapeutic Strategies. *Biol Psychiatry*, 78(5), 298–306. <https://doi.org/10.1016/j.biopsych.2015.03.017>
- Del-Ben, C. M., & Graeff, F. G. (2009). Panic Disorder: Is the PAG Involved? *Neural Plasticity*, 2009, 108135. <https://doi.org/10.1155/2009/108135>
- DiLeo, A., Wright, K. M., & McDannald, M. A. (2016). Sub-second fear discrimination in rats: Adult impairment in adolescent heavy alcohol drinkers. *Learning & Memory*, 23, 618–622.
- Duvarci, S., & Pare, D. (2014). Amygdala microcircuits controlling learned fear. *Neuron*, 82(5), 966–980. <https://doi.org/10.1016/j.neuron.2014.04.042>
- Estes, K. W., & Skinner, B. F. (1941). Some Quantitative Properties of Anxiety. *Journal of Experimental Psychology*, 29(5), 390–400.
- Etkin, A., & Wager, T. D. (2007). Functional neuroimaging of anxiety: A meta-analysis of emotional processing in PTSD, social anxiety disorder, and specific phobia. *Am J Psychiatry*, 164(10), 1476–1488. <https://doi.org/10.1176/appi.ajp.2007.07030504>
- Fanselow, M. S. (1991). The Midbrain Periaqueductal Gray as a Coordinator of Action in Response to Fear and Anxiety. *Midbrain Periaqueductal Gray Matter*, 213, 151–173.
- Fanselow, M. S. (1993). The Periaqueductal Gray and the Organization of Defensive Behavior. *Aggressive Behavior*, 19(1), 18–19.
- Fanselow, M. S. (1994). Neural Organization of the Defensive Behavior System Responsible for Fear. *Psychonomic Bulletin & Review*, 1(4), 429–438.

<https://doi.org/10.3758/Bf03210947>

Fanselow, M. S., & LeDoux, J. E. (1999). Why we think plasticity underlying Pavlovian fear conditioning occurs in the basolateral amygdala. *Neuron*, 23(2), 229–232.

Fanselow, M. S., & Lester, L. S. (1988). A functional behavioristic approach to aversively motivated behavior: Predatory imminence as a determinant of the topography of defensive behavior. In R. C. Bolles Beecher, M. D. (Ed.), *Evolution and Learning* (pp. 185–212). Erlbaum.

Farook, J. M., Wang, Q., Moochhala, S. M., Zhu, Z. Y., Lee, L., & Wong, P. T.-H. (2004). Distinct regions of periaqueductal gray (PAG) are involved in freezing behavior in hooded PVG rats on the cat-freezing test apparatus. *Neuroscience Letters*, 354(2), 139–142. <https://doi.org/10.1016/j.neulet.2003.10.011>

Faull, O. K., Jenkinson, M., Ezra, M., & Pattinson, Kt. (2016). Conditioned respiratory threat in the subdivisions of the human periaqueductal gray. *Elife*, 5. <https://doi.org/10.7554/eLife.12047>

Frank, M. J., & Surmeier, D. J. (2009). Do Substantia Nigra Dopaminergic Neurons Differentiate Between Reward and Punishment? *Journal of Molecular Cell Biology*, 1(1), 15–16. <https://doi.org/10.1093/jmcb/mjp010>

Giustino, T. F., & Maren, S. (2015). The Role of the Medial Prefrontal Cortex in the Conditioning and Extinction of Fear. *Frontiers in Behavioral Neuroscience*, 9, 298. <https://doi.org/10.3389/fnbeh.2015.00298>

Glotzbach-Schoon, E., Tadda, R., Andreatta, M., Tröger, C., Ewald, H., Grillon, C., Pauli, P., & Mühlberger, A. (2013). Enhanced discrimination between threatening and safe contexts in high-anxious individuals. *Biological Psychology*, 93(1), 159–166. <https://doi.org/10.1016/j.biopsycho.2013.01.011>

Gorka, A. X., Torrisi, S., Shackman, A. J., Grillon, C., & Ernst, M. (2018). Intrinsic functional connectivity of the central nucleus of the amygdala and bed nucleus of the stria

- terminalis. *NeuroImage*, 168, 392–402.
<https://doi.org/10.1016/j.neuroimage.2017.03.007>
- Greiner, E. M., Muller, I., Norris, M. R., Ng, K. H., & Sangha, S. (2019). Sex differences in fear regulation and reward-seeking behaviors in a fear safety-reward discrimination task. *Behavioural Brain Research*, 368, 131–139. <https://doi.org/10.1016/j.bbr.2019.111903>
- Groenewegen, H. J. (2003). The basal ganglia and motor control. *Neural Plasticity*, 10(1–2), 107–120. <https://doi.org/10.1155/NP.2003.107>
- Gruene, T. M., Flick, K., Stefano, A., Shea, S. D., & Shansky, R. M. (2015). Sexually divergent expression of active and passive conditioned fear responses in rats. *Elife*, 4. <https://doi.org/10.7554/eLife.11352>
- Hermans, E. J., Henckens, M. J. A. G., Roelofs, K., & Fernández, G. (2013). Fear bradycardia and activation of the human periaqueductal grey. *NeuroImage*, 66, 278–287. <https://doi.org/10.1016/j.neuroimage.2012.10.063>
- Insanally, M. N., Carcea, I., Field, R. E., Rodgers, C. C., DePasquale, B., Rajan, K., DeWeese, M. R., Albanna, B. F., & Froemke, R. C. (2019). Spike-timing-dependent ensemble encoding by non-classically responsive cortical neurons. *Elife*, 8. <https://doi.org/10.7554/eLife.42409>
- Johansen, J. P., Cain, C. K., Ostroff, L. E., & LeDoux, J. E. (2011). Molecular mechanisms of fear learning and memory. *Cell*, 147(3), 509–524. <https://doi.org/10.1016/j.cell.2011.10.009>
- Johnstone, T., Somerville, L. H., Alexander, A. L., Oakes, T. R., Davidson, R. J., Kalin, N. H., & Whalen, P. J. (2005). Stability of amygdala BOLD response to fearful faces over multiple scan sessions. *Neuroimage*, 25(4), 1112–1123. <https://doi.org/10.1016/j.neuroimage.2004.12.016>
- Jones, L. M., Fontanini, A., Sadacca, B. F., Miller, P., & Katz, D. B. (2007). Natural stimuli evoke dynamic sequences of states in sensory cortical ensembles. *Proc Natl Acad Sci U S A*,

- 104(47), 18772–18777. <https://doi.org/10.1073/pnas.0705546104>
- Keay, K. A., & Bandler, R. (2004). CHAPTER 10—Periaqueductal Gray. In G. Paxinos (Ed.), *The Rat Nervous System (Third Edition)* (Third Edition, pp. 243–257). Academic Press. <https://doi.org/10.1016/B978-012547638-6/50011-0>
- Kim, J. J., Rison, R. A., & Fanselow, M. S. (1993). Effects of amygdala, hippocampus, and periaqueductal gray lesions on short- and long-term contextual fear. *Behav Neurosci*, 107(6), 1093–1098.
- Kirouac, G. J., Li, S., & Mabrouk, G. (2004). GABAergic projection from the ventral tegmental area and substantia nigra to the periaqueductal gray region and the dorsal raphe nucleus. *The Journal of Comparative Neurology*, 469(2), 170–184. <https://doi.org/10.1002/cne.11005>
- Koutsikou, S., Crook, J. J., Earl, E. V., Leith, J. L., Watson, T. C., Lumb, B. M., & Apps, R. (2014). Neural substrates underlying fear-evoked freezing: The periaqueductal grey-cerebellar link. *J Physiol*, 592(10), 2197–2213. <https://doi.org/10.1113/jphysiol.2013.268714>
- Krout, K. E., & Loewy, A. D. (2000). Periaqueductal gray matter projections to midline and intralaminar thalamic nuclei of the rat. *J Comp Neurol*, 424(1), 111–141.
- LeDoux, J. E., Iwata, J., Cicchetti, P., & Reis, D. J. (1988). Different projections of the central amygdaloid nucleus mediate autonomic and behavioral correlates of conditioned fear. *Journal of Neuroscience*, 8(7), 2517–2529.
- Lee, J. L. C., Dickinson, A., & Everitt, B. J. (2005). Conditioned suppression and freezing as measures of aversive Pavlovian conditioning: Effects of discrete amygdala lesions and overtraining. *Behavioural Brain Research*, 159(2), 221–233.
- Liebman, J. M., Mayer, D. J., & Liebeskind, J. C. (1970). Mesencephalic central gray lesions and fear-motivated behavior in rats. *Brain Res*, 23(3), 353–370.
- Lutas, A., Kucukdereli, H., Alturkistani, O., Carty, C., Sugden, A. U., Fernando, K., Diaz, V.,

- Flores-Maldonado, V., & Andermann, M. L. (2019). State-specific gating of salient cues by midbrain dopaminergic input to basal amygdala. *BioRxiv*, 687707.
<https://doi.org/10.1101/687707>
- Mahan, A. L., & Ressler, K. J. (2012). Fear conditioning, synaptic plasticity and the amygdala: Implications for posttraumatic stress disorder. *Trends in Neurosciences*, 35(1), 24–35.
<https://doi.org/10.1016/j.tins.2011.06.007>
- Maren, S., Phan, K. L., & Liberzon, I. (2013). The contextual brain: Implications for fear conditioning, extinction and psychopathology. *Nat Rev Neurosci*, 14(6), 417–428.
<https://doi.org/10.1038/nrn3492>
- McDannald, M. A. (2010). Contributions of the amygdala central nucleus and ventrolateral periaqueductal grey to freezing and instrumental suppression in Pavlovian fear conditioning. *Behavioural Brain Research*, 211(1), 111–117.
- McDannald, M. A., & Galarce, E. M. (2011). Measuring Pavlovian fear with conditioned freezing and conditioned suppression reveals different roles for the basolateral amygdala. *Brain Research*, 1374, 82–89. <https://doi.org/10.1016/j.brainres.2010.12.050>
- McEchron, M. D., Bouwmeester, H., Tseng, W., Weiss, C., & Disterhoft, J. F. (1998). Hippocampectomy disrupts auditory trace fear conditioning and contextual fear conditioning in the rat. *Hippocampus*, 8(6), 638–646. [https://doi.org/10.1002/\(Sici\)1098-1063\(1998\)8:6<638::Aid-Hipo6>3.0.Co;2-Q](https://doi.org/10.1002/(Sici)1098-1063(1998)8:6<638::Aid-Hipo6>3.0.Co;2-Q)
- McNally, G. P., Johansen, J. P., & Blair, H. T. (2011). Placing prediction into the fear circuit. *Trends Neurosci*, 34(6), 283–292. <https://doi.org/10.1016/j.tins.2011.03.005>
- Milad, M. R., Orr, S. P., Lasko, N. B., Chang, Y., Rauch, S. L., & Pitman, R. K. (2008). Presence and acquired origin of reduced recall for fear extinction in PTSD: results of a twin study. *Journal of Psychiatric Research*, 42(7), 515–520.
<https://doi.org/10.1016/j.jpsychires.2008.01.017>
- Mobbs, D., Petrovic, P., Marchant, J. L., Hassabis, D., Weiskopf, N., Seymour, B., Dolan, R. J.,

- & Frith, C. D. (2007). When fear is near: Threat imminence elicits prefrontal-periaqueductal gray shifts in humans. *Science*, 317(5841), 1079–1083.
<https://doi.org/10.1126/science.1144298>
- Mobbs, D., Yu, R. J., Rowe, J. B., Eich, H., FeldmanHall, O., & Dalgleish, T. (2010). Neural activity associated with monitoring the oscillating threat value of a tarantula. *Proceedings of the National Academy of Sciences of the United States of America*, 107(47), 20582–20586. <https://doi.org/10.1073/pnas.1009076107>
- Nambu, A. (2008). Seven problems on the basal ganglia. *Current Opinion in Neurobiology*, 18(6), 595–604. <https://doi.org/10.1016/j.conb.2008.11.001>
- Neupane, S. P., Bramness, J. G., & Lien, L. (2017). Comorbid post-traumatic stress disorder in alcohol use disorder: Relationships to demography, drinking and neuroimmune profile. *BMC Psychiatry*, 17(1), 312. <https://doi.org/10.1186/s12888-017-1479-8>
- Oka, T., Tsumori, T., Yokota, S., & Yasui, Y. (2008). Neuroanatomical and neurochemical organization of projections from the central amygdaloid nucleus to the nucleus retroambiguus via the periaqueductal gray in the rat. *Neurosci Res*, 62(4), 286–298.
<https://doi.org/10.1016/j.neures.2008.10.004>
- Ono, M., Bishop, D. C., & Oliver, D. L. (2017). Identified GABAergic and glutamatergic Neurons in the Mouse Inferior Colliculus Share Similar Response Properties. *The Journal of Neuroscience : The Official Journal of the Society for Neuroscience*, 37(37), 8952–8964.
<https://doi.org/10.1523/JNEUROSCI.0745-17.2017>
- Ozawa, T., Ycu, E. A., Kumar, A., Yeh, L. F., Ahmed, T., Koivumaa, J., & Johansen, J. P. (2017). A feedback neural circuit for calibrating aversive memory strength. *Nature Neuroscience*, 20(1), 90–97. <https://doi.org/10.1038/nn.4439>
- Paredes, J., Winters, R. W., Schneiderman, N., & McCabe, P. M. (2000). Afferents to the central nucleus of the amygdala and functional subdivisions of the periaqueductal gray: Neuroanatomical substrates for affective behavior. *Brain Research*, 887(1), 157–173.

[https://doi.org/10.1016/S0006-8993\(00\)02972-3](https://doi.org/10.1016/S0006-8993(00)02972-3)

Paxinos, G., & Watson, C. (2007). *The rat brain in stereotaxic coordinates* (14605705; 6th ed., Vol. 1–1). Academic Press/Elsevier. Publisher description

<http://www.loc.gov/catdir/enhancements/fy0745/2006937142-d.html>

Perusini, J. N., & Fanselow, M. S. (2015). Neurobehavioral perspectives on the distinction between fear and anxiety. *Learning & Memory*, 22(9), 417–425.

<https://doi.org/10.1101/lm.039180.115>

Pickens, C. L., Golden, S. A., Adams-Deutsch, T., Nair, S. G., & Shaham, Y. (2009). Long-lasting incubation of conditioned fear in rats. *Biological Psychiatry*, 65(10), 881–886.

<https://doi.org/10.1016/j.biopsych.2008.12.010>

Pitman, R. K. (1988). Post-Traumatic Stress Disorder, Conditioning, and Network Theory.

Psychiatric Annals, 18(3), 182–189. <https://doi.org/10.3928/0048-5713-19880301-11>

Pitman, R. K., Rasmusson, A. M., Koenen, K. C., Shin, L. M., Orr, S. P., Gilbertson, M. W., Milad, M. R., & Liberzon, I. (2012). Biological studies of post-traumatic stress disorder.

Nature Reviews Neuroscience, 13(11), 769–787. <https://doi.org/10.1038/nrn3339>

Rauch, S. L., Whalen, P. J., Shin, L. M., McInerney, S. C., Macklin, M. L., Lasko, N. B., Orr, S. P., & Pitman, R. K. (2000). Exaggerated amygdala response to masked facial stimuli in posttraumatic stress disorder: A functional MRI study. *Biol Psychiatry*, 47(9), 769–776.

Rauch, Scott L., Shin, L. M., & Phelps, E. A. (2006). Neurocircuitry models of posttraumatic stress disorder and extinction: Human neuroimaging research—Past, present, and future.

Biological Psychiatry, 60(4), 376–382.

<https://doi.org/10.1016/j.biopsych.2006.06.004>

Ray, M. H., Hanlon, E., & McDannald, M. A. (2018). Lateral orbitofrontal cortex partitions mechanisms for fear regulation and alcohol consumption. *PLoS One*, 13(6), e0198043.

<https://doi.org/10.1371/journal.pone.0198043>

Ray, Madelyn H., Russ, A. N., Walker, R. A., & McDannald, M. A. (2020). The Nucleus

- Accumbens Core is Necessary to Scale Fear to Degree of Threat. *The Journal of Neuroscience*, 40(24), 4750. <https://doi.org/10.1523/JNEUROSCI.0299-20.2020>
- Rescorla, R. A. (1968). Probability of shock in the presence and absence of CS in fear conditioning. *Journal of Comparative and Physiological Psychology*, 66(1), 1–5.
- Robinson, J. E., Coughlin, G. M., Hori, A. M., Cho, J. R., Mackey, E. D., Turan, Z., Patriarchi, T., Tian, L., & Gradinaru, V. (2019). Optical dopamine monitoring with dLight1 reveals mesolimbic phenotypes in a mouse model of neurofibromatosis type 1. *ELife*, 8. <https://doi.org/10.7554/eLife.48983>
- Roesch, M. R., Calu, D. J., & Schoenbaum, G. (2007). Dopamine neurons encode the better option in rats deciding between differently delayed or sized rewards. *Nature Neuroscience*, 10(12), 1615–1624.
- Rosas, J. M., & Alonso, G. (1996). Temporal discrimination and forgetting of CS duration in conditioned suppression. *Learning and Motivation*, 27(1), 43–57. <https://doi.org/10.1006/lmot.1996.0003>
- Rozeske, R. R., Jercog, D., Karalis, N., Chaudun, F., Khoder, S., Girard, D., Winke, N., & Herry, C. (2018). Prefrontal-Periaqueductal Gray-Projecting Neurons Mediate Context Fear Discrimination. *Neuron*, 97(4), 898-910 e6. <https://doi.org/10.1016/j.neuron.2017.12.044>
- Satpute, A. B., Wager, T. D., Cohen-Adad, J., Bianciardi, M., Choi, J. K., Buhle, J. T., Wald, L. L., & Barrett, L. F. (2013). Identification of discrete functional subregions of the human periaqueductal gray. *Proceedings of the National Academy of Sciences of the United States of America*, 110(42), 17101–17106. <https://doi.org/10.1073/pnas.1306095110>
- Schultz, W. (1997). Dopamine neurons and their role in reward mechanisms. *Curr Opin Neurobiol*, 7(2), 191–197.
- Sengupta, A., & McNally, G. P. (2014). A role for midline and intralaminar thalamus in the associative blocking of Pavlovian fear conditioning. *Front Behav Neurosci*, 8, 148. <https://doi.org/10.3389/fnbeh.2014.00148>

- Shi, C., & Davis, M. (1999). Pain pathways involved in fear conditioning measured with fear-potentiated startle: Lesion studies. *J Neurosci*, *19*(1), 420–430.
- Shin, L. M., & Handwerker, K. (2009). Is posttraumatic stress disorder a stress-induced fear circuitry disorder? *Journal of Traumatic Stress*, *22*(5), 409–415.
<https://doi.org/10.1002/jts.20442>
- Silva, C., & McNaughton, N. (2019). Are periaqueductal gray and dorsal raphe the foundation of appetitive and aversive control? A comprehensive review. *Progress in Neurobiology*, *177*, 33–72. <https://doi.org/10.1016/j.pneurobio.2019.02.001>
- Sonne, J., Reddy, V., & Beato, M. R. (2020). Neuroanatomy, Substantia Nigra. In *StatPearls*. StatPearls Publishing.
- Strickland, J. A., Dileo, A. D., Moaddab, M., Ray, M. H., Walker, R. A., Wright, K. M., & McDannald, M. A. (2021). Foot shock facilitates reward seeking in an experience-dependent manner. *Behavioural Brain Research*, *399*, 112974.
<https://doi.org/10.1016/j.bbr.2020.112974>
- Tovote, P., Esposito, M. S., Botta, P., Chaudun, F., Fadok, J. P., Markovic, M., Wolff, S. B., Ramakrishnan, C., Fenno, L., Deisseroth, K., Herry, C., Arber, S., & Luthi, A. (2016). Midbrain circuits for defensive behaviour. *Nature*, *534*(7606), 206–212.
<https://doi.org/10.1038/nature17996>
- Tovote, P., Fadok, J. P., & Luthi, A. (2015). Neuronal circuits for fear and anxiety. *Nat Rev Neurosci*, *16*(6), 317–331. <https://doi.org/10.1038/nrn3945>
- Vertes, R. P., Linley, S. B., & Hoover, W. B. (2015). Limbic circuitry of the midline thalamus. *Neuroscience and Biobehavioral Reviews*, *54*, 89–107.
<https://doi.org/10.1016/j.neubiorev.2015.01.014>
- Vianna, D. M., Allen, C., & Carrive, P. (2008). Cardiovascular and behavioral responses to conditioned fear after medullary raphe neuronal blockade. *Neuroscience*, *153*(4), 1344–1353. <https://doi.org/10.1016/j.neuroscience.2008.03.033>

- Vianna, D. M. L., Graeff, F. G., Brandao, M. L., & Landeira-Fernandez, J. (2001). Defensive freezing evoked by electrical stimulation of the periaqueductal gray: Comparison between dorsolateral and ventrolateral regions. *Neuroreport*, *12*(18), 4109–4112. <https://doi.org/10.1097/00001756-200112210-00049>
- Walker, D. L., Cassella, J. V., Lee, Y., De Lima, T. C., & Davis, M. (1997). Opposing roles of the amygdala and dorsolateral periaqueductal gray in fear-potentiated startle. *Neurosci Biobehav Rev*, *21*(6), 743–753.
- Walker, R. A., Andreansky, C., Ray, M. H., & McDannald, M. A. (2018). Early adolescent adversity inflates threat estimation in females and promotes alcohol use initiation in both sexes. *Behav Neurosci*, *132*(3), 171–182. <https://doi.org/10.1037/bne0000239>
- Walker, R. A., Wright, K. M., Jhou, T. C., & McDannald, M. A. (2019). The ventrolateral periaqueductal gray updates fear via positive prediction error. *Eur J Neurosci*. <https://doi.org/10.1111/ejn.14536>
- Watson, T. C., Cerminara, N. L., Lumb, B. M., & Apps, R. (2016). Neural Correlates of Fear in the Periaqueductal Gray. *J Neurosci*, *36*(50), 12707–12719. <https://doi.org/10.1523/JNEUROSCI.1100-16.2016>
- Wright, K. M., DiLeo, A., & McDannald, M. A. (2015). Early adversity disrupts the adult use of aversive prediction errors to reduce fear in uncertainty. *Front Behav Neurosci*, *9*, 227. <https://doi.org/10.3389/fnbeh.2015.00227>
- Wright, K. M., Lee, E., & McDannald, M. A. (2019). Roles for dorsal raphe/periaqueductal gray and retrorubral field dopamine in adaptive fear. *Society for Neuroscience Meeting Planner, Program No. 722.01. 2019*.
- Wright, K. M., & McDannald, M. A. (2019). Ventrolateral periaqueductal gray neurons prioritize threat probability over fear output. *Elife*, *8*. <https://doi.org/10.7554/eLife.45013>
- Yamaguchi, T., Wang, H. L., & Morales, M. (2013). Glutamate neurons in the substantia nigra compacta and retrorubral field. *Eur J Neurosci*, *38*(11), 3602–3610.

<https://doi.org/10.1111/ejn.12359>

Yeh, L. F., Watanabe, M., Sulkes-Cuevas, J., & Johansen, J. P. (2017). Dysregulation of aversive signaling pathways: A novel circuit endophenotype for pain and anxiety disorders. *Curr Opin Neurobiol*, 48, 37–44. <https://doi.org/10.1016/j.conb.2017.09.006>

Zhou, J., Gardner, M. P. H., Stalnaker, T. A., Ramus, S. J., Wikenheiser, A. M., Niv, Y., & Schoenbaum, G. (2018). Rat orbitofrontal ensemble activity contains a multiplexed but value-invariant representation of task structure in an odor sequence task. *BioRxiv*, 507376. <https://doi.org/10.1101/507376>